

Design, Synthesis and Biological Evaluation of Novel DNA Gyrase Inhibitors and their Siderophore Mimic Conjugates

Andraž Lamut,^a Cristina D. Cruz,^b Žiga Skok,^a Michaela Barančoková,^a Nace Zidar,^a Anamarija Zega,^a Lucija Peterlin Mašič,^a Janez Ilaš,^a Päivi Tammela,^b Danijel Kikelj,^a and Tihomir Tomašič,^{a,*}

^aUniversity of Ljubljana, Faculty of Pharmacy, Aškerčeva cesta 7, 1000 Ljubljana, Slovenia

^bDrug Research Program, Division of Pharmaceutical Biosciences, Faculty of Pharmacy, University of Helsinki, P.O. Box 56 (Viikinkaari 5 E), FI-00014 Helsinki, Finland

***Corresponding author: Tihomir Tomašič**

University of Ljubljana, Faculty of Pharmacy,

Aškerčeva cesta 7, 1000 Ljubljana, Slovenia

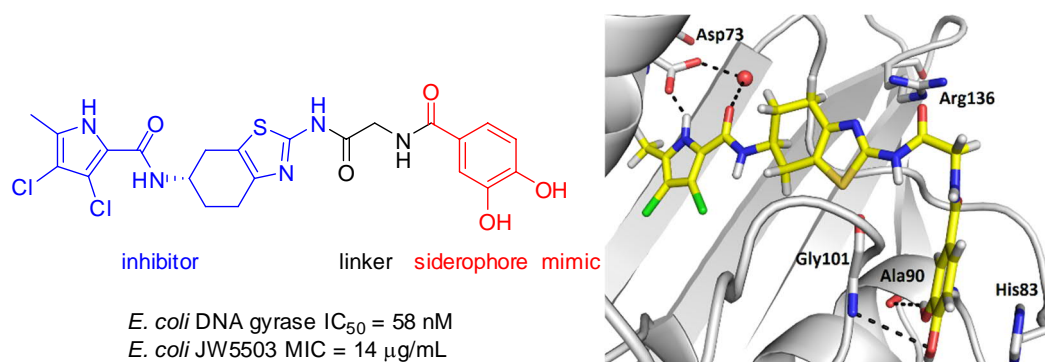
Tel: +386-1-4769556

E-mail: tihomir.tomasic@ffa.uni-lj.si

Abstract

Bacterial DNA gyrase is an important target for the development of novel antibacterial drugs, which are urgently needed because of high level of antibiotic resistance worldwide. We designed and synthesized new 4,5,6,7-tetrahydrobenzo[*d*]thiazole-based DNA gyrase B inhibitors and their conjugates with siderophore mimics, which were introduced to increase the uptake of inhibitors into the bacterial cytoplasm. The most potent conjugate **34** had an IC₅₀ of 58 nM against *Escherichia coli* DNA gyrase and displayed MIC of 14 µg/mL against *E. coli* ΔtolC strain. Only minor improvements in the antibacterial activities against wild-type *E. coli* in low-iron conditions were seen for DNA gyrase inhibitor – siderophore mimic conjugates.

Graphical abstract



Keywords: antibiotics; catechol; DNA gyrase; inhibitors; siderophore mimic;

Abbreviations

EDC, 1-ethyl-3-(3-(dimethylamino)propyl)-carbodiimide; GyrB, DNA gyrase subunit B; HOBt, 1-hydroxybenzotriazole; MIC, minimum inhibitory concentration; OM, outer membrane.

Highlights

- Siderophore mimics were conjugated with 4,5,6,7-tetrahydrobenzo[*d*]thiazole-based DNA gyrase B inhibitors.
- The most potent conjugate had an IC₅₀ of 58 nM against *Escherichia coli* DNA gyrase.
- Two conjugates displayed MICs of 14 µg/mL against *E. coli* ΔtolC strain.
- Most conjugates showed improved activities against wild-type *Escherichia coli* in iron-depleted medium.

1. Introduction

In recent decades, infectious diseases have been recognized as one of the most important global health issues, which is mainly attributed to the increasing problem of microbial resistance [1, 2]. According to the World Health Organization, the priority pathogens for which research and development of new treatment options are most urgently needed include 12 families of bacteria. Among these, *Staphylococcus aureus*, *Pseudomonas aeruginosa* and the *Enterobacteriaceae* family (including *Escherichia coli*) have been described as critical high-priority pathogens that are especially difficult to treat [3].

Unfortunately, the urgent need for development of new antibiotics is, however, accompanied by a lack of interest of the pharmaceutical industry for economic reasons and because of strict regulatory requirements [4]. Due to the problem of bacterial resistance, antibiotics with new mechanisms of action are needed, as they would then not be expected to be removed by the pre-existing resistance mechanisms, with the development of cross resistance also less likely to occur. In the last 10 years, some successful new drugs have been approved that have alternative mechanisms of action; e.g., antibiotics belonging to the class of oxazolidinones and lipopeptides [5]. In addition to overexpression of efflux pumps, reduced permeability of the outer membrane (OM) is recognized as a major mechanism that underlies resistance of Gram-negative bacteria and that can cause the failure of existing antibacterial therapies [6].

DNA gyrase is a validated target for antibacterial drug discovery [7, 8]. This enzyme belongs to the class of bacterial type IIa topoisomerases, and it is responsible for the introduction of negative supercoils during bacterial DNA replication. DNA gyrase is a heterotetrameric protein that is composed of two GyrA subunits and two ATP-binding GyrB subunits [7]. Many studies have already been carried out to develop clinically useful ATP-

competitive GyrB inhibitors; however, none are currently available for therapeutic use [8, 9]. In 2015 we discovered structurally novel GyrB inhibitors based on the 4,5,6,7-tetrahydrobenzo[*d*]thiazole-2,6-diamine core (**1-3**, Figure 1) [10,11]. Compounds **1** and **2** showed low-nanomolar inhibition of *E. coli* DNA gyrase, but did not show activity against wild-type Gram-negative strains of *E. coli* and *P. aeruginosa*, which was most likely the consequence of cell-wall penetration issues and/or active efflux from the bacterial cells that is mediated by their efflux pump machineries. This latter explanation was supported by the findings that some of these compounds showed improved antibacterial activities when tested against the *E. coli* JW5503 strain that has a defective efflux pump, with MICs as low as 31 μ M (e.g. **2**, Figure 1) [10]. Similar observations were also made for other structural classes of GyrB inhibitors, including benzo[*d*]thiazoles [12], *N*-phenylpyrrolamides [13] and ethyl ureas [14, 15].

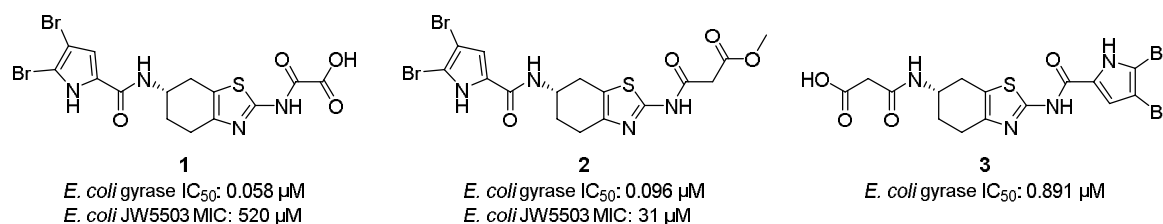


Figure 1. Representative structures of previously reported DNA gyrase inhibitors with the 4,5,6,7-tetrahydrobenzo[*d*]thiazole-2,6-diamine scaffold.

One strategy to overcome the problem of low bacterial cell-wall penetration is conjugation of small molecular weight siderophore mimics to molecules that have antibacterial properties [16, 17]. Siderophores are high-affinity iron-chelating compounds that are secreted by microorganisms and are among the strongest known soluble iron-binding agents [18]. Bacteria use siderophores to exploit the very limited amounts of freely available iron in the host environment during infection, and hence to survive the proliferation process [19]. Iron–siderophore complexes are then transported across the bacterial membrane into the cytoplasm

via iron-uptake machineries. Attaching a siderophore or a siderophore mimic to an antibacterial drug can therefore be used as a means to deliver antibiotics into bacteria [20, 21]. Siderophore mimics are small fragments of natural siderophores that have the similar structural features that are responsible for iron chelation. Commonly used siderophore mimics are shown in Figure 2, and these include catechols, hydroxypyranones, hydroxypyridones and dihydroxypyridones. Some antibiotic–siderophore mimic conjugates have recently been taken to clinical trials, such as the monosulfactam BAL30072 [22] and cephalosporin cefiderocol [23] (Figure 2). In November 2019 U.S. Food and Drug Administration approved cefiderocol for the treatment of complicated urinary tract infections [24].

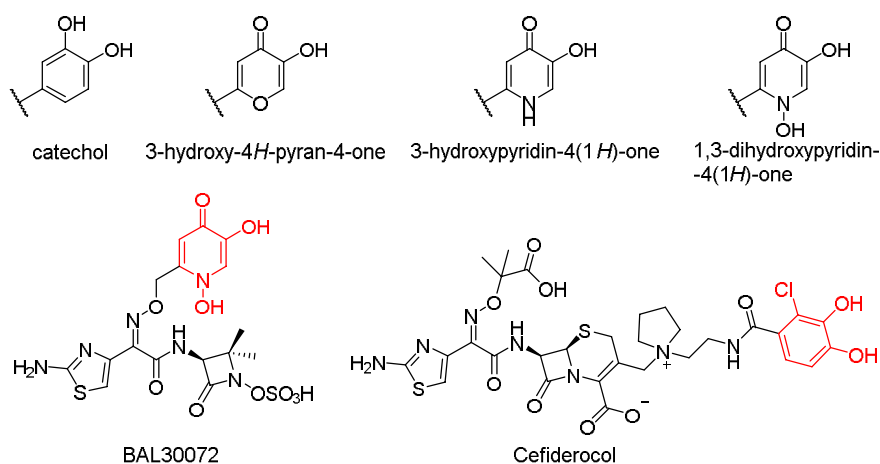


Figure 2. Structures of the commonly used siderophore mimics and the most developed antibiotic–siderophore mimic conjugates BAL30072 and cefiderocol.

In the present study, we designed new DNA gyrase inhibitors starting from compounds presented in Figure 1. Moreover, we attached the siderophore mimics to selected DNA gyrase inhibitors to evaluate their impact on enzyme inhibition and antibacterial activities against Gram-negative bacteria.

2. Design

New (*S*)-4,5,6,7-tetrahydrobenzo[*d*]thiazol-6-yl-1*H*-pyrrole-2-carboxamide derivatives were designed using co-crystal structures that we reported previously, where the inhibitors bind to the 43-kDa N-terminal fragment of *E. coli* GyrB (PDB codes: 4ZVI, 5L3J) [11, 25]. In these structures, the pyrrole-2-carboxamide moiety is bound deep in the hydrophobic pocket and forms hydrogen bonds with Asp73 of *E. coli* GyrB and a conserved water molecule. In addition, substituents on the 2-amino group of the central (*S*)-4,5,6,7-tetrahydrobenzo[*d*]thiazole-2,6-diamine scaffold can form additional interactions with Arg136 and adjacent amino acid residues of *E. coli* GyrB, as was predicted by molecular docking (Figure 3A) [10].

In the present designed series of DNA gyrase inhibitors and inhibitor–siderophore mimic conjugates, two different pyrrole moieties were used to achieve favorable interactions in the hydrophobic pocket of *E. coli* GyrB, namely dibromopyrrole and dichloromethylpyrrole, as halogen atoms have been shown to be important for binding [10, 26]. Further, based on the described orientation of these inhibitors in the GyrB ATP-binding site, the 2-amino group was identified as a suitable position on which to attach additional substituents or siderophore mimic moieties (Figure 3).

Based on molecular docking calculations (Figure 3A), substituents directly attached to the 2-amino group (Figure 3B and 3C, type **I**) can form additional interactions with the binding site residues. In addition, to explore the impact of siderophore mimics on DNA gyrase inhibition, we also designed analogs that had the siderophore mimic attached via different linkers to the 2-amino group of the central scaffold (Figure 3B and 3D, type **II**). Three different siderophore mimics were used: hydroxypyranone, hydroxypyridone and catechol. Different amino acid linkers were explored for the possibility of hydrophobic interactions of their lipophilic side chains with hydrophobic amino-acid residues in the binding site, or cation- π

interactions with the Arg136 for compounds with phenylalanine and tyrosine linkers. The length of the linkers was also examined, with this extended by one carbon atom using β -alanine. The catechol siderophore mimic was attached via two different substitution patterns, to obtain either 3,4-dihydroxyphenyl-based or 2,3-dihydroxyphenyl-based conjugates. To compare the effects of the siderophore moiety on DNA gyrase inhibition, the compounds were also prepared with free amino (**11**, **12**, **29**, **30**) or acetamido (**13**, **14**, **18-23**) groups.

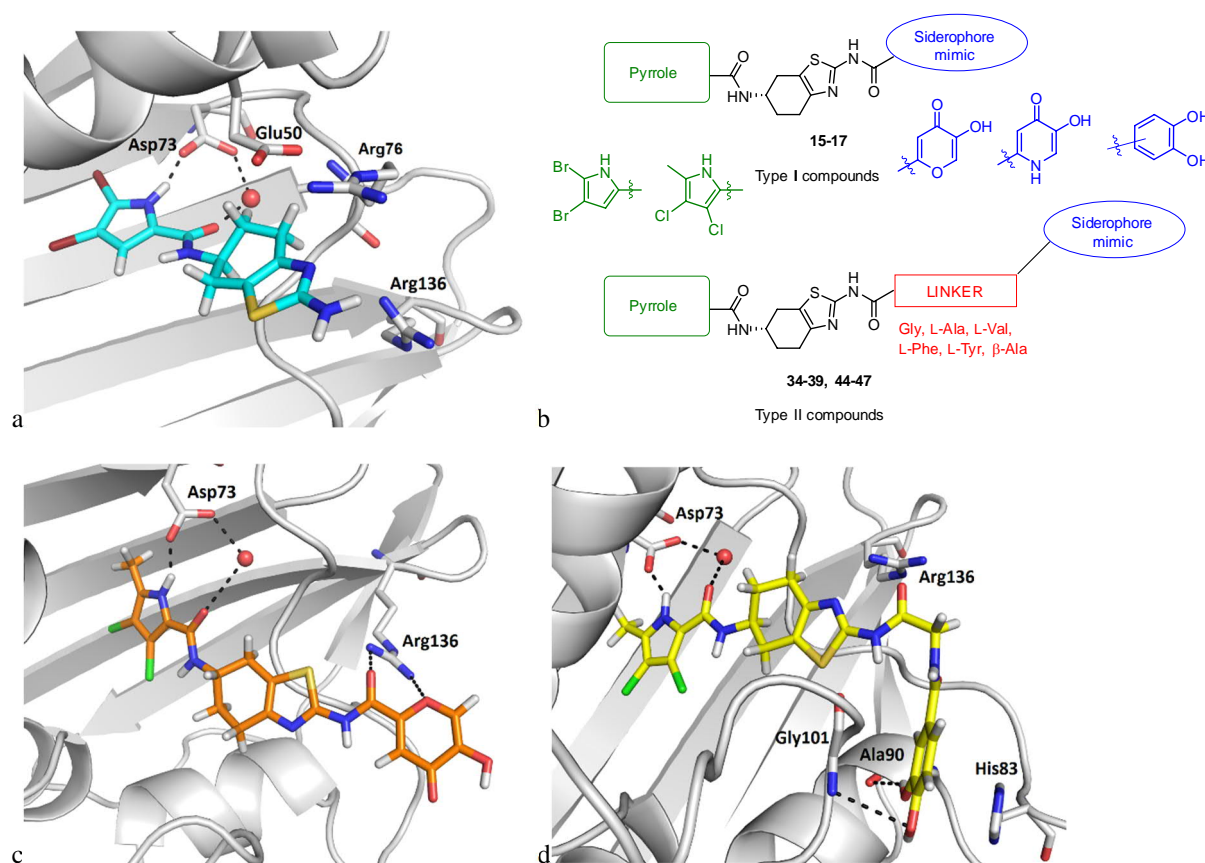
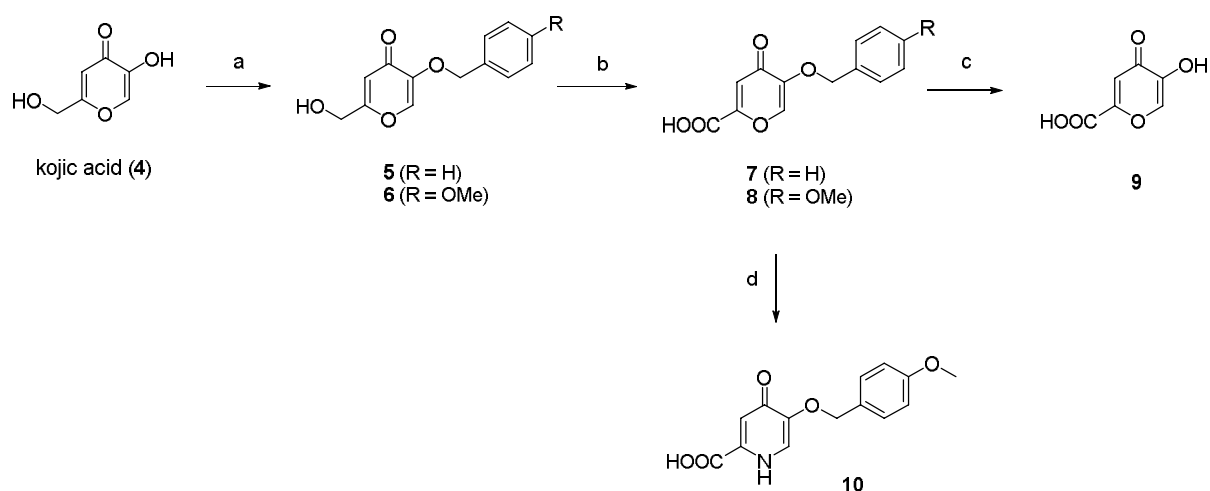


Figure 3. a) Molecular docking calculated binding mode of amine **11** (in cyan sticks) in the *E. coli* DNA gyrase ATP-binding site (PDB entry: 4DUH, in grey). b) Design of the DNA gyrase inhibitor–siderophore mimic conjugates, based on the binding mode of **11**. c, d) Docking binding modes of compounds **17** (in orange sticks) and **34** (in yellow sticks) in the *E. coli* DNA gyrase ATP-binding site (in grey). For clarity, only selected amino acid residues are presented as sticks. Conserved water molecule is presented as a red sphere. Hydrogen bonds are presented as black dashed lines.

3. Chemistry

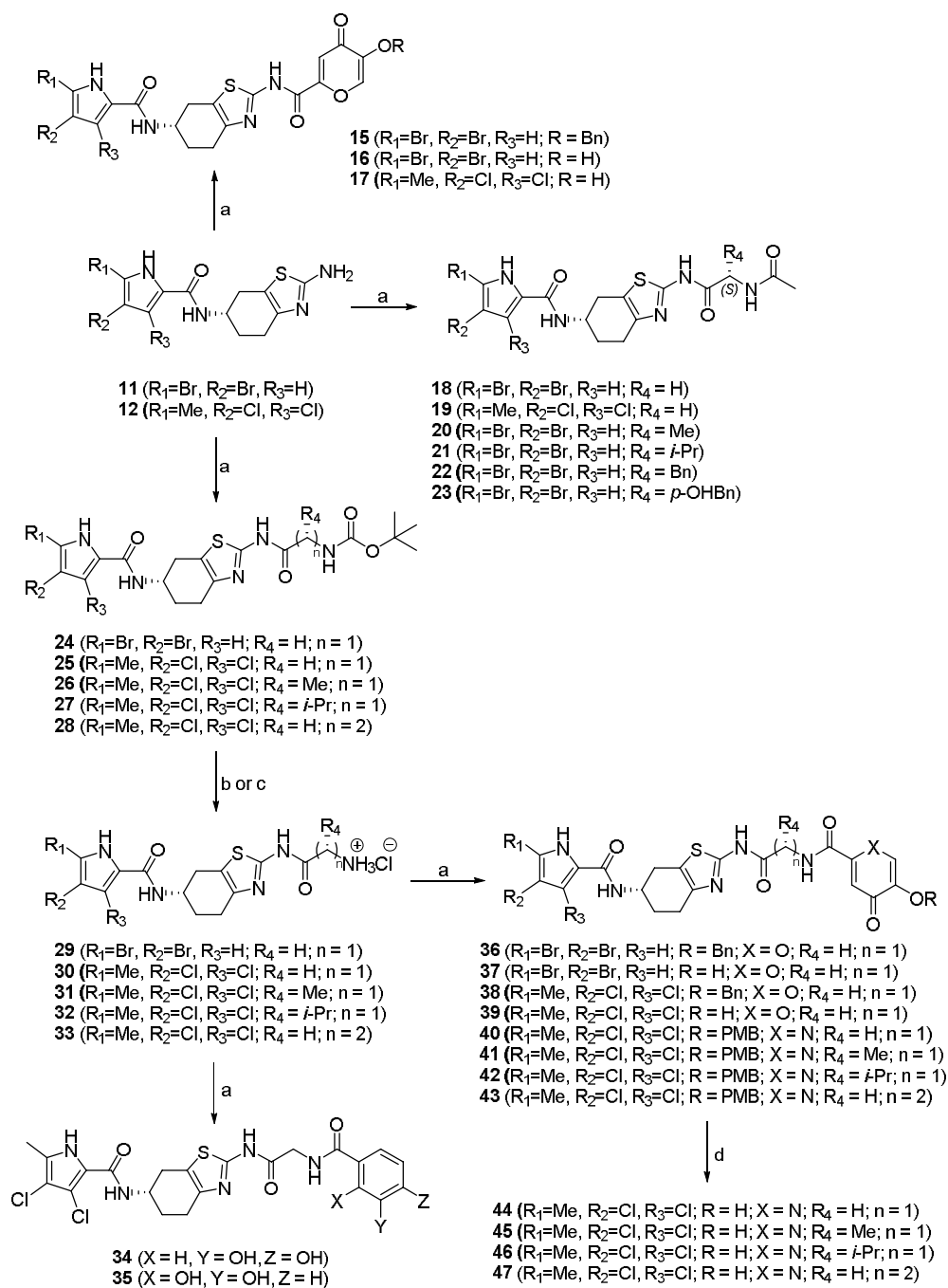
The synthesis of the siderophore mimics was performed starting from kojic acid (Scheme 1, **4**). First, the hydroxyl group directly attached to the ring was protected with either benzyl or *para*-methoxybenzyl functionality using benzyl bromide or 4-methoxybenzyl chloride under alkaline conditions, to obtain compounds **5** and **6**. Subsequent oxidation of the aliphatic hydroxyl group with Jones reagent (chromium trioxide in sulfuric acid) yielded compounds **7** and **8**. The removal of the *O*-benzyl group of **7** with catalytic hydrogenation using palladium on activated charcoal as catalyst resulted in siderophore mimic **9**, and treating **8** with 25% aqueous ammonia gave compound **10**.



Scheme 1. *Reagents and conditions.* (a) For **5**: benzyl bromide, 10 M NaOH, MeOH, 80 °C, overnight; for **6**: 4-methoxybenzyl chloride, K₂CO₃, DMF, 50 °C, 4 h. (b) CrO₃/ H₂SO₄, acetone, 30 min at -5 °C, then 3 h at 20 °C. (c) H₂, Pd/C, abs. EtOH, 20 °C, 60 min. (d) 25% NH₃ (aq), 80 °C, 4 h.

All of these final compounds were synthesized from the parent (*S*)-4,5,6,7-tetrahydrobenzo[*d*]thiazol-6-yl-1*H*-pyrrole-2-carboxamides **11** and **12** (Scheme 2), which were obtained according to previously reported procedures [10]. Also, acetamides **13** and **14** (Table 1) were obtained as reported previously [10]. Hydroxypyranone siderophore mimics in the form

of carboxylic acids and either *O*-benzyl protected or not (**7**, **9**) were coupled to the 2-amino group of **11** and **12** by 1-ethyl-3-(3-(dimethylamino)propyl)-carbodiimide (EDC)/ 1-hydroxybenzotriazole (HOBt)-promoted amide bond formation, to yield compounds **15-17**. In the same manner, compounds **18-23** were prepared using *N*-acetylated amino acids (Gly, L-Ala, L-Val, L-Phe, L-Tyr) and compounds **24-28**, using *N*-Boc-protected amino acids (Gly, L-Ala, L-Val, β -Ala). Removal of the Boc protecting group was performed with 4 M HCl in 1,4-dioxane or acetyl chloride in methanol, to obtain compounds **29-33**, which were used in another EDC/HOBt coupling to prepare analogs **34-43**. Finally, removal of the *para*-methoxybenzyl protection group from compounds **40-43** with 1 M HCl in acetic acid resulted in compounds **44-47**.



Scheme 2. Reagents and conditions. (a) For **15-17**: hydroxypyranone acid **7** or **9**; for **18-23** corresponding *N*-acetylated amino acid derivative; for **24-28** corresponding *N*-Boc-protected amino acid derivative; for **34**: 3,4-dihydroxybenzoic acid; for **35**: 2,3-dihydroxybenzoic acid; for **36-43**: corresponding hydroxypyranone acid **7** or **9** or hydroxypyridone acid **10**; EDC, HOBT, NMM, DMF, 0 °C, then 20 °C, overnight, except 60 h for **15** and **25**, 96 h for **17** and 72 h for **40**; additional heating 5 h at 60 °C for **16**. (b) **24**, acetyl chloride, MeOH, 90 min, 0 °C; then 20 °C, 18 h. (c) Corresponding *N*-Boc-protected compounds **25-28**, 4 M HCl in 1,4-dioxane, 20 °C, 16 h. (d) Corresponding 4-methoxybenzyl-protected compounds **40-43**, 1 M HCl in acetic acid, 20 °C, 16 h.

4. Results and Discussion

4.1 *In vitro* enzyme inhibition

In total, 23 compounds (**15-23**, **34-47**) were synthesized and tested in the DNA gyrase supercoiling assay to determine their *in vitro* inhibitory activities against *E. coli* DNA gyrase. These data are presented in Figures 4 and 5, and Tables S1 and S2 as IC₅₀ values.

Overall, 12 of the compounds showed *E. coli* DNA gyrase inhibitory activities with IC₅₀ <1 μM, with seven of these at <0.2 μM. Six of these seven were more potent inhibitors than the positive control novobiocin (IC₅₀, 0.17 μM): **19**, **20**, **21**, **34**, **35** and **39**. For the synthesized GyrB inhibitors bearing a siderophore mimic, six of 17 showed IC₅₀ against *E. coli* DNA gyrase <0.5 μM, with the most potent compound **34** with an IC₅₀ of 0.058 μM (Figure 5, Table S2). Moreover, this IC₅₀ for **34** is comparable to that of the oxalyl acid **1** (Figure 2), which is one of the most potent 4,5,6,7-tetrahydrobenzo[*d*]thiazole-based DNA gyrase inhibitors described to date [10].

The *E. coli* DNA gyrase inhibition was improved by acylation of the 2-amino group of the central scaffold (Figure 4, Table S1), as the acetamides **13** and **14** (IC₅₀, 0.15 μM, 0.48 μM, respectively) were more potent than their free amino counterparts **11** and **12** (IC₅₀, >10 μM). The same was seen for the acetamides **18** and **19** and the amines **29** and **30** with glycine as the linker (Figure 4, Table S1). Amino acids with small side chains as linkers (Gly, L-Ala, L-Val, β-Ala) were well tolerated (IC₅₀, 0.10-0.52 μM for **18-21**), while bulkier side chains in the linkers (L-Phe, L-Tyr) led to a loss of activity (IC₅₀, 7.0 μM, 2.8 μM for **22**, **23**, respectively). Therefore, only DNA gyrase inhibitors with non-aromatic amino acids as linkers were considered for the synthesis of the conjugates.

In the type **I** compounds (Figure 5, Table S2), the dibromopyrrole analog **16** (IC₅₀, 0.18 μM) was significantly more potent than its dichloromethylpyrrole counterpart **17** (IC₅₀, 2.1

μM). The attached hydroxypyranone siderophore mimic did not affect the binding, as starting compound **13** (IC_{50} , 0.15 μM) and its conjugate analog **16** had comparable IC_{50} values. Furthermore, the additional benzyl group in **15** (IC_{50} , 3.4 μM) largely reduced the affinity for *E. coli* DNA gyrase, which was also observed in the type **II** compounds **36** and **38** (Figure 5, Table S2, IC_{50} , 2.0 μM , 2.1 μM , respectively). Catechol-based conjugates **34** (IC_{50} , 0.058 μM) and **35** (IC_{50} , 0.11 μM) with a glycine linker were more potent *E. coli* DNA gyrase inhibitors than the hydroxypyranone **37** (IC_{50} , 0.69 μM) and the hydroxypyridinone **44** (IC_{50} , 1.6 μM) and had comparable activities to the hydroxypyranone conjugate **39** (IC_{50} , 0.090 μM). Increasing the linker length of **44** in the β -Ala analog **47** (IC_{50} , 0.35 μM) improved the DNA gyrase inhibition. Moreover, introduction of a methyl (**45**; IC_{50} , 0.26 μM) or *i*-Pr (**46**; IC_{50} , 0.64 μM) group into the linker also increased the DNA gyrase inhibitory activities.

Figure 4. Enzyme inhibition data of the (*S*)-4,5,6,7-tetrahydrobenzo[*d*]thiazol-6-yl-1*H*-pyrrole-2-carboxamide-based compounds against *Escherichia coli* DNA gyrase.

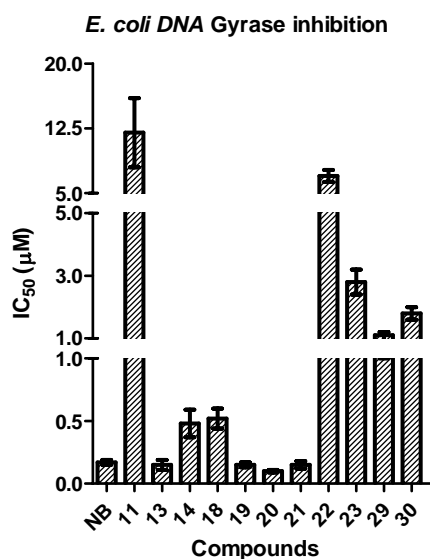
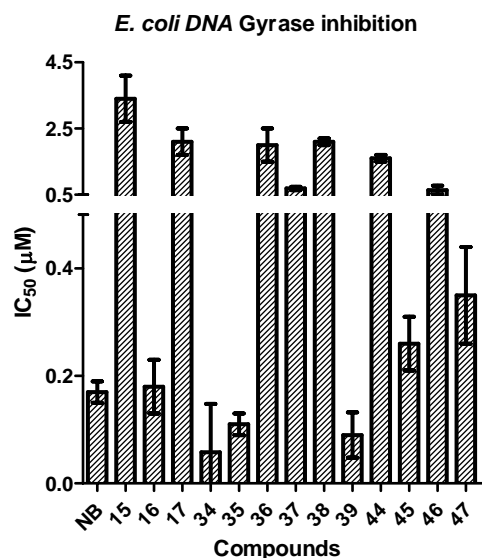


Figure 5. Enzyme inhibition data of DNA gyrase inhibitor – siderophore mimic conjugates against *Escherichia coli* DNA gyrase.



4.2 Antibacterial activities

All of these compounds were evaluated for their *in vitro* antibacterial activities against two Gram-positive (*Enterococcus faecalis* ATCC 29212, *S. aureus* ATCC 25923 or 29213) and two Gram-negative (*E. coli* ATCC 25922, *P. aeruginosa* ATCC 27853) bacterial strains. In addition, they were tested against two *E. coli* mutant strains: JD17464, as an *lpxC* deletion mutant with an impaired outer membrane; and JW5503, as a *tolC* deletion mutant with a defective efflux pump. Preliminary tests were performed at 50 µM, and growth inhibition was measured after 24 h incubation. These data are presented in Figures S1 and S2 in the Supplementary Information. MICs were determined in dose-response assays for compounds that showed >90% growth in the preliminary assay (Table S3) [27]. The compounds containing the siderophore mimics were evaluated also against *E. coli* (ATCC 25922), *P. aeruginosa* (ATCC 27853) and *A. baumannii* (ATCC 19606) in cation-adjusted Mueller-Hinton broth (CAMHB) as iron-depleted (ID-CAMHB) or when supplemented with iron, to determine the effects of the attached siderophore mimics on the antibacterial activities in iron depleted conditions. These data are presented in Table S4 in the Supplementary Information as

percentages of bacterial growth inhibition at 50 μ M of the tested compounds and in Figure 6. Data of growth inhibition for non-conjugated compounds **13**, **14**, **18**, **20**, **21** and **29** against *E. coli* ATCC 25922, in CAMHB and ID-CAMHB, are also shown in Table S4. Since there is no difference in activity, any possible direct effect due to different culture medium composition can be excluded.

These antibacterial activity assays revealed activity of compounds **30** and **35** against the Gram-positive bacterial strain of *E. faecalis* with MICs of 11 μ g/mL and 14 μ g/mL, respectively. On the other hand, tested compounds were generally inactive against the wild-type Gram-negative bacterial strains in iron-supplemented medium. However, weak correlations between *in vitro* inhibitory activities and antibacterial properties have also been reported previously for other structural classes of DNA gyrase B inhibitors [8]. In addition, the inhibitory activities here in the iron-depleted medium were generally also weak against all of the bacterial strains tested, with only two compounds (**45**, **46**) showing >50% growth inhibition against *A. baumannii* (Figure 6). For compounds **35**, **44**, **45** and **47** we observed an opposite effect on bacterial growth of *P. aeruginosa*, since they showed a drop in growth inhibition in iron-supplemented compared to iron-depleted medium. Several groups have investigated the effect of introducing siderophores mimics into the structure of fluoroquinolones, well-known DNA gyrase inhibitors, but the activities of most of these conjugates were also not greater compared to those of the parent antibiotics, or in many cases activities were even lost [28].

However, increases in the inhibitory effects were seen for iron-depleted *versus* iron-supplemented media for almost all of the compounds tested against wild-type *E. coli*, presumably as a consequence of the attached siderophore mimics. Moreover, inhibition against the Δ tolC *E. coli* JW5503 strain was seen (Supplementary Figures S1, S2 and Table S3). For this *E. coli* mutant with a defective efflux pump, the most potent bacterial growth inhibition was for compound **19** with an MIC of 1 μ g/mL. Among the siderophore mimic conjugates, the

most promising activities were shown by the catechol derivatives **34** and **35**, with MICs of 14 $\mu\text{g/mL}$ against the ΔtolC *E. coli* JW5503 strain, which is more effective than for the best compounds from the first generation 4,5,6,7-tetrahydrobenzo[*d*]thiazoles [10]. In contrast, none of the tested compounds showed significantly improved antibacterial activity against ΔlpxC *E. coli* JD17464 compared to wild-type strain. These data suggest that efflux problems, but not cell wall penetration, remain the issue in terms of the weak antibacterial activities of the 4,5,6,7-tetrahydrobenzo[*d*]thiazole derivatives.

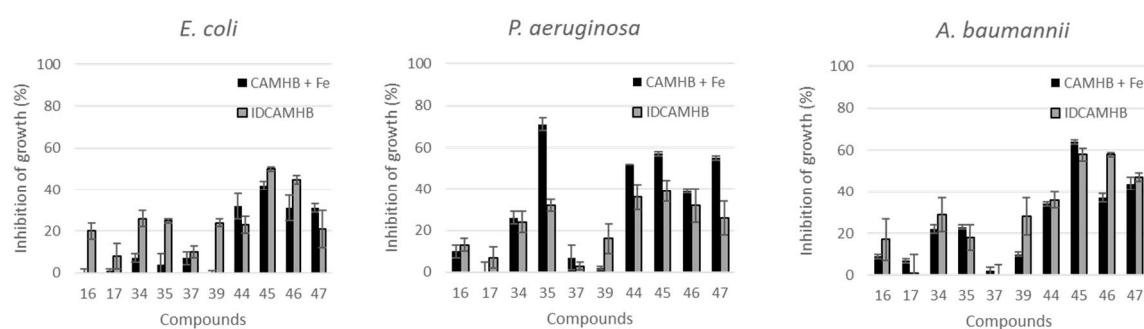


Figure 6. Antibacterial activity of DNA gyrase B inhibitor-siderophore mimic conjugates against *E. coli*, *P. aeruginosa* and *A. baumannii* in iron-depleted (ID-CAMHB) and iron-supplemented CAMHB media at 50 μM concentration. Cefiderocol MICs in CAMHB were 0.25, 1.0, and 2.0 $\mu\text{g/mL}$, and in ID-CAMHB 0.25, 0.5 and 0.25 $\mu\text{g/mL}$ against *E. coli*, *P. aeruginosa* and *A. baumannii*, respectively (complying with approved CLSI values) [29]. Ceftazidime was used as a negative control and MICs were 0.25, 2, and > 4 $\mu\text{g/mL}$ both in CAMHB and ID-CAMHB against *E. coli*, *P. aeruginosa* and *A. baumannii*, respectively.

Recent studies revealed that not only siderophore-mimic moieties, but also other groups present in the molecule could contribute to iron chelation [30, 31]. For example, BAL30072 (Figure 1) has been found to form compact complex in solution comprising two BAL30072 molecules and one Fe^{3+} ion. In this complex sulfate group of BAL30072 participates as a chelating functionality in addition to the dihydroxypyridone moiety [30]. In another study with (pre)acinetobactin, a siderophore secreted by *A. baumannii*, the same ligand to metal stoichiometry in the solution was found to be favorable in low iron conditions and such complex

is readily recognized and transported by the outer membrane (OM) transporter into the periplasm of *A. baumannii*. Interestingly, only one oxygen from a catechol moiety of preacinetobactin participates in complex formation, together with three other atoms in the scaffold [31]. Thus, more focused investigation of the interactions of our DNA gyrase inhibitor–siderophore mimic conjugates with Fe^{3+} is required in the future to completely elucidate stoichiometry of these complexes as well as to identify functional groups responsible for iron chelation. Moreover, since the interactions with the OM transporters also play a key role in circumventing poor permeation in Gram-negative bacteria, further studies on affinity and binding mode of our conjugates in OM transporters are needed, such as recently published study on enterobactin-iron complex with *P. aeruginosa* OM transporter PfeA [32]. Inappropriate shape and size of our conjugates and consequentially their poor affinity toward OM transporters might be a reason for only slight improvements in antibacterial activities in iron-depleted *versus* iron-supplemented media against tested wild-type Gram-negative bacterial strains. Moreover, the solving of the efflux problems should be considered as equally important to achieve improved antibacterial activities against Gram-negative bacterial strains.

5. Conclusion

These new 4,5,6,7-tetrahydrobenzo[*d*]thiazole derivatives conjugated with three types of siderophore mimics were designed, synthesized and evaluated in biological assays. *In vitro* enzyme inhibition of *E. coli* DNA gyrase revealed that compounds **34** and **35**, which include a catechol siderophore mimic moiety, are more potent inhibitors than the positive control novobiocin, with IC_{50} in the low nanomolar range ($<0.2 \mu\text{M}$). The most potent among all of the compounds tested was **34**, with IC_{50} of $0.058 \mu\text{M}$, which is comparable to the best 4,5,6,7-tetrahydrobenzo[*d*]thiazole-based DNA gyrase inhibitors described to date [10]. This shows

that it is possible to design potent DNA gyrase inhibitor–siderophore mimic conjugates with non-cleavable linkers. *In vitro* antibacterial assays showed no significant activities against wild-type Gram-negative bacterial strains. For the efflux pump mutant strain, both of these potent catechol mimic conjugates **34** and **35** showed a MIC of 14 $\mu\text{g}/\text{mL}$ against *E. coli* JW5503, demonstrating that active efflux together with permeability remains the issue for these compounds. Both **34** and **35** also showed minor improvements in their antibacterial activities against wild-type *E. coli* in iron-depleted medium. Therefore, the use of catechols as siderophore mimics appears to be a promising approach for further investigations into DNA gyrase inhibitor–siderophore mimic conjugates with sufficient antibacterial activity against wild-type Gram-negative bacterial strains.

6. Experimental Section

6.1 Materials and Methods

The chemicals were obtained from Acros Organics (Geel, Belgium), Sigma-Aldrich (St. Louis, MO, USA), TCI Europe N.V. (Zwijndrecht, Belgium) and Apollo Scientific (Stockport, UK), and were used without further purification. Analytical TLC was performed on silica gel Merck 60 F₂₅₄ plates (0.25 mm), with visualization with UV light and spray reagents. Column chromatography was carried out on silica gel 60 (particle size, 240-400 mesh). HPLC analyses were performed on: (i) an Agilent Technologies 1100 instrument with a UV-VIS detector (G1365B), a thermostat (G1316A), an autosampler (G1313A) and a C18 column (Eclipse Plus; 5 μm , 4.6 \times 150 mm; Agilent); (ii) a Thermo Scientific Dionex Ultimate 3000 Binary Rapid Separation LC System (Thermo Fisher Scientific, Waltham, MA, USA) with an autosampler, a binary pump system, a photodiode array detector, a thermostated column compartment and a C18 column (Zorbax Extend; 3.5 μm , 4.6 \times 150 mm; Agilent). The following gradient elution

was used with mobile phases A (0.1% trifluoroacetic acid in water) and B (acetonitrile): 0-16 min, 95%-5% A; 16-21 min, 5% A. The flow rate was 1.0 mL/min, and the injection volume was 20 μ L. All of the tested compounds were \geq 95% pure by HPLC. Melting points were determined on a Reichert hot-stage microscope, and are uncorrected. ^1H and ^{13}C NMR spectra were recorded at 400 MHz and 100 MHz, respectively, on a spectrometer (AVANCE III 400; Bruker Corporation, Billerica, MA, USA) in DMSO- d_6 or CDCl_3 solutions, with TMS as the internal standard. Mass spectra were obtained using Advion expression CMS mass spectrometer (Advion Inc., Ithaca, USA) and high resolution mass spectra were obtained using a Q-TOF Premier mass spectrometer (Micromass, Waters, Manchester, UK) or an Exactive Plus Orbitrap mass spectrometer (Thermo Fischer Scientific Inc., Waltham, MA, USA). Optical rotations were measured on a polarimeter (241 MC; Perkin-Elmer). The reported values for specific rotation were the means of five successive measurements, using an integration time of 5 s.

6.2 Synthesis

6.2.1 Synthesis of siderophore mimics

Siderophore mimics were synthesized according to the reported procedures [33, 34].

6.2.1.1 General procedure A. Chromium trioxide (2.8 mmol) was suspended in water (1 mL) and concentrated sulfuric acid (0.3 mL) was added dropwise on an ice bath. The mixture was quantitatively introduced into a solution of corresponding alcohol (1 mmol), which was previously dissolved in acetone (10 mL) with additional heating and then cooled on an ice bath. Reaction mixture was stirred for 30 min at 0 $^\circ\text{C}$ and then for 3 h at room temperature. The precipitate was filtered off through a layer of Celite and mother liquid was evaporated under reduced pressure. Water (2 mL) was added to the residue and precipitate formed was filtered off and dried at 40 $^\circ\text{C}$.

6.2.1.1.1 5-(Benzyloxy)-2-(hydroxymethyl)-4H-pyran-4-one (**5**). Kojic acid (10.0 g, 70.4 mmol) was suspended in methanol (80 mL) and 10 M NaOH (7.74 mL, 77.4 mmol) was added. Then benzyl bromide (9.61 mL, 80.9 mmol) was added dropwise and reaction mixture was stirred at 80 °C overnight. Reaction mixture was allowed to cool to room temperature and solvent was evaporated under reduced pressure. Acetone (12 mL) and water (120 mL) were added to the crude residue and precipitate was formed, which was filtered off and dried at 40 °C. Yield 16.845 g (99.0 %); yellow solid; m. p. 123-125 °C; ¹H NMR (400 MHz, CDCl₃) δ 4.48 (s, 2H, CH₂), 5.08 (s, 2H, CH₂), 6.57 (s, 1H, pyran-H), 7.31-7.42 (m, 5H, Ar-H), 7.56 (s, 1H, pyran-H) ppm, signal for OH not seen in the spectrum.

6.2.1.1.2 2-(Hydroxymethyl)-5-((4-methoxybenzyl)oxy)-4H-pyran-4-one (**6**). Kojic acid (5.0 g, 35.2 mmol) and potassium carbonate (10.7 g, 77.4 mmol) were suspended in dry *N,N*-dimethylformamide (DMF) (80 mL). The round-bottom flask was filled with argon and 4-methoxybenzyl chloride (5.23 mL, 38.7 mmol) was added dropwise. Reaction mixture was stirred at 50 °C for 4 h. Then DMF was evaporated under reduced pressure and water (100 mL) was added. A precipitate was formed, which was filtered off and dried at 60 °C. Yield 8.145 g (88 %); yellow solid; m. p. 114-116 °C; ¹H NMR (400 MHz, DMSO-*d*₆) δ 3.77 (s, 3H, CH₃), 4.30 (d, 2H, *J* = 4.0 Hz, CH₂OH), 4.86 (s, 2H, CH₂), 5.75 (br s, 1H, OH), 6.32 (t, 1H, *J* = 0.9 Hz, pyran-H), 6.92-6.99 (m, 2H, Ar-H), 7.31-7.39 (m, 2H, Ar-H), 8.16 (s, 1H, pyran-H) ppm; HRMS ESI⁺ *m/z* for C₁₄H₁₅O₅ ([M+H]⁺): calcd 263.0919, found 263.0921.

6.2.1.1.3 5-(Benzyloxy)-4-oxo-4H-pyran-2-carboxylic acid (**7**). Prepared from **5** (5.0 g, 21.5 mmol) and chromium trioxide (6.02 g, 60.2 mmol) according to the general procedure A. Yield 3.437 g (65 %); yellow solid; m. p. 162 - 164 °C; ¹H NMR (400 MHz, DMSO-*d*₆) δ 4.99 (s, 2H, CH₂), 6.93 (s, 1H, pyran-H), 7.34-7.47 (m, 5H, Ar-H), 8.37 (s, 1H, pyran-H) ppm, signal for COOH not seen in the spectrum; HRMS ESI⁻ *m/z* for C₁₃H₉O₅ ([M-H]⁻): calcd 245.0450, found 245.0451.

6.2.1.1.4 *5-((4-Methoxybenzyl)oxy)-4-oxo-4H-pyran-2-carboxylic acid (8)*. Prepared from **6** (2.05 g, 7.82 mmol) and chromium trioxide (2.19 g, 21.9 mmol) according to the general procedure **A**. Precipitate was additionally washed with hot MeOH (2 × 30 mL). Yield 0.980 g (45 %); yellow solid; m. p. 165 - 167 °C; ¹H NMR (400 MHz, DMSO-*d*₆) δ 3.77 (s, 3H, CH₃), 4.90 (s, 2H, CH₂), 6.93 (s, 1H, pyran-H); 6.94-7.00 (m, 2H, Ar-H), 7.34-7.40 (m, 2H, Ar-H), 8.36 (s, 1H, pyran-H) ppm; HRMS ESI⁻ m/z for C₁₄H₁₁O₆ ([M-H]⁻): calcd 275.0556, found 275.0562.

6.2.1.1.5 *5-Hydroxy-4-oxo-4H-pyran-2-carboxylic acid (9)*. Compound **7** (0.400 g, 1.22 mmol) was dissolved in dry ethanol (80 mL) and put under argon. Then 5 % m/m of Pd/C (0.020 g) was added and reaction mixture was stirred for 1 h at room temperature under hydrogen atmosphere. Then Pd/C was filtered off and the solvent evaporated under reduced pressure. Yield 0.236 g (93 %); yellow amorphous powder; ¹H NMR (400 MHz, DMSO-*d*₆) δ 6.96 (s, 1H, pyran-H); 8.21 (s, 1H, pyran-H), 9.67 (br s, 1H, OH) ppm; HRMS ESI⁻ m/z for C₆H₃O₅ ([M-H]⁻): calcd 154.9986, found 154.9981.

6.2.1.1.6 *5-((4-Methoxybenzyl)oxy)-4-oxo-1,4-dihydropyridine-2-carboxylic acid (10)*. Compound **8** (0.390 g, 1.41 mmol) was dissolved in 25% aqueous ammonia (10 mL) and refluxed for 4 h at 80 °C. Then reaction mixture was concentrated to about 5 mL and slowly acidified with concentrated hydrochloric acid to pH = 2. Precipitate formed was filtered off and dried under reduced pressure (co-evaporation with 2 × 5 mL diethyl ether). Yield 0.325 g (84 %); white amorphous solid; ¹H NMR (400 MHz, DMSO-*d*₆) δ 3.76 (s, 3H, CH₃), 5.12 (s, 2H, CH₂), 6.96 (m, 2H, Ar-H), 7.24 (br s, 1H, pyridine-H), 7.39 (m, 2H, Ar-H), 7.93 (br s, 1H, pyridine-H) ppm, signals for NH and COOH not seen in the spectrum; HRMS ESI⁻ m/z for C₁₄H₁₂NO₅ ([M-H]⁻): calcd 274.0715, found 274.0723.

6.2.2 Synthesis of compounds

6.2.2.1 General procedure B. A solution of carboxylic acid (1 mmol) in *N,N*-dimethylformamide (10 mL) was cooled to 0 °C and then EDC (1.2 mmol) and HOBT (1.3 mmol) were added. pH was adjusted to 8 with *N*-methylmorpholine and the reaction mixture stirred for 20 min at 0 °C. Then amine (1 mmol) was added and reaction mixture stirred overnight at room temperature. The solvent was evaporated *in vacuo* and the residue dissolved in ethyl acetate (30 mL) and washed successively with 1 % citric acid (2 × 30 mL), saturated aqueous NaHCO₃ solution (2 × 30 mL), and brine (30 mL). The organic phase was dried over Na₂SO₄, filtered and solvent evaporated under reduced pressure.

6.2.2.1.1 *(S)*-*N*-(2-(5-(Benzyloxy)-4-oxo-4*H*-pyran-2-carboxamido)-4,5,6,7-tetrahydrobenzo[*d*]thiazol-6-yl)-4,5-dibromo-1*H*-pyrrole-2-carboxamide (**15**). Prepared from **11** (0.300 g, 0.714 mmol) and **7** (0.176 g, 0.714 mmol) according to the general procedure **B**. Product was purified by flash column chromatography using dichloromethane/methanol (15:1) as eluent. Yield 0.094 g (20 %); yellow solid; m. p. 168 - 170 °C; [α]_D+32.8 (*c* 0.19, DMF); ¹H NMR (400 MHz, DMSO-*d*₆) δ 1.83-1.94 (m, 1H, H_A-7), 1.95-2.08 (m, 1H, H_B-7), 2.57-2.66 (m, 1H, H_A-5), 2.70-2.78 (m, 2H, H_B-5, H_A-4), 2.94-3.06 (m, 1H, H_B-4), 4.16-4.31 (m, 1H, CHNH), 5.02 (s, 2H, OCH₂), 7.01 (d, 1H, *J* = 2.6 Hz, pyrrole-H), 7.10 (s, 1H, pyran-H), 7.35-7.49 (m, 5H, Ar-H), 8.12 (d, 1H, *J* = 7.8 Hz, CHNH), 8.33 (s, 1H, pyran-H), 12.72 (d, 1H, *J* = 2.5 Hz, pyrrole-NH) ppm; ¹³C NMR (100 MHz, DMSO-*d*₆) δ 27.8, 70.1, 97.2, 104.0, 112.4, 114.7, 127.4, 127.7, 127.9, 135.3, 140.3, 147.5, 157.8 ppm; HRMS ESI⁻ *m/z* for C₂₅H₁₉Br₂N₄O₅S ([M-H]⁻): calcd 644.9443, found 644.9439; HPLC: t_r 13.15 min (95 % at 254 nm).

6.2.2.1.2 *(S)*-4,5-Dibromo-*N*-(2-(5-hydroxy-4-oxo-4*H*-pyran-2-carboxamido)-4,5,6,7-tetrahydrobenzo[*d*]thiazol-6-yl)-1*H*-pyrrole-2-carboxamide (**16**). Prepared from **11** (0.300 g, 0.714 mmol) and **9** (0.111 g, 0.714 mmol) according to the general procedure **B**. After addition of 10 % citric acid and ethyl acetate, precipitate was formed, which was filtered off and dried.

Crude residue was suspended in a small volume of ethyl acetate, heated until boiling and filtered off. Product was dried in *vacuo*. Yield 0.044 g (11 %); brown amorphous solid; $[\alpha]_D +41.5$ (*c* 0.20, DMF); ^1H NMR (400 MHz, DMSO-*d*₆) δ 1.81-1.96 (m, 1H, H_A-7), 1.96-2.07 (m, 1H, H_B-7), 2.60-2.80 (m, 3H, H-5, H_A-4), 3.00 (m, 1H, H_B-4), 4.16-4.29 (m, 1H, CHNH), 7.01 (d, 1H, *J* = 2.4 Hz, pyrrole-H), 7.12 (s, 1H, pyran-H), 8.12 (d, 1H, *J* = 7.6 Hz, CHNH), 8.18 (s, 1H, pyran-H), 9.62 (s, 1H, OH), 12.72 (d, 1H, *J* = 2.4 Hz, pyrrole-NH) ppm; ^{13}C NMR (100 MHz, DMSO-*d*₆) δ 27.9, 28.4, 44.9, 97.8, 104.6, 113.0, 114.1, 128.0, 139.7, 147.5, 158.4, 173.7 ppm; HRMS ESI⁻ *m/z* for C₁₈H₁₃Br₂N₄O₅S ([M-H]⁻): calcd 554.8968, found 554.8984; HPLC: *t*_r 10.77 min (95 % at 254 nm).

6.2.2.1.3 (*S*)-3,4-Dichloro-*N*-(2-(5-hydroxy-4-oxo-4*H*-pyran-2-carboxamido)-4,5,6,7-tetrahydrobenzo[*d*]thiazol-6-yl)-5-methyl-1*H*-pyrrole-2-carboxamide (**17**). Prepared from **12** (0.126 g, 0.365 mmol) and **9** (0.057 g, 0.365 mmol) according to the general procedure **B**. After addition of 10% citric acid, precipitate was formed, which was filtered off and washed with ethyl acetate (3 × 10 mL) and hot methanol (3 × 1 mL). Yield 0.030 g (17 %); brown amorphous solid; $[\alpha]_D -17.7$ (*c* 0.19, DMSO); ^1H NMR (400 MHz, DMSO-*d*₆) δ 1.90-2.11 (m, 2H, H-7), 2.19 (s, 3H, CH₃), 2.65-2.84 (m, 3H, H-5, H_A-4), 3.02 (d, 1H, *J*₁ = 14.1 Hz, H_B-4), 4.20-4.35 (m, 1H, CHNH), 7.12 (s, 1H, pyran-H), 7.39 (d, 1H, *J* = 7.9 Hz, CHNH), 8.18 (s, 1H, pyran-H), 9.63 (s, 1H, OH), 12.02 (s, 1H, pyrrole-NH) ppm; ^{13}C NMR (100 MHz, DMSO-*d*₆) δ 10.7, 27.5, 28.3, 44.9, 108.0, 110.0, 114.1, 119.2, 127.3, 139.7, 147.5, 158.3, 173.7 ppm; HRMS ESI⁺ *m/z* for C₁₉H₁₇N₄O₅SCl₂ ([M+H]⁺): calcd 483.0291, found 483.0282; HPLC: *t*_r 11.42 min (95 % at 254 nm).

6.2.2.1.4 (*S*)-*N*-(2-(2-Acetamidoacetamido)-4,5,6,7-tetrahydrobenzo[*d*]thiazol-6-yl)-4,5-dibromo-1*H*-pyrrole-2-carboxamide (**18**). Prepared from **11** (0.200 g, 0.476 mmol) and *N*-acetylglycine (0.058 g, 0.476 mmol) according to the general procedure **B**. Product was purified by flash column chromatography using ethyl acetate to ethyl acetate/methanol (5:2) as eluent.

Yield 0.086 g (35 %); yellow solid; m. p. 196-198 °C; $[\alpha]_D -7.4$ (c 0.30, MeOH); $^1\text{H NMR}$ (400 MHz, DMSO- d_6) δ 1.83-1.91 (m, 4H, H_A-7, CH₃), 1.96-2.03 (m, 1H, H_B-7), 2.58-2.77 (m, 3H, H-5, H_A-4), 2.99 (dd, 1H, $J_1 = 15.5$ Hz, $J_2 = 5.2$ Hz, H_B-4), 3.94 (d, 2H, $J = 5.8$ Hz, CH₂NH), 4.13-4.24 (m, 1H, CHNH), 7.01 (d, 1H, $J = 2.8$ Hz, pyrrole-H), 8.11 (d, 1H, $J = 7.7$ Hz, CHNH), 8.26 (t, 1H, $J = 5.9$ Hz, CH₂NH), 11.98 (s, 1H, NHCO), 12.71 (d, 1H, $J = 2.6$ Hz, pyrrole-NH) ppm; $^{13}\text{C NMR}$ (100 MHz, DMSO- d_6) δ 22.3, 24.6, 28.4, 28.6, 41.9, 45.3, 97.8, 104.5, 112.9, 119.3, 128.0, 143.5, 155.3, 158.4, 167.9, 169.8 ppm; HRMS ESI⁻ m/z for C₁₆H₁₆Br₂N₅O₃S ([M-H]⁻): calcd 515.9341, found 515.9346; HPLC: t_r 11.48 min (99 % at 254 nm).

6.2.2.1.5 (S)-N-(2-(2-Acetamidoacetamido)-4,5,6,7-tetrahydrobenzo[d]thiazol-6-yl)-3,4-dichloro-5-methyl-1H-pyrrole-2-carboxamide (**19**). Prepared from **12** (0.150 g, 0.435 mmol) and N-acetylglycine (0.051 g, 0.435 mmol) according to the general procedure **B**. Crude product was crystallized from methanol. Yield 0.078 g (40 %); yellow solid; m. p. 168 – 171 °C; $[\alpha]_D -9.6$ (c 0.13, DMF); $^1\text{H NMR}$ (400 MHz, DMSO- d_6) δ 1.88 (s, 3H, CH₃), 1.91-2.07 (m, 2H, H-7), 2.19 (s, 3H, pyrrole-CH₃), 2.65-2.78 (m, 3H, H-5, H_A-4), 3.01 (m, 1H, H_B-4), 3.94 (d, 2H, $J = 5.8$ Hz, CH₂NH), 4.20-4.31 (m, 1H, CHNH), 7.32 (d, 1H, $J = 7.8$ Hz, CHNH), 8.27 (t, 1H, $J = 5.8$ Hz, CH₂NH), 11.99 (s, 1H, NHCO), 12.02 (s, 1H, pyrrole-NH) ppm; $^{13}\text{C NMR}$ (100 MHz, DMSO- d_6) δ 11.1, 22.8, 24.7, 28.5, 28.8, 42.4, 45.6, 108.5, 110.5, 112.6, 119.7, 127.8, 143.8, 155.8, 158.7, 168.4, 170.3 ppm; HRMS ESI⁻ m/z for C₁₇H₁₈N₅O₃SCl₂ ([M-H]⁻): calcd 442.0507, found 442.0496; HPLC: t_r 10.55 min (97 % at 254 nm).

6.2.2.1.6 N-((S)-2-((S)-2-Acetamidopropanamido)-4,5,6,7-tetrahydrobenzo[d]thiazol-6-yl)-4,5-dibromo-1H-pyrrole-2-carboxamide (**20**). Prepared from **11** (0.160 g, 0.381 mmol) and N-acetyl-L-alanine (0.050 g, 0.381 mmol) according to the general procedure **B**. Product was purified by flash column chromatography using ethyl acetate to ethyl acetate/methanol (5:2) as eluent. Yield 0.081 g (40 %); yellow solid; m. p. 160-162 °C; $[\alpha]_D +10.3$ (c 0.18, DMF); $^1\text{H NMR}$ (400 MHz, DMSO- d_6) δ 1.27 (dd, 3H, $J_1 = 7.2$ Hz, $J_2 = 1.6$ Hz, CHCH₃), 1.81-1.90 (m,

4H, H_A-7, COCH₃), 1.94-2.03 (m, 1H, H_B-7), 2.59-2.75 (m, 3H, H-5, H_A-4), 2.98 (m, 1H, H_B-4), 4.14-4.24 (m, 1H, CHNH), 4.40-4.48 (m, 1H, CHCH₃), 7.00 (d, 1H, *J* = 2.5 Hz, pyrrole-H), 8.09 (t, 1H, *J* = 7.2 Hz, CHNH), 8.25 (d, 1H, *J* = 6.8 Hz, CHNH), 11.98 (d, 1H, *J* = 1.9 Hz, pyrrole-NH), 12.70 (s, 1H, NHCO) ppm; ¹³C NMR (100 MHz, DMSO-*d*₆) δ 18.1, 22.8, 25.1, 28.8, 29.1, 45.7, 48.8, 98.3, 105.0, 113.4, 119.9, 128.6, 144.0, 155.9, 158.9, 169.8, 171.9 ppm; HRMS ESI⁻ *m/z* for C₁₇H₁₈Br₂N₅O₃S ([M-H]⁻): calcd 529.9497, found 529.9496; HPLC: *t*_r 11.77 min (97.6 % at 254 nm).

6.2.2.1.7 *N*-((*S*)-2-((*S*)-2-Acetamido-3-methylbutanamido)-4,5,6,7-tetrahydrobenzo[*d*]thiazol-6-yl)-4,5-dibromo-1*H*-pyrrole-2-carboxamide (**21**). Prepared from **11** (0.180 g, 0.428 mmol) and *N*-acetyl-L-valine (0.068 g, 0.428 mmol) according to the general procedure **B**. Product was purified by flash column chromatography using dichloromethane/methanol (20:1) as eluent. Yield 0.047 g (20 %); white solid; m. p. 180-182 °C; ¹H NMR (400 MHz, DMSO-*d*₆) δ 0.88 (t, 6H, *J* = 7.5 Hz, 2 × CH₃), 1.80-1.92 (m, 4H, H_A-7, COCH₃), 1.94-2.06 (m, 2H, H_B-7, CH(CH₃)₂), 2.59-2.74 (m, 3H, H-5, H_A-4), 2.98 (dd, 1H, *J*₁ = 14.4 Hz, *J*₂ = 5.4 Hz, H_B-4), 4.16-4.23 (m, 1H, CHNH), 4.32-4.39 (m, 1H, CHCH), 7.00 (d, 1H, *J* = 2.5 Hz, pyrrole-H), 8.08-8.13 (m, 2H, 2 × CHNH), 12.04 (s, 1H, NHCO), 12.70 (d, 1H, *J* = 2.6 Hz, pyrrole-NH) ppm; HRMS ESI⁻ *m/z* for C₁₉H₂₂Br₂N₅O₃S ([M-H]⁻): calcd 557.9810, found 557.9823; HPLC: *t*_r 12.38 min (100 % at 254 nm).

6.2.2.1.8 *N*-((*S*)-2-((*S*)-2-Acetamido-3-phenylpropanamido)-4,5,6,7-tetrahydrobenzo[*d*]thiazol-6-yl)-4,5-dibromo-1*H*-pyrrole-2-carboxamide (**22**). Prepared from **11** (0.180 g, 0.428 mmol) and *N*-acetyl-L-phenylalanine (0.089 g, 0.428 mmol) according to the general procedure **B**. Product was purified by flash column chromatography using dichloromethane/methanol (20:1) as eluent. Yield 0.023 g (9 %); white solid; m. p. 143-145 °C; [α]_D +10.3 (*c* 0.18, DMF); ¹H NMR (400 MHz, DMSO-*d*₆) δ 1.77-1.91 (m, 4H, H_A-7, COCH₃), 1.95-2.04 (m, 1H, H_B-7), 2.60-2.74 (m, 3H, H-5, H_A-4), 2.84 (dd, 1H, *J*₁ = 13.1 Hz, *J*₂ = 3.2

Hz, H_B-4), 2.95-3.06 (m, 2H, PhCH₂), 4.14-4.24 (m, 1H, CHNH), 4.68-4.74 (m, 1H, CHCH₂), 7.01 (d, 1H, *J* = 2.6 Hz, pyrrole-H), 7.18-7.31 (m, 5H, Ar-H), 8.07-8.13 (m, 1H, CHNH), 8.33 (d, 1H, *J* = 7.8 Hz, CHNH), 12.18 (s, 1H, NHCO), 12.71 (d, 1H, *J* = 1.9 Hz, pyrrole-NH) ppm; HRMS ESI⁺ *m/z* for C₂₃H₂₄Br₂N₅O₃S ([M+H]⁺): calcd 607.9961, found 607.9959; HPLC: *t*_r 13.08 min (100 % at 254 nm).

6.2.2.1.9 *N*-((*S*)-2-((*S*)-2-Acetamido-3-(4-hydroxyphenyl)propanamido)-4,5,6,7-tetrahydrobenzo[*d*]thiazol-6-yl)-4,5-dibromo-1*H*-pyrrole-2-carboxamide (**23**). Prepared from **11** (0.100 g, 0.238 mmol) and *N*-acetyl-L-tyrosine (0.053 g, 0.238 mmol) according to the general procedure **B**. Product was purified by flash column chromatography using dichloromethane/methanol (20:1) as eluent. Yield 0.037 g (25 %); white solid; m. p. 188-190 °C; [α]_D +13.2 (*c* 0.08, DMF); ¹H NMR (400 MHz, DMSO-*d*₆) δ 1.80 (s, 3H, COCH₃), 1.83-1.91 (m, 1H, H_A-7), 1.95-2.04 (m, 1H, H_B-7), 2.59-2.74 (m, 4H, H-5, H_A-4, PhCH₂-H_A), 2.87-2.92 (m, 1H, PhCH₂-H_B), 2.99 (dd, 1H, *J*₁ = 15.8 Hz, *J*₂ = 5.1 Hz, H_B-4), 4.13-4.24 (m, 1H, CHNH), 4.57-4.67 (m, 1H, CHCH₂), 6.64 (d, 2H, *J* = 8.5 Hz, Ar-H), 7.01 (dd, 1H, *J*₁ = 2.6 Hz, *J*₂ = 1.1 Hz, pyrrole-H), 7.07 (d, 2H, *J* = 8.5 Hz, Ar-H), 8.10 (dd, 1H, *J*₁ = 7.4 Hz, *J*₂ = 2.1 Hz, CHNH), 8.25 (d, 1H, *J* = 7.8 Hz, CHNH), 9.21 (d, 1H, *J* = 1.1 Hz, OH), 12.11 (s, 1H, NHCO), 12.70 (d, 1H, *J* = 2.7 Hz, pyrrole-NH) ppm; ¹³C NMR (100 MHz, DMSO-*d*₆) δ 22.8, 25.1, 28.9, 37.1, 45.7, 55.0, 98.3, 105.0, 113.4, 115.4, 119.9, 127.8, 128.5, 130.6, 144.0, 155.7, 156.4, 158.9, 169.9, 170.9 ppm; HRMS ESI⁻ *m/z* for C₂₃H₂₂Br₂N₅O₄S ([M-H]⁻): calcd 621.9759, found 621.9741; HPLC: *t*_r 12.19 min (97.6 % at 254 nm).

6.2.2.1.10 *tert*-Butyl (*S*)-(2-((6-(4,5-dibromo-1*H*-pyrrole-2-carboxamido)-4,5,6,7-tetrahydrobenzo[*d*]thiazol-2-yl)amino)-2-oxoethyl)carbamate (**24**). Prepared from **11** (0.918 g, 2.19 mmol) and *N*-Boc-glycine (0.383 g, 2.19 mmol) according to the general procedure **B**. Product was purified by flash column chromatography using dichloromethane/methanol (20:1) as eluent. Yield 0.672 g (53 %); yellow solid; m. p. 156-158 °C; [α]_D -2.96 (*c* 0.15, MeOH);

^1H NMR (400 MHz, DMSO- d_6) δ 1.35 (s, 9H, 3 \times CH₃), 1.79-1.93 (m, 1H, H_A-7), 1.95-2.04 (m, 1H, H_B-7), 2.57-2.76 (m, 3H, H-5, H_A-4), 2.98 (dd, 1H, $J_1 = 15.6$ Hz, $J_2 = 4.9$ Hz, H_B-4), 3.81 (d, 2H, $J = 6.2$ Hz, CH₂NH), 4.12-4.26 (m, 1H, CHNH), 7.00 (d, 1H, $J = 1.9$ Hz, pyrrole-H), 7.14 (t, 1H, $J = 6.1$ Hz, CH₂NH), 8.10 (d, 1H, $J = 7.7$ Hz, CHNH), 11.94 (s, 1H, NHCO), 12.70 (s, 1H, pyrrole-NH) ppm; ^{13}C NMR (100 MHz, DMSO- d_6) δ 24.6, 28.1, 28.4, 28.6, 42.9, 45.2, 78.2, 97.8, 104.5, 112.9, 119.2, 128.0, 143.5, 155.3, 155.8, 158.4, 168.2 ppm; HRMS ESI⁻ m/z for C₁₉H₂₂Br₂N₅O₄S ([M-H]⁻): calcd 573.9759, found 573.9752; HPLC: t_r 13.23 min (96 % at 254 nm).

6.2.2.1.11 *tert*-Butyl (*S*)-(2-((6-(3,4-dichloro-5-methyl-1*H*-pyrrole-2-carboxamido)-4,5,6,7-tetrahydrobenzo[*d*]thiazol-2-yl)amino)-2-oxoethyl)carbamate (**25**). Prepared from **12** (0.220 g, 0.637 mmol) and *N*-Boc-glycine (0.112 g, 0.637 mmol) according to the general procedure **B**. Yield 0.128 g (40 %); yellow amorphous solid; $[\alpha]_D +3.3$ (c 0.43, DMF); ^1H NMR (400 MHz, DMSO- d_6) δ 1.30 and 1.39 (2 \times s, 9H, 3 \times CH₃), 1.89-2.07 (m, 2H, H-7), 2.18 (s, 3H, pyrrole-CH₃), 2.66-2.77 (m, 3H, H-5, H_A-4), 3.02 (dd, 1H, $J_1 = 15.9$ Hz, $J_2 = 5.0$ Hz, H_B-4), 3.81 (d, 2H, $J = 6.1$ Hz, CH₂NH), 4.21-4.32 (m, 1H, CHNH), 7.14 (t, 1H, $J = 6.1$ Hz, CH₂NH), 7.32 (d, 1H, $J = 7.8$ Hz, CHNH), 11.95 (s, 1H, NHCO), 12.02 (s, 1H, pyrrole-NH) ppm; ^{13}C NMR (100 MHz, DMSO- d_6) δ 10.6, 24.1, 27.9, 28.1, 28.2, 42.9, 45.1, 78.1, 107.9, 109.8, 119.0, 119.1, 127.3, 143.3, 155.3, 155.8, 158.1, 168.1 ppm; HRMS ESI⁺ m/z for C₂₀H₂₆N₅O₄SCl₂ ([M+H]⁺): calcd 502.1077, found 502.1074; HPLC: t_r 11.09 min (97.7 % at 254 nm).

6.2.2.1.12 *tert*-Butyl ((*S*)-1-(((*S*)-6-(3,4-dichloro-5-methyl-1*H*-pyrrole-2-carboxamido)-4,5,6,7-tetrahydrobenzo[*d*]thiazol-2-yl)amino)-1-oxopropan-2-yl)carbamate (**26**). Prepared from **12** (0.301 g, 0.872 mmol) and *N*-Boc-L-alanine (0.165 g, 0.872 mmol) according to the general procedure **B**. Product was purified by flash column chromatography using dichloromethane/methanol (20:1) as eluent. Yield 0.216 g (48 %); brown solid; m. p. 142-144 °C; $[\alpha]_D -23.5$ (c 0.19, DMF); ^1H NMR (400 MHz, DMSO- d_6) δ 1.18-1.30 (m, 4H, CH₃), 1.38

(s, 8H, CH₃), 1.89-2.07 (m, 2H, H-7), 2.19 (s, 3H, pyrrole-CH₃), 2.66-2.77 (m, 3H, H-5, H_A-4), 3.01 (dd, 1H, $J_1 = 15.9$ Hz, $J_2 = 5.1$ Hz, H_B-4), 4.15-4.32 (m, 2H, 2 × CHNH), 7.22 (d, 1H, $J = 7.1$ Hz, COCHNH), 7.34 (d, 1H, $J = 7.7$ Hz, CHNH), 11.96 (s, 1H, NHCO), 12.01 (s, 1H, pyrrole-NH) ppm; ¹³C NMR (100 MHz, DMSO-*d*₆) δ 11.1, 18.1, 24.7, 28.5, 28.7, 28.8, 45.6, 50.1, 78.6, 108.5, 110.4, 119.7, 127.8, 143.9, 155.6, 156.0, 158.7, 172.3 ppm; HRMS ESI⁺ *m/z* for C₂₁H₂₈N₅O₄SCl₂ ([M+H]⁺): calcd 516.12336, found 516.12366 ; HPLC: *t_r* 13.82 min (96 % at 254 nm).

6.2.2.1.13 *tert*-Butyl ((*S*)-1-(((*S*)-6-(3,4-dichloro-5-methyl-1*H*-pyrrole-2-carboxamido)-4,5,6,7-tetrahydrobenzo[*d*]thiazol-2-yl)amino)-3-methyl-1-oxobutan-2-yl)carbamate (27).

Prepared from **12** (0.305 g, 0.883 mmol) and *N*-Boc-L-valine (0.192 g, 0.883 mmol) according to the general procedure **B**. Product was purified by flash column chromatography using dichloromethane/methanol (20:1) as eluent. Yield 0.158 g (33 %); brown solid; m. p. 144-146 °C; [α]_D -10.2 (*c* 0.20, DMF); ¹H NMR (400 MHz, DMSO-*d*₆) δ 0.80-0.95 (m, 6H, 2 × CHCH₃), 1.28 and 1.38 (2 × s, 9H, 3 × CH₃), 1.89-2.06 (m, 3H, H-7, CHCH₃), 2.19 (s, 3H, pyrrole-CH₃), 2.66-2.77 (m, 3H, H-5, H_A-4), 2.96-3.06 (m, 1H, H_B-4), 4.01 (t, 1H, $J = 8.0$ Hz, COCHNH), 4.21-4.32 (m, 1H, CHNH), 7.07 (d, 1H, $J = 8.1$ Hz, COCHNH), 7.35 (d, 1H, $J = 7.5$ Hz, CHNH), 11.98 (s, 1H, NHCO), 12.01 (s, 1H, pyrrole-NH) ppm; ¹³C NMR (100 MHz, DMSO-*d*₆) δ 11.1, 19.0, 19.5, 24.7, 28.5, 28.6, 28.8, 30.5, 45.6, 60.3, 78.7, 108.5, 110.4, 119.7, 127.8, 143.9, 156.0, 158.7, 171.2 ppm; HRMS ESI⁺ *m/z* for C₂₃H₃₂N₅O₄SCl₂ ([M+H]⁺): calcd 544.15466, found 544.15472; HPLC: *t_r* 15.10 min (96 % at 254 nm).

6.2.2.1.14 *tert*-Butyl (*S*)-(3-(((6-(3,4-dichloro-5-methyl-1*H*-pyrrole-2-carboxamido)-4,5,6,7-tetrahydrobenzo[*d*]thiazol-2-yl)amino)-3-oxopropyl)carbamate (28). Prepared from **12** (0.339 g, 0.982 mmol) and *N*-Boc-β-alanine (0.186 g, 0.982 mmol) according to the general procedure **B**. Yield 0.361 g (71 %); brown solid; m. p. 167-169 °C; [α]_D -6.8 (*c* 0.32, DMF); ¹H NMR (400 MHz, DMSO-*d*₆) δ 1.37 (s, 9H, 3 × CH₃), 1.87-2.07 (m, 2H, H-7), 2.19 (s, 3H, pyrrole-

CH₃), 2.52-2.58 (m, 2H, COCH₂), 2.65-2.73 (m, 3H, H-5, H_A-4), 2.94-3.06 (m, 1H, H_B-4), 3.22 (dd, 2H, $J_1 = 12.9$ Hz, $J_2 = 6.8$ Hz, CH₂NH), 4.18-4.32 (m, 1H, CHNH), 6.89 (t, 1H, $J = 5.5$ Hz, CH₂NH), 7.33 (d, 1H, $J = 7.7$ Hz, CHNH), 11.91 (s, 1H, NHCO), 12.03 (s, 1H, pyrrole-NH) ppm; ¹³C NMR (100 MHz, DMSO-*d*₆) δ 11.1, 24.7, 28.6, 28.7, 28.8, 35.9, 36.6, 45.7, 78.1, 108.4, 110.5, 119.4, 119.7, 127.8, 143.7, 155.9, 156.0, 158.7, 169.7 ppm; HRMS ESI⁺ m/z for C₂₁H₂₈N₅O₄SCl₂ ([M+H]⁺): calcd 516.12336, found 516.12366; HPLC: t_r 13.44 min (95 % at 254 nm).

6.2.2.1.15 (S)-2-((6-(4,5-Dibromo-1H-pyrrole-2-carboxamido)-4,5,6,7-tetrahydrobenzo[d]thiazol-2-yl)amino)-2-oxoethan-1-aminium chloride (**29**). To an ice-cold anhydrous methanol (70 mL) acetyl chloride (1.2 mL, 12.0 mmol) was added dropwise. Reaction mixture was stirred for 30 min at 0 °C. Then a solution of **24** (0.691 g, 1.20 mmol) in anhydrous methanol (40 mL) was added and reaction mixture was stirred for 1 h at 0 °C and then for 18 h at room temperature. Solvent was evaporated under reduced pressure. Yield 0.493 g (80 %); white solid; m. p. 197-199 °C; [α]_D -4.42 (c 0.24, MeOH); ¹H NMR (400 MHz, DMSO-*d*₆) δ 1.81-1.93 (m, 1H, H_A-7), 1.96-2.04 (m, 1H, H_B-7), 2.63-2.74 (m, 3H, H-5, H_A-4), 2.98 (dd, 1H, $J_1 = 15.5$ Hz, $J_2 = 5.4$ Hz, H_B-4), 3.86 (dd, 2H, $J_1 = 8.6$ Hz, $J_2 = 3.3$ Hz, CH₂NH₃⁺), 4.14-4.24 (m, 1H, CHNH), 7.02 (d, 1H, $J = 2.8$ Hz, pyrrole-H), 8.23 (d, 1H, $J = 7.8$ Hz, CHNH), 8.31 (br s, 3H, NH₃⁺), 12.77 (d, 1H, $J = 2.7$ Hz, pyrrole-NH) ppm; ¹³C NMR (100 MHz, DMSO-*d*₆) δ 24.6, 28.4, 28.6, 40.6, 45.2, 97.8, 104.5, 113.1, 120.0, 128.0, 142.0, 157.3, 157.7, 158.3 ppm; HRMS ESI⁻ m/z for C₁₄H₁₄Br₂N₅O₂S ([M-H]⁻): calcd 473.9235, found 473.9230; HPLC: t_r 10.80 min (100 % at 254 nm).

6.2.2.2. General procedure C. Starting compound (1 mmol) was dissolved in anhydrous 1,4-dioxane (10 mL) under argon atmosphere and cooled on an ice bath. Then a solution of 4 M HCl in 1,4-dioxane (2.5 mL, 10 mmol) was added dropwise and the mixture was stirred

overnight at room temperature. After reaction was completed solvent was evaporated under reduced pressure and co-evaporation with diethyl ether was performed (2×10 mL).

6.2.2.2.1 *(S)*-2-(((*S*)-6-(3,4-Dichloro-5-methyl-1*H*-pyrrole-2-carboxamido)-4,5,6,7-tetrahydrobenzo[*d*]thiazol-2-yl)amino)-2-oxoethan-1-aminium chloride (**30**). Prepared from **25** (0.133 g, 0.265 mmol) according to the general procedure **C**. Yield 0.116 g (100 %); grey amorphous solid; $[\alpha]_D -6.2$ (*c* 0.24, DMF); $^1\text{H NMR}$ (400 MHz, DMSO-*d*₆) δ 1.86-2.08 (m, 2H, H-7), 2.18 (s, 3H, pyrrole-CH₃), 2.66-2.80 (m, 3H, H-5, H_A-4), 3.02 (dd, 1H, $J_1 = 15.9$ Hz, $J_2 = 5.2$ Hz, H_B-4), 3.83-3.91 (m, 2H, CH₂NH₃⁺), 4.18-4.29 (m, 1H, CHNH), 7.72 (d, 1H, $J = 7.6$ Hz, CHNH), 8.42 (br s, 3H, NH₃⁺), 12.38 (s, 1H, pyrrole-NH) ppm; $^{13}\text{C NMR}$ (100 MHz, DMSO-*d*₆) δ 10.5, 24.1, 28.0, 28.2, 40.5, 45.0, 107.9, 110.4, 119.0, 119.8, 127.1, 158.1, 164.9 ppm; HRMS ESI⁺ *m/z* for C₁₅H₁₈N₅O₂SCl₂ ([M+H]⁺): calcd 402.0564, found 402.0555; HPLC: *t*_r 9.33 min (95 % at 254 nm).

6.2.2.2.2 *(S)*-1-(((*S*)-6-(3,4-Dichloro-5-methyl-1*H*-pyrrole-2-carboxamido)-4,5,6,7-tetrahydrobenzo[*d*]thiazol-2-yl)amino)-1-oxopropan-2-aminium chloride (**31**). Prepared from **26** (0.186 g, 0.360 mmol) according to the general procedure **C**. Yield 0.120 g (74 %); brown solid; m. p. 177-179 °C; $[\alpha]_D -12.6$ (*c* 0.24, DMF); $^1\text{H NMR}$ (400 MHz, DMSO-*d*₆) δ 1.46 (d, 3H, $J = 7.0$ Hz, CH₃), 1.89-2.08 (m, 2H, H-7), 2.19 (s, 3H, pyrrole-CH₃), 2.70-2.81 (m, 3H, H-5, H_A-4), 3.03 (dd, 1H, $J_1 = 15.5$ Hz, $J_2 = 4.8$ Hz, H_B-4), 4.05-4.16 (m, 1H, CHNH₃⁺), 4.18-4.30 (m, 1H, CHNH), 7.61 (d, 1H, $J = 7.7$ Hz, CHNH), 8.46 (br s, 3H, NH₃⁺), 12.28 (s, 1H, pyrrole-NH) ppm; HRMS ESI⁺ *m/z* for C₁₆H₂₀N₅O₂SCl₂ ([M+H]⁺): calcd 416.07093, found 416.07080; HPLC: *t*_r 9.48 min (96 % at 254 nm).

6.2.2.2.3 *(S)*-1-(((*S*)-6-(3,4-Dichloro-5-methyl-1*H*-pyrrole-2-carboxamido)-4,5,6,7-tetrahydrobenzo[*d*]thiazol-2-yl)amino)-3-methyl-1-oxobutan-2-aminium chloride (**32**). Prepared from **27** (0.136 g, 0.249 mmol) according to the general procedure **C**. Yield 0.120 g

(100 %); brown solid; m. p. 200-202 °C; $[\alpha]_{\text{D}} +25.6$ (c 0.16, DMF); ^1H NMR (400 MHz, DMSO- d_6) δ 0.97 (dd, 6H, $J_1 = 6.8$ Hz, $J_2 = 1.1$ Hz, $2 \times \text{CHCH}_3$), 1.89-2.08 (m, 3H, H-7, CHCH_3), 2.19 (s, 3H, pyrrole- CH_3), 2.69-2.82 (m, 3H, H-5, H_A -4), 2.97-3.08 (m, 1H, H_B -4), 3.82-3.92 (m, 1H, COCH), 4.20-4.30 (m, 1H, CHNH), 7.57 (d, 1H, $J = 7.7$ Hz, CHNH), 8.48 (br s, 3H, NH_3^+), 12.24 (s, 1H, pyrrole-NH) ppm; HRMS ESI $^+$ m/z for $\text{C}_{18}\text{H}_{24}\text{N}_5\text{O}_2\text{SCl}_2$ ($[\text{M}+\text{H}]^+$): calcd 444.10223, found 444.10208; HPLC: t_{r} 9.91 min (95 % at 254 nm).

6.2.2.2.4 *(S)*-3-((6-(3,4-Dichloro-5-methyl-1H-pyrrole-2-carboxamido)-4,5,6,7-tetrahydrobenzo[d]thiazol-2-yl)amino)-3-oxopropan-1-aminium chloride (**33**). Prepared from **28** (0.247 g, 0.478 mmol) according to the general procedure **C**. Yield 0.181 g (83 %); grey solid; m. p. 210-212 °C; $[\alpha]_{\text{D}} -16.6$ (c 0.24, DMF); ^1H NMR (400 MHz, DMSO- d_6) δ 1.87-2.07 (m, 2H, H-7), 2.19 (s, 3H, pyrrole- CH_3), 2.66-2.79 (m, 3H, H-5, H_A -4), 2.82 (t, 2H, $J = 6.9$ Hz, COCH_2), 2.96-3.05 (m, 1H, H_B -4), 3.05-3.14 (m, 2H, CH_2NH_3^+), 4.19-4.30 (m, 1H, CHNH), 7.57 (d, 1H, $J = 7.8$ Hz, CHNH), 7.97 (br s, 3H, NH_3^+), 12.17 (br s, 1H, NHCO), 12.25 (s, 1H, pyrrole-NH) ppm; ^{13}C NMR (100 MHz, DMSO- d_6) δ 11.1, 24.8, 28.6, 28.8, 32.8, 34.8, 45.7, 108.5, 111.1, 119.5, 119.8, 127.5, 143.7, 155.7, 158.6, 168.7 ppm; HRMS ESI $^+$ m/z for $\text{C}_{16}\text{H}_{20}\text{N}_5\text{O}_2\text{SCl}_2$ ($[\text{M}+\text{H}]^+$): calcd 416.07093, found 416.07077; HPLC: t_{r} 9.46 min (97 % at 254 nm).

6.2.2.3.1. *(S)*-3,4-Dichloro-*N*-(2-(2-(3,4-dihydroxybenzamido)acetamido)-4,5,6,7-tetrahydrobenzo[d]thiazol-6-yl)-5-methyl-1H-pyrrole-2-carboxamide (**34**). Prepared from **30** (0.142 g, 0.324 mmol) and 3,4-dihydroxybenzoic acid (0.050 g, 0.324 mmol) according to the general procedure **B**. Yield 0.089 g (51 %); brown solid; m. p. 203-205 °C; $[\alpha]_{\text{D}} +4.3$ (c 0.28, DMF); ^1H NMR (400 MHz, DMSO- d_6) δ 1.87-2.06 (m, 2H, H-7), 2.18 (s, 3H, pyrrole- CH_3), 2.65-2.77 (m, 3H, H-5, H_A -4), 3.01 (dd, 1H, $J_1 = 15.7$ Hz, $J_2 = 5.2$ Hz, H_B -4), 4.07 (d, 2H, $J = 6.5$ Hz, CH_2NH), 4.20-4.32 (m, 1H, CHNH), 6.78 (d, 1H, $J = 8.2$ Hz, CHNH), 7.23 (dd, 1H, $J_1 = 8.3$ Hz, $J_2 = 2.2$ Hz, Ar-H), 7.28-7.35 (m, 2H, Ar-H), 8.52 (t, 1H, $J = 5.9$ Hz, CH_2NH), 9.15

(br s, 1H, OH), 9.50 (br s, 1H, OH), 12.01 (s, 2H, pyrrole-NH, NHCO) ppm; ^{13}C NMR (100 MHz, $\text{DMSO-}d_6$) δ 11.1, 24.7, 28.5, 28.8, 43.0, 45.6, 108.5, 110.4, 115.3, 115.6, 119.6, 119.7, 125.4, 127.8, 143.8, 145.3, 149.1, 155.9, 158.7, 167.0, 168.6 ppm; HRMS ESI $^-$ m/z for $\text{C}_{22}\text{H}_{20}\text{N}_5\text{O}_5\text{SCl}_2$ ($[\text{M-H}]^-$): calcd 536.0562, found 536.0555; HPLC: t_r 10.89 min (95 % at 254 nm).

6.2.2.3.2 *(S)*-3,4-Dichloro-*N*-(2-(2-(2,3-dihydroxybenzamido)acetamido)-4,5,6,7-tetrahydrobenzo[*d*]thiazol-6-yl)-5-methyl-1*H*-pyrrole-2-carboxamide (**35**). Prepared from **30** (0.142 g, 0.324 mmol) and 2,3-dihydroxybenzoic acid (0.050 g, 0.324 mmol) according to the general procedure **B**. Yield 0.043 g (25 %); yellow solid; m. p. 173-175 °C; $[\alpha]_D +29.8$ (*c* 0.20, DMF); ^1H NMR (400 MHz, $\text{DMSO-}d_6$) δ 1.89-2.06 (m, 2H, H-7), 2.18 (s, 3H, pyrrole- CH_3), 2.55-2.73 (m, 3H, H-5, H_A -4), 3.01 (dd, 1H, $J_1 = 15.7$ Hz, $J_2 = 5.2$ Hz, H_B -4), 4.18 (d, 2H, $J = 5.7$ Hz, CH_2NH), 4.21-4.30 (m, 1H, CHNH), 6.69 (t, 1H, $J = 7.7$ Hz, CH_2NH), 6.93 (d, 1H, $J = 6.9$ Hz, Ar-H), 7.29-7.36 (m, 2H, Ar-H), 9.31 (br s, 1H, OH), 11.78-12.30 (m, 2H, pyrrole-NH, NHCO) ppm; ^{13}C NMR (100 MHz, $\text{DMSO-}d_6$) δ 11.1, 24.7, 28.5, 28.8, 42.7, 45.6, 108.5, 110.4, 115.5, 118.3, 119.2, 119.7, 119.8, 127.8, 146.7, 155.8, 158.7, 167.9, 170.3 ppm; HRMS ESI $^-$ m/z for $\text{C}_{22}\text{H}_{20}\text{N}_5\text{O}_5\text{SCl}_2$ ($[\text{M-H}]^-$): calcd 536.0562, found 536.0556; HPLC: t_r 12.00 min (95 % at 254 nm).

6.2.2.3.3 *(S)*-*N*-(2-(2-(5-(Benzyloxy)-4-oxo-4*H*-pyran-2-carboxamido)acetamido)-4,5,6,7-tetrahydrobenzo[*d*]thiazol-6-yl)-4,5-dibromo-1*H*-pyrrole-2-carboxamide (**36**). Prepared from **29** (0.150 g, 0.292 mmol) and **7** (0.072 g, 0.292 mmol) according to the general procedure **B**. Crude product was crystallized from dichloromethane/methanol (20:1). Yield 0.028 g (14 %); yellow solid; m. p. 166-168 °C; $[\alpha]_D +18.4$ (*c* 0.08, DMF); ^1H NMR (400 MHz, $\text{DMSO-}d_6$) δ 1.81-1.92 (m, 1H, H_A -7), 1.95-2.05 (m, 1H, H_B -7), 2.65-2.76 (m, 3H, H-5, H_A -4), 2.98 (dd, 1H, $J_1 = 15.7$ Hz, $J_2 = 4.5$ Hz, H_B -4), 4.13 (d, 2H, $J = 6.0$ Hz, CH_2NH), 4.16-4.23 (m, 1H, CHNH), 5.03 (s, 2H, OCH_2), 6.91 (s, 1H, pyran-H), 7.01 (s, 1H, pyrrole-H), 7.35-7.47 (m, 5H, Ph-H),

8.18 (d, 1H, $J = 8.4$ Hz, CHNH), 8.32 (s, 1H, pyran-H), 9.32 (t, 1H, $J = 6.0$ Hz, CH₂NH), 12.13 (s, 1H, NHCO), 12.74 (s, 1H, pyrrole-NH) ppm; HRMS ESI⁻ m/z for C₂₇H₂₂Br₂N₅O₆S ([M-H]⁻): calcd 701.9658, found 701.9658; HPLC: t_r 12.39 min (95 % at 254 nm).

6.2.2.3.4 (*S*)-4,5-Dibromo-*N*-(2-(2-(5-hydroxy-4-oxo-4*H*-pyran-2-carboxamido)acetamido)-4,5,6,7-tetrahydrobenzo[*d*]thiazol-6-yl)-1*H*-pyrrole-2-carboxamide (**37**). Prepared from **29** (0.100 g, 0.195 mmol) and **9** (0.030 g, 0.195 mmol) according to the general procedure **B**. Crude product was purified by flash column chromatography using dichloromethane/methanol (9:1) to dichloromethane/methanol (4:1) as eluent. Yield 0.008 g (12 %); yellow amorphous solid; ¹H NMR (400 MHz, DMSO-*d*₆) δ 1.83-1.91 (m, 1H, H_A-7), 1.95-2.03 (m, 1H, H_B-7), 2.65-2.73 (m, 3H, H-5, H_A-4), 2.98 (dd, 1H, $J_1 = 15.6$ Hz, $J_2 = 5.2$ Hz, H_B-4), 4.13 (d, 2H, $J = 5.8$ Hz, CH₂NH), 4.15-4.21 (m, 1H, CHNH), 6.92 (s, 1H, pyran-H), 7.00 (s, 1H, pyrrole-H), 8.18-8.23 (m, 2H, CHNH, pyran-H), 9.28 (t, 1H, $J = 5.9$ Hz, CH₂NH), 9.52-9.92 (br s, 1H, OH), 12.14 (s, 1H, pyrrole-NH), 12.62-12.96 (br s, 1H, NHCO) ppm; HRMS ESI⁻ m/z for C₂₀H₁₆Br₂N₅O₆S ([M-H]⁻): calcd 611.9188, found 611.9180.

6.2.2.3.5 (*S*)-*N*-(2-(2-(5-(Benzyloxy)-4-oxo-4*H*-pyran-2-carboxamido)acetamido)-4,5,6,7-tetrahydrobenzo[*d*]thiazol-6-yl)-3,4-dichloro-5-methyl-1*H*-pyrrole-2-carboxamide (**38**). Prepared from **30** (0.125 g, 0.287 mmol) and **7** (0.071 g, 0.287 mmol) according to the general procedure **B**. Crude product was purified by crystallization from methanol. Yield 0.045 g (25 %); yellow solid; m. p. 183-185 °C; [α]_D -10.9 (c 0.11, DMF); ¹H NMR (400 MHz, DMSO-*d*₆) δ 1.91-2.05 (m, 2H, H-7), 2.19 (s, 3H, pyrrole-CH₃), 2.70-2.78 (m, 3H, H-5, H_A-4), 2.99-3.05 (m, 1H, H_B-4), 4.13 (d, 2H, $J = 6.0$ Hz, CH₂NH), 4.22-4.31 (m, 1H, CHNH), 5.03 (s, 2H, OCH₂), 6.91 (s, 1H, pyran-H), 7.33 (d, 1H, $J = 7.6$ Hz, CHNH), 7.36-7.47 (m, 5H, Ph-H), 8.32 (s, 1H, pyran-H), 9.31 (t, 1H, $J = 6.0$ Hz, CH₂NH), 12.02 (s, 1H, pyrrole-NH), 12.13 (s, 1H, NHCO) ppm; HRMS ESI⁻ m/z for C₂₈H₂₄N₅O₆SCl₂ ([M-H]⁻): calcd 628.0824, found 628.0812; HPLC: t_r 12.82 min (95 % at 254 nm).

6.2.2.3.6 (S)-3,4-Dichloro-N-(2-(2-(5-hydroxy-4-oxo-4H-pyran-2-carboxamido)acetamido)-4,5,6,7-tetrahydrobenzo[d]thiazol-6-yl)-5-methyl-1H-pyrrole-2-carboxamide (**39**). Prepared from **30** (0.100 g, 0.228 mmol) and **9** (0.036 g, 0.228 mmol) according to the general procedure **B**. Product was precipitated from the reaction mixture after addition of 10 % citric acid (5 mL) and was filtered off. Precipitate was then washed with hot ethyl acetate (3 × 5 mL) and hot methanol (3 × 5 mL) and dried. Yield 0.030 g (24 %); brown amorphous solid; $[\alpha]_D +10.9$ (*c* 0.17, DMF); $^1\text{H NMR}$ (400 MHz, DMSO-*d*₆) δ 1.88-2.07 (m, 2H, H-7), 2.18 (s, 3H, pyrrole-CH₃), 2.65-2.77 (m, 3H, H-5, H_A-4), 3.02 (dd, 1H, $J_1 = 15.8$ Hz, $J_2 = 5.1$ Hz, H_B-4), 4.12 (d, 2H, $J = 5.8$ Hz, CH₂NH), 4.20-4.32 (m, 1H, CHNH), 6.92 (s, 1H, pyran-H), 7.33 (d, 1H, $J = 7.8$ Hz, CHNH), 8.19 (s, 1H, pyran-H), 9.27 (t, 1H, $J = 5.8$ Hz, CH₂NH), 9.64 (br s, 1H, OH), 12.02 (s, 1H, pyrrole-NH), 12.12 (s, 1H, NHCO) ppm; $^{13}\text{C NMR}$ (100 MHz, DMSO-*d*₆) δ 10.1, 23.6, 27.4, 27.7, 41.7, 44.5, 107.4, 109.4, 112.6, 118.6, 118.8, 126.8, 138.8, 142.8, 146.9, 154.1, 154.7, 157.6, 158.6, 166.4, 173.1 ppm; HRMS ESI⁺ *m/z* for C₂₁H₂₀N₅O₆SCl₂ ([M+H]⁺): calcd 540.0517, found 540.0503; HPLC: *t*_r 10.68 min (95 % at 254 nm).

6.2.2.3.7 (S)-N-(2-((6-(3,4-Dichloro-5-methyl-1H-pyrrole-2-carboxamido)-4,5,6,7-tetrahydrobenzo[d]thiazol-2-yl)amino)-2-oxoethyl)-5-((4-methoxybenzyl)oxy)-4-oxo-1,4-dihydropyridine-2-carboxamide (**40**). Prepared from **30** (0.080 g, 0.182 mmol) and **10** (0.050 g, 0.182 mmol) according to the general procedure **B**. Yield 0.053 g (45 %); yellow solid; m. p. 168-170 °C; $[\alpha]_D +9.0$ (*c* 0.16, DMF); $^1\text{H NMR}$ (400 MHz, DMSO-*d*₆) δ 1.90-2.05 (m, 2H, H-7), 2.18 (s, 3H, pyrrole-CH₃), 2.65-2.75 (m, 3H, H-5, H_A-4), 3.02 (dd, 1H, $J_1 = 15.8$ Hz, $J_2 = 5.1$ Hz, H_B-4), 3.76 (s, 3H, OCH₃), 4.15 (d, 2H, $J = 6.0$ Hz, CH₂NH), 4.22-4.32 (m, 1H, CHNH), 5.19 (s, 2H, OCH₂), 6.92-7.01 (m, 2H, Ar-H), 7.33 (d, 1H, $J = 7.7$ Hz, CHNH), 7.37-7.45 (m, 2H, Ar-H), 7.49 (s, 1H, pyridine-H), 8.23 (s, 1H, pyridine-H), 8.81 (t, 1H, $J = 6.0$ Hz, CH₂NH), 10.82 (br s, 1H, pyridine-NH), 12.02 (s, 1H, pyrrole-NH), 12.08 (br s, 1H, NHCO) ppm; $^{13}\text{C NMR}$ (100 MHz, DMSO-*d*₆) δ 11.2, 28.5, 28.8, 55.5, 70.8, 108.4, 110.4, 114.3, 119.7,

127.8, 128.9, 130.3, 158.7, 159.6, 168.1 ppm; HRMS ESI⁺ m/z for C₂₉H₂₉N₆O₆SCl₂ ([M+H]⁺): calcd 659.1252, found 659.1237; HPLC: t_r 12.53 min (95 % at 254 nm).

6.2.2.3.8 *N-((S)-1-(((S)-6-(3,4-Dichloro-5-methyl-1H-pyrrole-2-carboxamido)-4,5,6,7-tetrahydrobenzo[d]thiazol-2-yl)amino)-1-oxopropan-2-yl)-5-((4-methoxybenzyl)oxy)-4-oxo-1,4-dihydropyridine-2-carboxamide (41)*. Prepared from **31** (0.088 g, 0.194 mmol) and **10** (0.053 g, 0.194 mmol) according to the general procedure **B**. Product was purified by flash column chromatography using dichloromethane/methanol (20:1) as eluent. Yield 0.035 g (27 %); brown solid; m. p. 147-149 °C; [α]_D +15.7 (c 0.04, DMF); ¹H NMR (400 MHz, DMSO-*d*₆) δ 1.43 (d, 3H, *J* = 7.1 Hz, CHCH₃), 1.89-2.06 (m, 2H, H-7), 2.19 (s, 3H, pyrrole-CH₃), 2.66-2.78 (m, 3H, H-5, H_A-4), 2.97-3.06 (m, 1H, H_B-4), 3.76 (s, 3H, OCH₃), 4.21-4.32 (m, 1H, CHNH), 4.60-4.71 (m, 1H, CHCH₃), 5.19 (s, 2H, OCH₂), 6.93-6.99 (m, 2H, Ar-H), 7.34 (d, 1H, *J* = 7.8 Hz, CHNH), 7.38-7.45 (m, 2H, Ar-H), 7.48 (s, 1H, pyridine-H), 8.23 (s, 1H, pyridine-H), 8.60-8.67 (m, 1H, COCHNH), 10.87 (s, 1H, pyridine-NH), 12.02 (s, 1H, pyrrole-NH), 12.17 (s, 1H, NHCO) ppm; HRMS ESI⁺ m/z for C₃₀H₃₁N₆O₆SCl₂ ([M+H]⁺): calcd 673.13974, found 673.13977; HPLC: t_r 12.92 min (95 % at 254 nm).

6.2.2.3.9 *N-((S)-1-(((S)-6-(3,4-Dichloro-5-methyl-1H-pyrrole-2-carboxamido)-4,5,6,7-tetrahydrobenzo[d]thiazol-2-yl)amino)-3-methyl-1-oxobutan-2-yl)-5-((4-methoxybenzyl)oxy)-4-oxo-1,4-dihydropyridine-2-carboxamide (42)*. Prepared from **32** (0.095 g, 0.198 mmol) and **10** (0.054 g, 0.198 mmol) according to the general procedure **B**. Product was purified by flash column chromatography using dichloromethane/methanol (20:1) as eluent. Yield 0.038 g (27 %); brown solid; m. p. 153-155 °C; ¹H NMR (400 MHz, DMSO-*d*₆) δ 0.91 (t, 6H, *J* = 6.7 Hz, 2 × CHCH₃), 1.92-2.07 (m, 2H, H-7), 2.21-2.24 (m, 4H, CHCH₃, pyrrole-CH₃), 2.68-2.77 (m, 3H, H-5, H_A-4), 2.97-3.05 (m, 1H, H_B-4), 3.77 (s, 3H, OCH₃), 4.21-4.31 (m, 1H, CHNH), 4.51-4.60 (m, 1H, COCHNH), 5.19 (s, 2H, OCH₂), 6.93-6.99 (m, 2H, Ar-H), 7.35 (d, 1H, *J* = 7.9 Hz, CHNH), 7.39-7.45 (m, 2H, Ar-H), 7.49 (s, 1H, pyridine-H), 8.26 (s, 1H, pyridine-H), 8.50-

8.57 (m, 1H, COCHNH), 10.90 (s, 1H, pyridine-NH), 12.01 (s, 1H, pyrrole-NH), 12.28 (s, 1H, NHCO) ppm; HRMS ESI⁺ m/z for C₃₂H₃₅N₆O₆SCl₂ ([M+H]⁺): calcd 701.17104, found 701.17084; HPLC: t_r 14.25 min (96 % at 254 nm).

6.2.2.3.10 (S)-N-(3-((6-(3,4-Dichloro-5-methyl-1H-pyrrole-2-carboxamido)-4,5,6,7-tetrahydrobenzo[d]thiazol-2-yl)amino)-3-oxopropyl)-5-((4-methoxybenzyl)oxy)-4-oxo-1,4-dihydropyridine-2-carboxamide (**43**). Prepared from **33** (0.178 g, 0.393 mmol) and **10** (0.180 g, 0.393 mmol) according to the general procedure **B**. Crude product was recrystallized from ethyl acetate. Yield 0.066 g (25 %); brown solid; m. p. 184-186 °C; [α]_D -8.8 (c 0.24, DMF); ¹H NMR (400 MHz, DMSO-*d*₆) δ 1.89-2.07 (m, 2H, H-7), 2.19 (s, 3H, pyrrole-CH₃), 2.65-2.77 (m, 5H, H-5, H_A-4, COCH₂), 3.02 (dd, 1H, J₁ = 16.2 Hz, J₂ = 4.9 Hz, H_B-4), 3.55 (dd, 2H, J₁ = 13.4 Hz, J₂ = 7.1 Hz, CH₂NH), 3.76 (s, 3H, OCH₃), 4.20-4.31 (m, 1H, CHNH), 5.17 (s, 2H, OCH₂), 6.92-6.98 (m, 2H, Ar-H), 7.34 (d, 1H, J = 7.7 Hz, CHNH), 7.37-7.43 (m, 2H, Ar-H), 7.49 (s, 1H, pyridine-H), 8.18 (s, 1H, pyridine-H), 8.60 (t, 1H, J = 6.1 Hz, CH₂NH), 10.81 (s, 1H, pyridine-NH), 11.99 (s, 1H, NHCO), 12.02 (s, 1H, pyrrole-NH) ppm; ¹³C NMR (100 MHz, DMSO-*d*₆) δ 11.1, 24.7, 28.5, 28.8, 35.3, 35.4, 45.7, 55.6, 70.8, 108.5, 110.1, 110.4, 114.3, 119.5, 119.7, 127.8, 128.8, 130.3, 135.5, 143.7, 144.9, 146.1, 154.8, 155.8, 158.7, 159.6, 164.2, 170.0 ppm; HRMS ESI⁻ m/z for C₃₀H₂₉N₆O₆SCl₂ ([M-H]⁻): calcd 671.12409, found 671.12640; HPLC: t_r 12.22 min (96 % at 254 nm).

6.2.2.4 General procedure D. Starting compound (1 mmol) was dissolved in acetic acid (50 mL) and a solution of 1 M HCl in acetic acid (20 mL, 20 mmol) was added dropwise. The mixture was stirred overnight at room temperature. Volume of the solvent was reduced *in vacuo* to only a few milliliters and diethyl ether (100 mL) was added. A precipitate was formed, which was filtered off and dried *in vacuo*.

6.2.2.4.1 (S)-N-(2-((6-(3,4-Dichloro-5-methyl-1H-pyrrole-2-carboxamido)-4,5,6,7-tetrahydrobenzo[d]thiazol-2-yl)amino)-2-oxoethyl)-5-hydroxy-4-oxo-1,4-dihydropyridine-2-carboxamide (**44**). Prepared from **40** (0.030 g, 0.0455 mmol) according to the general procedure **D**. Yield 0.019 g (75 %); pink solid; m. p. > 300 °C; $[\alpha]_D -25.3$ (c 0.08, DMF); $^1\text{H NMR}$ (400 MHz, DMSO- d_6) δ 1.93-2.07 (m, 2H, H-7), 2.18 (s, 3H, pyrrole-CH₃), 2.66-2.76 (m, 3H, H-5, H_A-4), 3.01 (dd, 1H, $J_1 = 15.8$ Hz, $J_2 = 5.2$ Hz, H_B-4), 4.18 (d, 2H, $J = 5.7$ Hz, CH₂NH), 4.22-4.29 (m, 1H, CHNH), 7.42 (d, 1H, $J = 7.6$ Hz, CHNH), 7.64 (s, 1H, pyridine-H) 8.05 (s, 1H, pyridine-H), 9.24 (br s, 1H, OH), 12.07-12.20 (m, 2H, pyrrole-NH, NHCO) ppm; $^{13}\text{C NMR}$ (100 MHz, DMSO- d_6) δ 11.1, 24.7, 28.6, 28.8, 42.9, 45.6, 108.5, 110.7, 111.1, 119.6, 119.8, 127.7, 143.8, 146.6, 155.8, 158.7, 167.8 ppm; HRMS ESI⁻ m/z for C₂₁H₁₉N₆O₅SCl₂ ([M-H]⁻): calcd 537.0515, found 537.0518; HPLC: t_r 10.08 min (95 % at 254 nm).

6.2.2.4.2 N-((S)-1-(((S)-6-(3,4-Dichloro-5-methyl-1H-pyrrole-2-carboxamido)-4,5,6,7-tetrahydrobenzo[d]thiazol-2-yl)amino)-1-oxopropan-2-yl)-5-hydroxy-4-oxo-1,4-dihydropyridine-2-carboxamide (**45**). Prepared from **41** (0.027 g, 0.040 mmol) according to the general procedure **D**. Yield 0.014 g (62 %); orange solid; m. p. 207-209 °C; $[\alpha]_D -51.8$ (c 0.07, DMF); $^1\text{H NMR}$ (400 MHz, DMSO- d_6) δ 1.44 (d, 3H, $J = 7.1$ Hz, CHCH₃), 1.89-2.07 (m, 2H, H-7), 2.19 (s, 3H, pyrrole-CH₃), 2.66-2.79 (m, 3H, H-5, H_A-4), 2.97-3.06 (m, 1H, H_B-4), 4.20-4.31 (m, 1H, CH₂CHNH), 4.62-4.72 (m, 1H, COCHNH), 7.38 (d, 1H, $J = 7.7$ Hz, CH₂CHNH), 7.60 (s, 1H, pyridine-H), 8.02 (s, 1H, pyridine-H), 8.93 (s, 1H, OH), 12.06 (s, 1H, pyrrole-NH), 12.18 (br s, 1H, NHCO) ppm; $^{13}\text{C NMR}$ (100 MHz, DMSO- d_6) δ 11.1, 18.1, 24.7, 28.6, 28.8, 45.6, 49.7, 108.5, 110.6, 119.6, 120.0, 127.7, 143.9, 146.7, 158.7, 171.1 ppm; HRMS ESI⁺ m/z for C₂₂H₂₃N₆O₅SCl₂ ([M+H]⁺): calcd 553.08222, found 553.08264; HPLC: t_r 10.27 min (96 % at 254 nm).

6.2.2.4.3 N-((S)-1-(((S)-6-(3,4-Dichloro-5-methyl-1H-pyrrole-2-carboxamido)-4,5,6,7-tetrahydrobenzo[d]thiazol-2-yl)amino)-3-methyl-1-oxobutan-2-yl)-5-hydroxy-4-oxo-1,4-

dihydropyridine-2-carboxamide (46). Prepared from **42** (0.033 g, 0.047 mmol) according to the general procedure **D**. Yield 0.021 g (77 %); brown solid; m. p. 213-215 °C; $[\alpha]_D +8.9$ (c 0.13, DMF); $^1\text{H NMR}$ (400 MHz, DMSO- d_6) δ 0.92 (d, 4H, $J = 6.6$ Hz, CHCH $\underline{\text{H}}$ ₃), 1.10 (t, 2H, $J = 7.0$ Hz, CHCH $\underline{\text{H}}$ ₃), 1.89-2.07 (m, 2H, H-7), 2.13-2.24 (m, 4H, CHCH $\underline{\text{H}}$ ₃, pyrrole-CH $\underline{\text{H}}$ ₃), 2.66-2.79 (m, 3H, H-5, H_A-4), 2.97-3.06 (m, 1H, H_B-4), 4.20-4.31 (m, 1H, CH $\underline{\text{H}}$ ₂CHNH), 4.51-4.59 (m, 1H, COCH $\underline{\text{H}}$ ₂NH), 7.39 (d, 1H, $J = 7.6$ Hz, CH $\underline{\text{H}}$ ₂CHNH), 7.58 (s, 1H, pyridine-H), 8.04 (s, 1H, pyridine-H), 8.73 (br s, 1H, OH), 12.06 (s, 1H, pyrrole-NH), 12.28 (s, 1H, NHCO) ppm; HRMS ESI⁺ m/z for C₂₄H₂₇N₆O₅SCl₂ ([M+H]⁺): calcd 581.11352, found 581.11365; HPLC: t_r 11.09 min (95 % at 254 nm).

6.2.2.4.4 (S)-N-(3-((6-(3,4-Dichloro-5-methyl-1H-pyrrole-2-carboxamido)-4,5,6,7-tetrahydrobenzo[d]thiazol-2-yl)amino)-3-oxopropyl)-5-hydroxy-4-oxo-1,4-dihydropyridine-2-carboxamide (**47**). Prepared from **43** (0.054 g, 0.080 mmol) according to the general procedure **D**. Yield 0.036 g (80 %); brown solid; m. p. 220-222 °C; $[\alpha]_D -4.7$ (c 0.24, DMF); $^1\text{H NMR}$ (400 MHz, DMSO- d_6) δ 1.87-1.97 (m, 1H, H_A-7), 1.97-2.07 (m, 1H, H_B-7), 2.19 (s, 3H, pyrrole-CH $\underline{\text{H}}$ ₃), 2.65-2.80 (m, 5H, H-5, H_A-4, COCH $\underline{\text{H}}$ ₂), 2.96-3.05 (m, 1H, H_B-4), 4.20-4.30 (m, 1H, CH $\underline{\text{H}}$ ₂NH), 7.41 (d, 1H, $J = 7.7$ Hz, CHNH), 7.64 (s, 1H, pyridine-H), 8.02 (s, 1H, pyridine-H), 9.06 (br s, 1H, OH), 12.03 (s, 1H, NHCO), 12.10 (s, 1H, pyrrole-NH) ppm; $^{13}\text{C NMR}$ (100 MHz, DMSO- d_6) δ 11.1, 24.8, 28.6, 28.8, 35.0, 36.1, 45.7, 108.5, 110.8, 111.3, 119.6, 127.7, 143.7, 146.9, 155.9, 158.7, 169.5 ppm; HRMS ESI⁺ m/z for C₂₂H₂₃N₆O₅SCl₂ ([M+H]⁺): calcd 553.08222, found 553.08258; HPLC: t_r 10.04 min (95 % at 254 nm).

6.3 Determination of inhibitory activities against *E. coli* DNA gyrase

The assays for determination of IC₅₀ against *E. coli* DNA gyrase were performed according to previously reported procedures [10]. IC₅₀ values were determined with seven concentrations of the inhibitors. GraphPad Prism program was used for calculating an IC₅₀ value, which

represents the concentration of inhibitor where the activity of the enzyme is reduced by 50%. IC₅₀ values were determined in three independent measurements, and their average value is given as a final result.

6.4 Determination of antibacterial activities

The clinical microbiology control strains of *E. faecalis* (ATCC 29212), *S. aureus* (ATCC 25923 and 29213), *E. coli* (ATCC 25922), *P. aeruginosa* (ATCC 27853) and *A. baumannii* (ATCC 19606) were obtained from Microbiologics Inc. (St. Cloud, MN, USA). The single-gene knock-out mutant strains of *E. coli* JW5503 (*tolC* knock-out) and JD17464 (*lpxC* knock-out) were obtained from the *E. coli* collection of the National BioResource Project at the National Institute of Genetics (Japan) [35]. To determine the antibacterial activities, broth microdilution assays were carried out in 96-well plates following the Clinical and Laboratory Standards Institute guidelines [27]. Preliminary screening was performed at 50 µM, and growth inhibition was measured after 24 h incubation. For compounds displaying >90% growth inhibition in the preliminary assay, the MICs were determined in dose–response assays (from at least two independent experiments, each with three replicates per concentration, except when stated otherwise). Cation-adjusted Mueller-Hinton broth (CAMHB, BD) was used in all assays. CAMHB was prepared according to manufacturer’s instructions and iron-depleted CAMHB (ID-CAMHB) according to CLSI guidelines [36]. Iron-depleted conditions mimic the conditions faced by bacteria during infections of human tissues and fluids. Thus, the use of iron-depleted conditions was required to induce the ferric iron transport. In brief, ID-CAMHB was prepared by adding 100 g of Chelex 100 resin (Bio-Rad) to 1 L of autoclaved CAMHB and stirred for 2 h at room temperature, in order to remove cations from the medium. Then, broth was filtered using a 0.2 µm filter to remove the resin and pH adjusted to 7.3 using 5 M hydrochloric acid. ID-CAMHB was then supplemented with calcium (CaCl₂), magnesium

(MgCl₂) and zinc (ZnSO₄) to final concentrations of 22.5 µg/mL, 11.25 µg/mL and 0.56 µg/mL, respectively, and filtered again. To evaluate the effect of iron concentration on antibacterial effect of compounds, an appropriate amount of iron (III) chloride was added to ID-CAMHB, and this supplemented media was used as control CAMHB. The iron concentration in CAMHB and ID-CAMHB were approximately 0.2 mg/L and ≤0.03 mg/L, respectively. Cefiderocol MICs were determined against *E. coli*, *P. aeruginosa* and *A. baumannii*, and used as quality control in the assays. Cefiderocol was purchased from MedChemExpress Europe.

Molecular docking. Three-dimensional models of the designed DNA gyrase inhibitors and their conjugates with siderophore mimics were built in Chem3D 18.0 (PerkinElmer Inc., Massachusetts, USA). The geometries and charges of the ligands were optimized using the MM2 force field and partial atomic charges were assigned. The energy was minimized until the gradient value was smaller than 0.001 kcal/ (mol×Å). Molecular docking calculations were performed in Schrödinger Release 2019-1 (Schrödinger, LLC, New York, NY, USA, 2019). Crystal structure of *E. coli* DNA gyrase B in complex with bithiazole inhibitor (PDB entry: 4DUH) was retrieved from Protein Data Bank. Protein was then prepared by Protein Preparation Wizard using default settings. Receptor grid was calculated for the ligand-binding site and designed compounds were docked using Glide XP protocol as implemented in Schrödinger Release 2019-1 (Glide, Schrödinger, LLC, New York, NY, USA, 2019). The highest ranked docking pose was used for visualization.

Associated content

Appendix A. Supplementary Information

The full data for the synthetic procedures of the siderophore mimics, and ¹H and ¹³C NMR spectra are given in the Supplementary Information. This material is available via the internet.

Author information

Corresponding author: Tihomir Tomašič

E-mail: tihomir.tomasic@ffa.uni-lj.si

Tel: +386-1-4769556

Fax: +386-1-4258031

Author contributions

The manuscript was written with contributions from all of the authors. All of the authors have given approval to the final version of the manuscript.

Funding sources

The work was funded by the Slovenian Research Agency (Grant No. P1-0208) and the Academy of Finland (Grant Nos. 277001, 304697, 312503).

Conflicts of interest

The authors declare that they have no conflicts of interest, including no financial, personal or other relationships with other people or organizations.

Acknowledgements

The authors thank Dušan Žigon (Mass Spectrometry Centre, Jožef Stefan Institute, Ljubljana, Slovenia) for the mass spectra, Heidi Mäkkylä, Cristina Carbonell Duacastella and Heli Parviainen for their technical assistance in the antibacterial assays, and Christopher Berrie for scientific editing of the manuscript.

References

- [1] G.V. Asokan, R.K. Kasimanickam, Emerging infectious diseases, antimicrobial resistance and millennium development goals: resolving the challenges through one health, *Cent. Asian J. Glob. Health* 2 (2013) 76.
- [2] E. Toner, A. Adalja, G.K. Gronvall, A. Cicero, T.V. Inglesby, Antimicrobial resistance is a global health emergency, *Health Secur.* 13 (2015) 153-155.
- [3] World Health Organization, WHO publishes list of bacteria for which new antibiotics are urgently needed, <https://www.who.int/news-room/detail/27-02-2017-who-publishes-list-of-bacteria-for-which-new-antibiotics-are-urgently-needed>, 2017 (accessed 27 August 2019).
- [4] P. Fernandes, E. Martens, Antibiotics in late clinical development, *Biochem. Pharmacol.* 133 (2017) 152-163.
- [5] M. Mazer-Amishahi, A. Pourmand, L. May, Newly approved antibiotics and antibiotics reserved for resistant infections: implications for emergency medicine, *Am. J. Emerg. Med.* 35 (2017) 154-158.
- [6] X.Z. Li, P. Plesiat, H. Nikaido, The challenge of efflux-mediated antibiotic resistance in Gram-negative bacteria, *Clin. Microbiol. Rev.* 28 (2015) 337-418.
- [7] T. Tomašič, L. Peterlin Mašič, Prospects for developing new antibacterials targeting bacterial type IIA topoisomerases, *Curr. Top. Med. Chem.* 14 (2014) 130-151.
- [8] G.S. Bisacchi, J.I. Manchester, A new-class antibacterial-almost. Lessons in drug discovery and development: a critical analysis of more than 50 years of effort toward ATPase inhibitors of DNA gyrase and topoisomerase IV, *ACS Infect. Dis.* 1 (2015) 4-41.
- [9] M. Durcik, T. Tomašič, N. Zidar, A. Zega, D. Kikelj, L. Peterlin Mašič, J. Ilaš, ATP-competitive DNA gyrase and topoisomerase IV inhibitors as antibacterial agents, *Expert Opin. Ther. Pat.* 29 (2019) 171-180.

- [10] T. Tomašič, S. Katsamakas, Ž. Hodnik, J. Ilaš, M. Brvar, T. Šolmajer, S. Montalvao, P. Tammela, M. Banjanac, G. Ergović, M. Anderluh, L. Peterlin Mašič, D. Kikelj, Discovery of 4,5,6,7-tetrahydrobenzo[1,2-*d*]thiazoles as novel DNA gyrase inhibitors targeting the ATP-binding site, *J. Med. Chem.* 58 (2015) 5501-5521.
- [11] T. Tomašič, M. Mirt, M. Barančokova, J. Ilaš, N. Zidar, P. Tammela, D. Kikelj, Design, synthesis and biological evaluation of 4,5-dibromo-*N*-(thiazol-2-yl)-1*H*-pyrrole-2-carboxamide derivatives as novel DNA gyrase inhibitors, *Bioorg. Med. Chem.* 25 (2017) 338-349.
- [12] M. Gjorgjieva, T. Tomašič, M. Barančokova, S. Katsamakas, J. Ilaš, P. Tammela, L. Peterlin Mašič, D. Kikelj, Discovery of benzothiazole scaffold-based DNA gyrase B inhibitors, *J. Med. Chem.* 59 (2016) 8941-8954.
- [13] D. Benedetto Tiz, Ž. Skok, M. Durcik, T. Tomašič, L. Peterlin Mašič, J. Ilaš, A. Zega, G. Draskovits, T. Revesz, A. Nyerges, C. Pal, C.D. Cruz, P. Tammela, D. Žigon, D. Kikelj, N. Zidar, An optimised series of substituted *N*-phenylpyrrolamides as DNA gyrase B inhibitors, *Eur. J. Med. Chem.* 167 (2019) 269-290.
- [14] I.A. Yule, L.G. Czaplewski, S. Pommier, D.T. Davies, S.K. Narramore, C.W. Fishwick, Pyridine-3-carboxamide-6-yl-ureas as novel inhibitors of bacterial DNA gyrase: structure based design, synthesis, SAR and antimicrobial activity, *Eur. J. Med. Chem.* 86 (2014) 31-38.
- [15] T. Tomašič, M. Barančokova, N. Zidar, J. Ilaš, P. Tammela, D. Kikelj, Design, synthesis, and biological evaluation of 1-ethyl-3-(thiazol-2-yl)urea derivatives as *Escherichia coli* DNA gyrase inhibitors, *Arch. Pharm. (Weinheim)* 351 (2018).
- [16] D. Benedetto Tiz, D. Kikelj, N. Zidar, Overcoming problems of poor drug penetration into bacteria, *Expert Opin. Drug Discov.* 13 (2018) 497-507.
- [17] H.I. Zgurskaya, C.A. Lopez, S. Gnanakaran, Permeability barrier of Gram-negative cell envelopes and approaches to bypass it, *ACS Infect. Dis.* 1 (2015) 512-522.

- [18] E. Ahmed, S.J. Holmstrom, Siderophores in environmental research: roles and applications, *Microb. Biotechnol.* 7 (2014) 196-208.
- [19] R. Golonka, B.S. Yeoh, M. Vijay-Kumar, The iron tug-of-war between bacterial siderophores and innate immunity, *J. Innate Immun.* 11 (2019) 249-262.
- [20] U. Bilitewski, J.A.V. Blodgett, A.K. Duhme-Klair, S. Dallavalle, S. Laschat, A. Routledge, R. Schobert, Chemical and biological aspects of nutritional immunity-perspectives for new anti-infectives that target iron uptake systems, *Angew. Chem. Int. Ed. Engl.* 56 (2017) 14360-14382.
- [21] G.L. Mislin, I.J. Schalk, Siderophore-dependent iron uptake systems as gates for antibiotic Trojan horse strategies against *Pseudomonas aeruginosa*, *Metallomics* 6 (2014) 408-420.
- [22] M.E. Falagas, A.D. Mavroudis, K.Z. Vardakas, The antibiotic pipeline for multi-drug resistant Gram negative bacteria: what can we expect?, *Expert Rev. Anti-infect. Ther.* 14 (2016) 747-763.
- [23] G.G. Zhanel, A.R. Golden, S. Zelenitsky, K. Wiebe, C.K. Lawrence, H.J. Adam, T. Idowu, R. Domalaon, F. Schweizer, M.A. Zhanel, P.R.S. Lagace-Wiens, A.J. Walkty, A. Noreddin, J.P. Lynch III, J.A. Karlowsky, Cefiderocol: a siderophore cephalosporin with activity against carbapenem-resistant and multidrug-resistant Gram-negative Bacilli, *Drugs* 79 (2019) 271-289.
- [24] U.S. Food & Drug administration, FDA approves new antibacterial drug to treat complicated urinary tract infections as part of ongoing efforts to address antimicrobial resistance, <https://www.fda.gov/news-events/press-announcements/fda-approves-new-antibacterial-drug-treat-complicated-urinary-tract-infections-part-ongoing-efforts>, 2019 (accessed 18 December 2019).
- [25] N. Zidar, H. Macut, T. Tomašič, M. Brvar, S. Montalvao, P. Tammela, T. Šolmajer, L. Peterlin Mašič, J. Ilaš, D. Kikelj, *N*-Phenyl-4,5-dibromopyrrolamides and *N*-phenylindolamides as ATP competitive DNA gyrase B inhibitors: design, synthesis, and evaluation, *J. Med. Chem.* 58 (2015) 6179-6194.

- [26] B.A. Sherer, K. Hull, O. Green, G. Basarab, S. Hauck, P. Hill, J.T. Loch 3rd, G. Mullen, S. Bist, J. Bryant, A. Boriack-Sjodin, J. Read, N. DeGrace, M. Uria-Nickelsen, R.N. Illingworth, A.E. Eakin, Pyrrolamide DNA gyrase inhibitors: optimization of antibacterial activity and efficacy, *Bioorg. Med. Chem. Lett.* 21 (2011) 7416-7420.
- [27] Methods for dilution antimicrobial susceptibility tests for bacteria that grow aerobically, approved standard, CLSI, Wayne, Pennsylvania, 2012.
- [28] M.G.P. Page, Siderophore conjugates, *Ann. NY Acad. Sci.* 1277 (2013) 115-126.
- [29] M.D. Huband, A. Ito, M. Tsuji, H.S. Sader, K.A. Fedler, R.K. Flamm, Cefiderocol MIC quality control ranges in iron-depleted cation-adjusted Mueller-Hinton broth using a CLSI M23-A4 multi-laboratory study design, *Diagn. Microbiol. Infect. Dis.* 88 (2017) 198-200.
- [30] M.A. Scorciapino, G. Malloci, I. Serra, S. Milenkovic, L. Moynie, J.H. Naismith, E. Desarbre, M.G.P. Page, M. Ceccarelli, Complexes formed by the siderophore-based monosulfactam antibiotic BAL30072 and their interaction with the outer membrane receptor PiuA of *P. aeruginosa*, *Biomaterials* 32 (2019) 155-170.
- [31] L. Moynie, I. Serra, M.A. Scorciapino, E. Oueis, M.G. Page, M. Ceccarelli, J.H. Naismith, Preacinetobactin not acinetobactin is essential for iron uptake by the BauA transporter of the pathogen *Acinetobacter baumannii*, *Elife* 7 (2018).
- [32] L. Moynie, S. Milenkovic, G.L.A. Mislin, V. Gasser, G. Malloci, E. Baco, R.P. McCaughan, M.G.P. Page, I.J. Schalk, M. Ceccarelli, J.H. Naismith, The complex of ferric-enterobactin with its transporter from *Pseudomonas aeruginosa* suggests a two-site model, *Nat. Commun.* 10 (2019) 3673.
- [33] Y.L. Cho, H.J. Heo, K.M. Oh, H.S. Lee, C.S. Park, S.E. Chae, J.Y. Yun, H.J. Kwon, Y.J. Yang, D.H. Kang, Y.Z. Kim, S.H. Woo, T.K. Park, US Patent, 2012, 0264727 A1.
- [34] M.E. Flanagan, S.J. Brickner, M. Lall, J. Casavant, L. Deschenes, S.M. Finegan, D.M. George, K. Granskog, J.R. Hardink, M.D. Huband, T. Hoang, L. Lamb, A. Marra, M. Mitton-

Fry, J.P. Mueller, L.M. Mullins, M.C. Noe, J.P. O'Donnell, D. Pattavina, J.B. Penzien, B.P. Schuff, J. Sun, D.A. Whipple, J. Young, T.D. Gootz, Preparation, Gram-negative antibacterial activity, and hydrolytic stability of novel siderophore-conjugated monocarbam diols, ACS Med. Chem. Lett. 2 (2011) 385-390.

[35] T. Baba, T. Ara, M. Hasegawa, Y. Takai, Y. Okumura, M. Baba, K.A. Datsenko, M. Tomita, B.L. Wanner, H. Mori, Construction of *Escherichia coli* K-12 in-frame, single-gene knockout mutants: the Keio collection, Mol. Syst. Biol. 2 (2006) 2006 0008.

[36] Subcommittee on antimicrobial susceptibility testing, meeting minutes and presentations, CLSI, 2016.

Supplementary Information for:

Design, Synthesis and Biological Evaluation of Novel DNA Gyrase Inhibitors and their Siderophore Mimic Conjugates

Andraž Lamut,^a Cristina D. Cruz,^b Žiga Skok,^a Michaela Barančoková,^a Nace Zidar,^a Anamarija Zega,^a Lucija Peterlin Mašič,^a Janez Ilaš,^a Päivi Tammela,^b Danijel Kikelj,^a and Tihomir Tomašič,^{a,*}

^a*University of Ljubljana, Faculty of Pharmacy, Aškerčeva cesta 7, 1000 Ljubljana, Slovenia*

^b*Drug Research Program, Division of Pharmaceutical Biosciences, Faculty of Pharmacy, University of Helsinki, P.O. Box 56 (Viikinkaari 5 E), FI-00014 Helsinki, Finland*

***Corresponding author: Tihomir Tomašič**

University of Ljubljana, Faculty of Pharmacy,

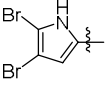
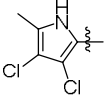
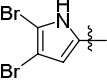
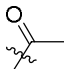
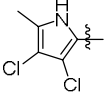
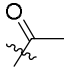
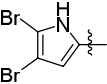
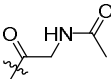
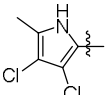
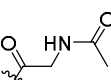
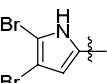
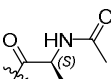
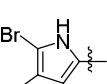
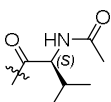
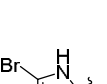
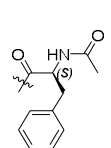
Aškerčeva cesta 7, 1000 Ljubljana, Slovenia

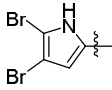
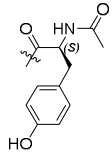
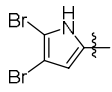
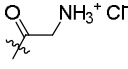
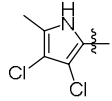
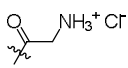
Tel: +386-1-4769556

E-mail: tihomir.tomasic@ffa.uni-lj.si

1. ENZYME INHIBITION

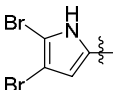
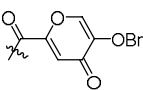
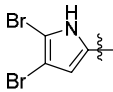
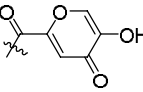
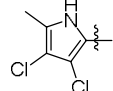
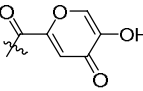
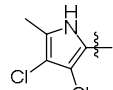
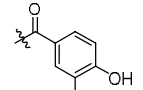
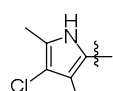
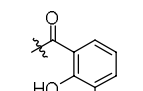
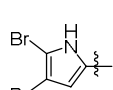
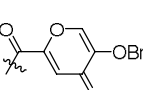
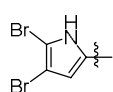
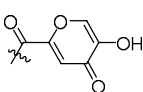
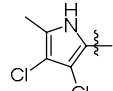
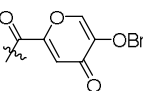
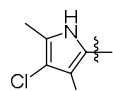
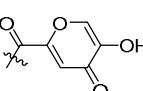
Table S1. Structures of the (*S*)-4,5,6,7-tetrahydrobenzo[*d*]thiazol-6-yl-1*H*-pyrrole-2-carboxamide derivatives and their inhibition of *Escherichia coli* DNA gyrase.

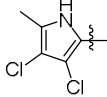
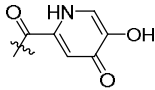
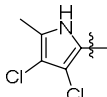
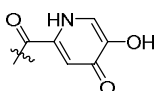
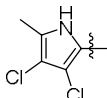
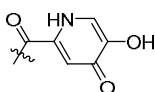
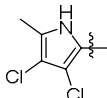
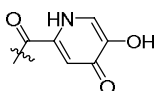
Compound	R ¹	R ²	<i>E. coli</i> DNA gyrase
			IC ₅₀ [μM]
Novobiocin ^a	-	-	0.17
11[10]		H	12
12		H	> 10
13[10]			0.15 ± 0.04
14			0.48 ± 0.11
18			0.52 ± 0.08
19			0.15 ± 0.02
20			0.10 ± 0.01
21			0.15 ± 0.03
22			7.0 ± 0.7

23			2.8 ± 0.4
29			1.1 ± 0.1
30			1.8 ± 0.2

^aNovobiocin used as positive control in enzyme assays

Table S2. Structures of the (*S*)-4,5,6,7-tetrahydrobenzo[*d*]thiazol-6-yl-1*H*-pyrrole-2-carboxamide GyrB inhibitor–siderophore mimic conjugates (**15-17**, **34-39**, **44-47**) and their inhibition of *Escherichia coli* DNA gyrase.

Compound	R ₁	R ₂	R ₃	n	<i>E. coli</i> DNA gyrase
					IC ₅₀ [μM]
Novobiocin ^a	-	-	-	-	0.17
15			-	-	3.4 ± 0.7
16			-	-	0.18 ± 0.05
17			-	-	2.1 ± 0.4
34			H	1	0.058 ± 0.090
35			H	1	0.11 ± 0.02
36			H	1	2.0 ± 0.5
37			H	1	0.69 ± 0.05
38			H	1	2.1 ± 0.1
39			H	1	0.090 ± 0.042

44			H	1	1.6 ± 0.1
45			Me	1	0.26 ± 0.05
46			<i>i</i> -Pr	1	0.64 ± 0.13
47			H	2	0.35 ± 0.09

^aNovobiocin used as positive control in enzyme assays

2. ANTIBACTERIAL ACTIVITY

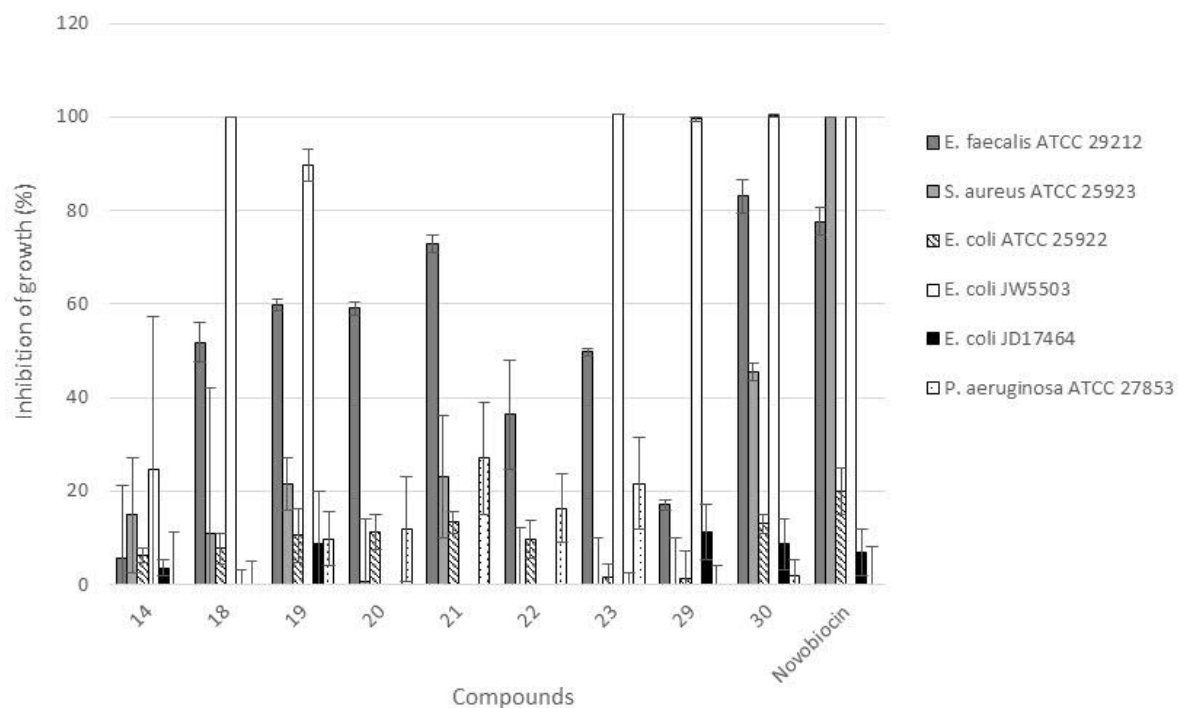


Figure S1. Antibacterial activities of new DNA gyrase inhibitors **14**, **18-23**, **29** and **30** against selected Gram-positive and Gram-negative bacterial strains in CAMHB media. Inhibition of growth was determined at 50 μ M of the tested compound relative to untreated control. Novobiocin at 4 μ g/mL was used as a positive control. Compounds **20-22** were not tested against *E. coli* mutant strains.

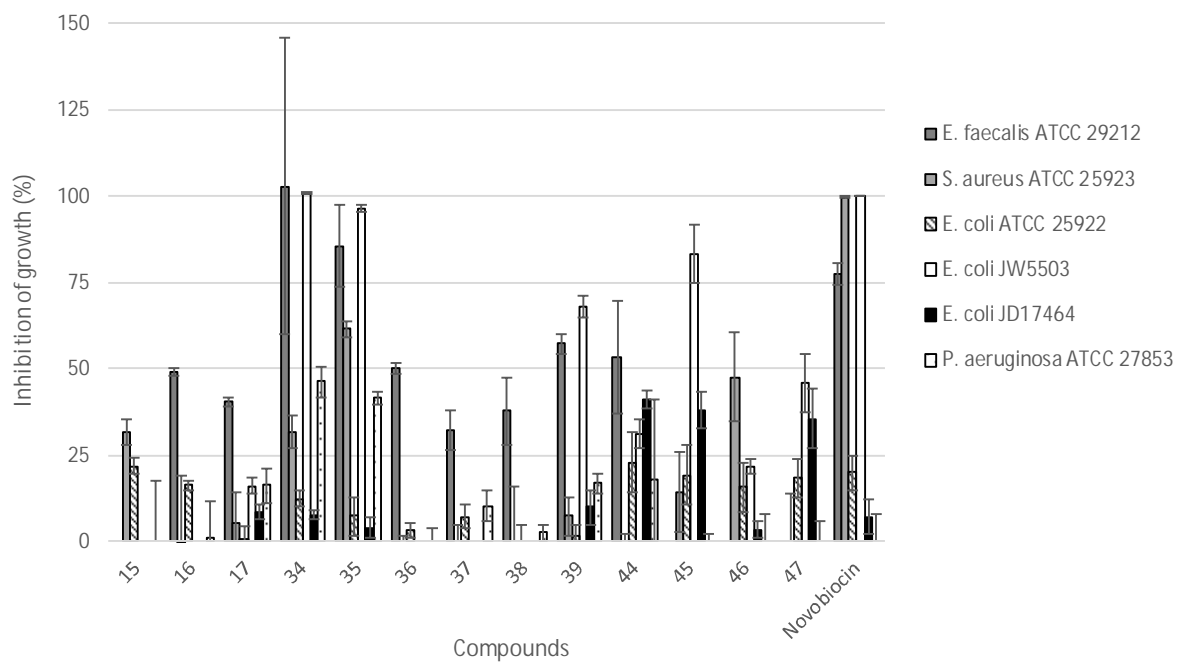


Figure S2. Antibacterial activities of new DNA gyrase inhibitor–siderophore mimic conjugates **15-17**, **34-39** and **44-47** against selected Gram-positive and Gram-negative bacterial strains, in CAMHB media. Inhibition of growth was determined at 50 μ M of the tested compound relative to untreated control. Novobiocin at 4 μ g/mL was used as a positive control. Compounds **15**, **16** and **36-38** were not tested against *E. coli* mutant strains. Compounds **15**, **16**, **34**, **35**, **39** and **44-47** were tested against *S. aureus* ATCC29213.

Table S3. Minimum inhibitory concentration (MIC) of the most potent compounds from initial screening at 50 μ M against *E. faecalis* ATCC 29212 and *E. coli* JW5503.

Compounds	MIC [μ g/mL] ^a	
	<i>E. faecalis</i>	<i>E. coli</i>
	ATCC 29212	JW5503
Inhibitor + linker		
18	nt ^b	13
19	nt	1
23	nt	16
29	nt	26
30	55	11
Inhibitor + siderophore mimic		
34	> 40	14
35	40	14
Controls		
Ciprofloxacin	1	0.005
Novobiocin	> 4	1

^aMIC, minimum inhibitory concentration that inhibits the growth of bacteria by $\geq 90\%$

^bnot tested: screening assays performed with compound's concentration at 50 μ M did not reach inhibition $\geq 90\%$

Table S4. Antibacterial activities of the DNA gyrase inhibitors and inhibitor-siderophore mimic conjugates against *Escherichia coli*, *Pseudomonas aeruginosa* and *Acinetobacter baumannii* in cation-adjusted Mueller-Hinton broth as either iron-depleted (-Fe) or iron-supplemented (+Fe).

	<i>E. coli</i> ATCC 25922		<i>P. aeruginosa</i> ATCC 27853		<i>A. baumannii</i> ATCC 19606	
	-Fe	+Fe	-Fe	+Fe	-Fe	+Fe
Minimum inhibitory concentrations [$\mu\text{g/mL}$]^a						
Cefiderocol ^c	0.25	0.25	0.5	1	0.25	2
Ceftazidime ^d	0.25	0.25	2	2	>4	>4
Growth inhibition [%]^b \pm SD						
Inhibitor + linker						
13	3 \pm 5	2 \pm 5	nt ^e	nt	nt	nt
14	0 \pm 4	0 \pm 1	nt	nt	nt	nt
18	5 \pm 3	5 \pm 5	nt	nt	nt	nt
20	5 \pm 1	4 \pm 7	nt	nt	nt	nt
21	4 \pm 10	10 \pm 1	nt	nt	nt	nt
29	14 \pm 1	19 \pm 4	nt	nt	nt	nt
Inhibitor + siderophore mimic						
16	20 \pm 4	0 \pm 2	13 \pm 3	10 \pm 3	17 \pm 10	9 \pm 1
17	8 \pm 6	1 \pm 1	7 \pm 5	0 \pm 5	1 \pm 9	7 \pm 1
34	26 \pm 4	7 \pm 2	24 \pm 5	26 \pm 3	29 \pm 8	22 \pm 2
35	25 \pm 1	4 \pm 5	32 \pm 3	71 \pm 3	18 \pm 6	23 \pm 1
37	10 \pm 3	7 \pm 3	3 \pm 2	7 \pm 6	0 \pm 5	2 \pm 2
39	24 \pm 2	0 \pm 1	16 \pm 7	2 \pm 1	28 \pm 9	10 \pm 1
44	23 \pm 4	32 \pm 6	36 \pm 6	52 \pm 0	36 \pm 4	34 \pm 1
45	50 \pm 1	42 \pm 2	39 \pm 5	57 \pm 1	58 \pm 3	64 \pm 1
46	45 \pm 2	31 \pm 6	32 \pm 8	39 \pm 1	58 \pm 1	37 \pm 2
47	21 \pm 9	31 \pm 2	26 \pm 8	55 \pm 1	47 \pm 2	44 \pm 3

^aMinimum inhibitory concentration that inhibits growth of the bacteria by $\geq 90\%$

^bInhibition of growth at 50 μM of the tested compound relative to the control

^cCefiderocol used as positive control

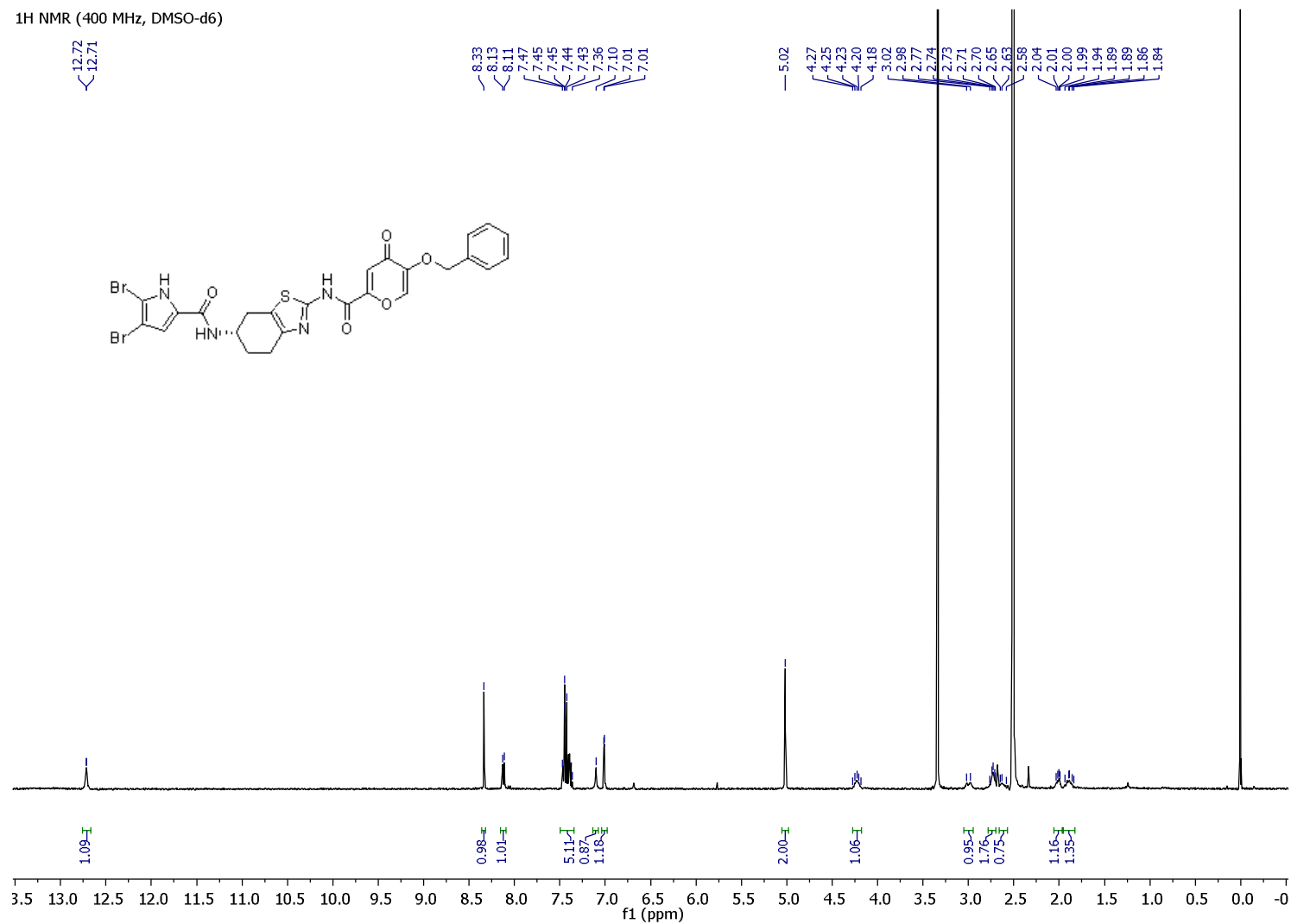
^dCeftazidime used as negative control

^enot tested

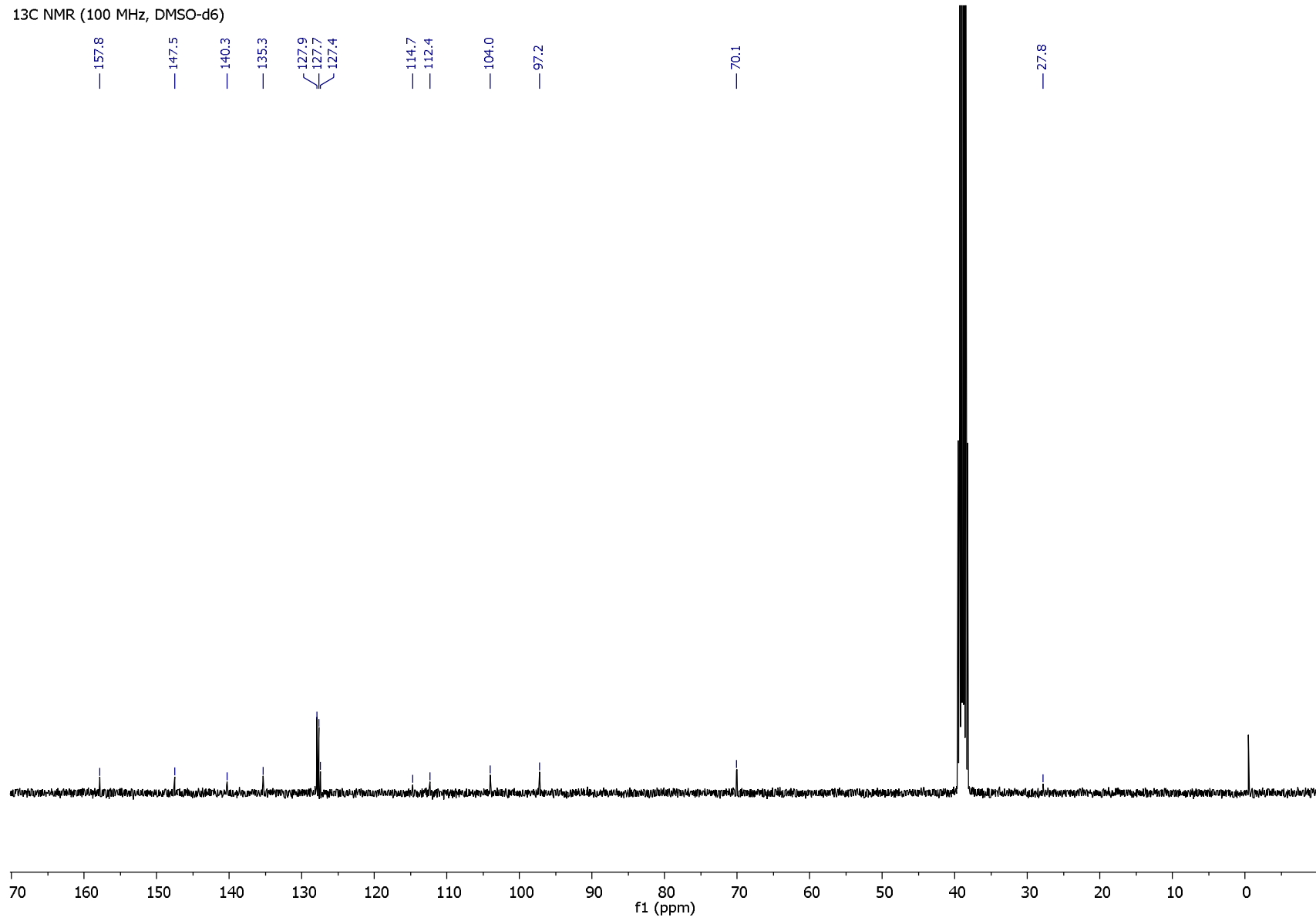
3. ¹H AND ¹³C NMR SPECTRA OF THE REPRESENTATIVE COMPOUNDS

(*S*)-*N*-(2-(5-(Benzyloxy)-4-oxo-4*H*-pyran-2-carboxamido)-4,5,6,7-tetrahydrobenzo[*d*]thiazol-6-yl)-4,5-dibromo-1*H*-pyrrole-2-carboxamide (**15**).

¹H NMR (400 MHz, DMSO-*d*₆)

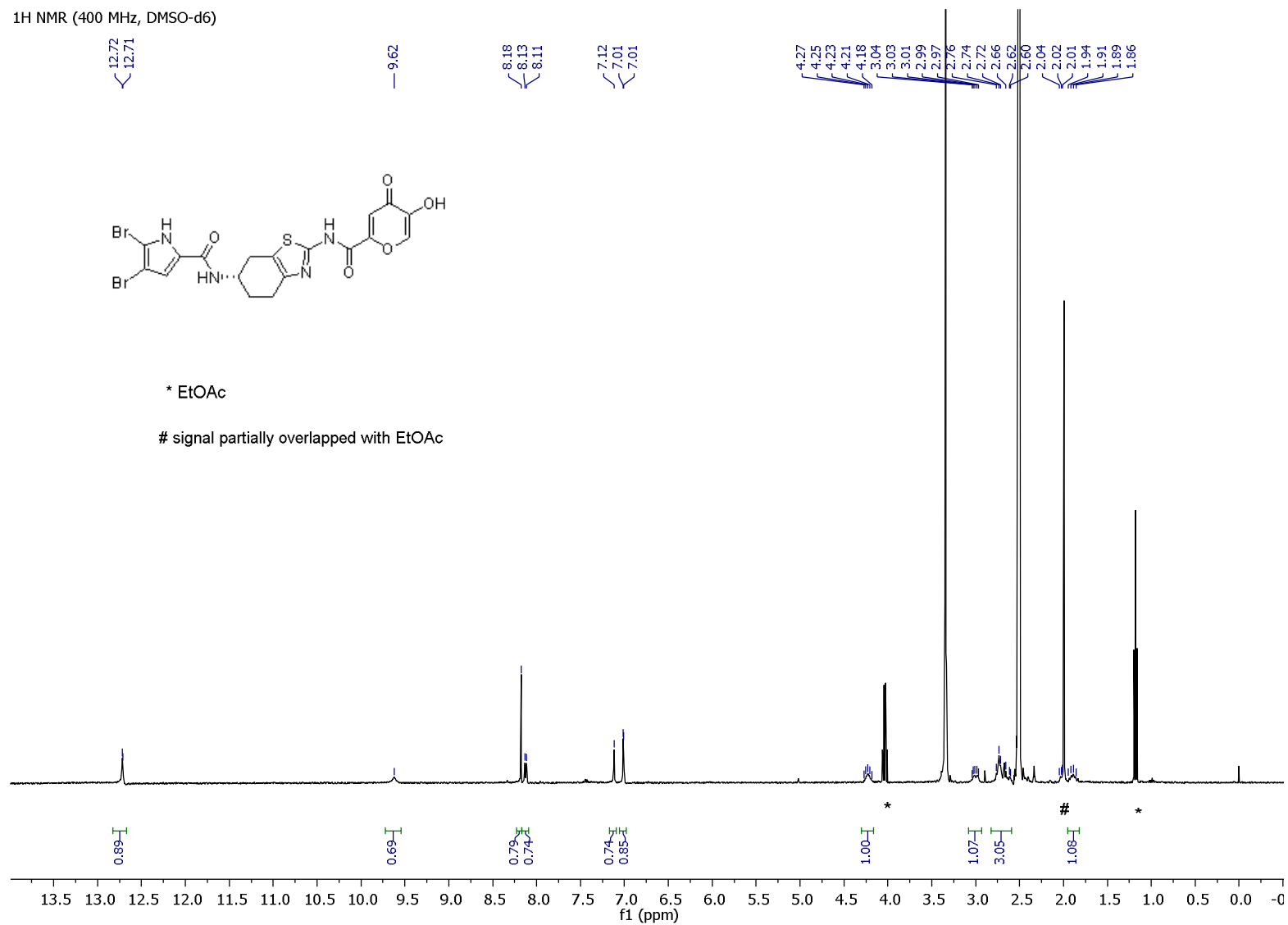


¹³C NMR (100 MHz, DMSO-d₆)

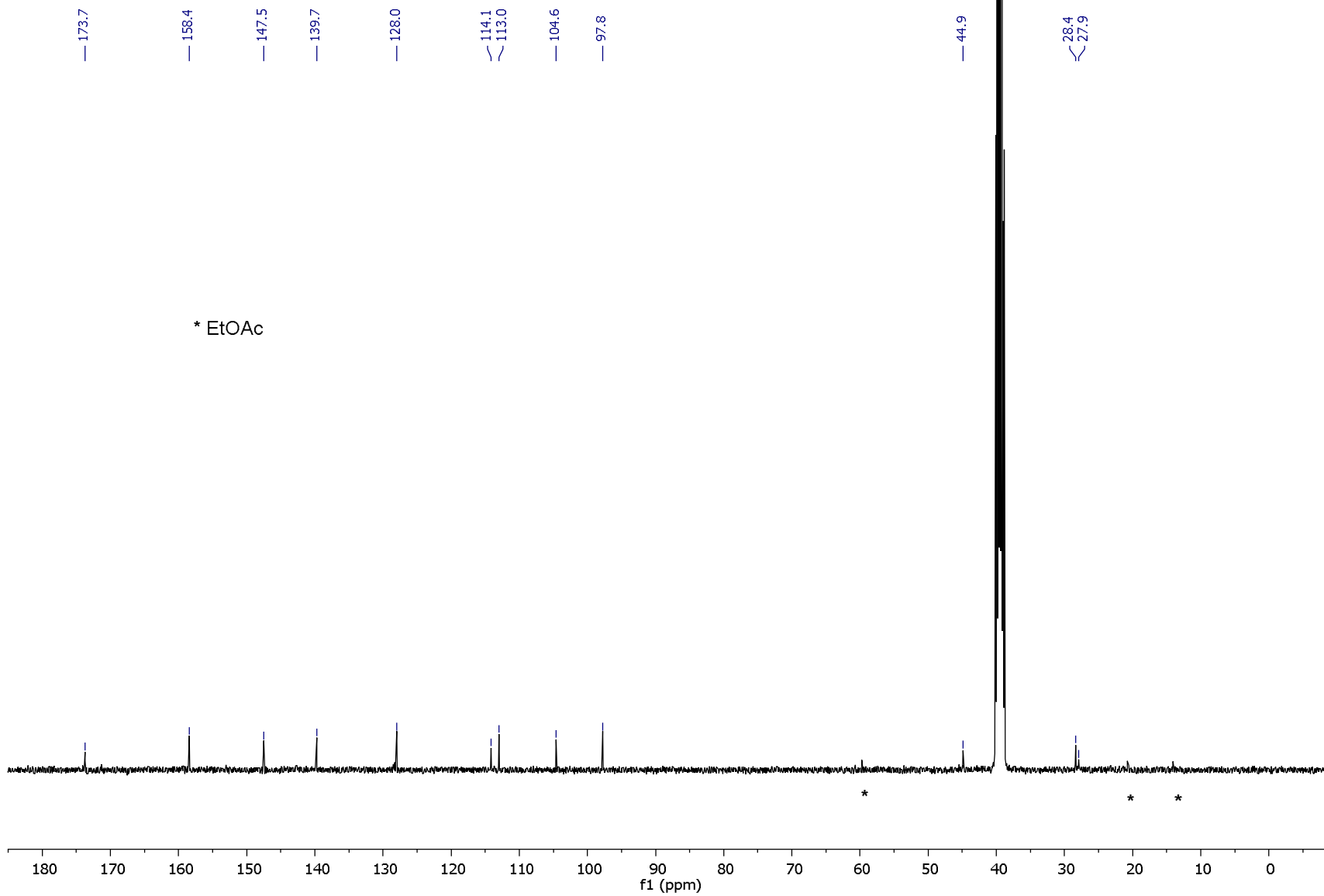


(S)-4,5-Dibromo-N-(2-(5-hydroxy-4-oxo-4H-pyran-2-carboxamido)-4,5,6,7-tetrahydrobenzo[d]thiazol-6-yl)-1H-pyrrole-2-carboxamide (**16**).

¹H NMR (400 MHz, DMSO-d₆)

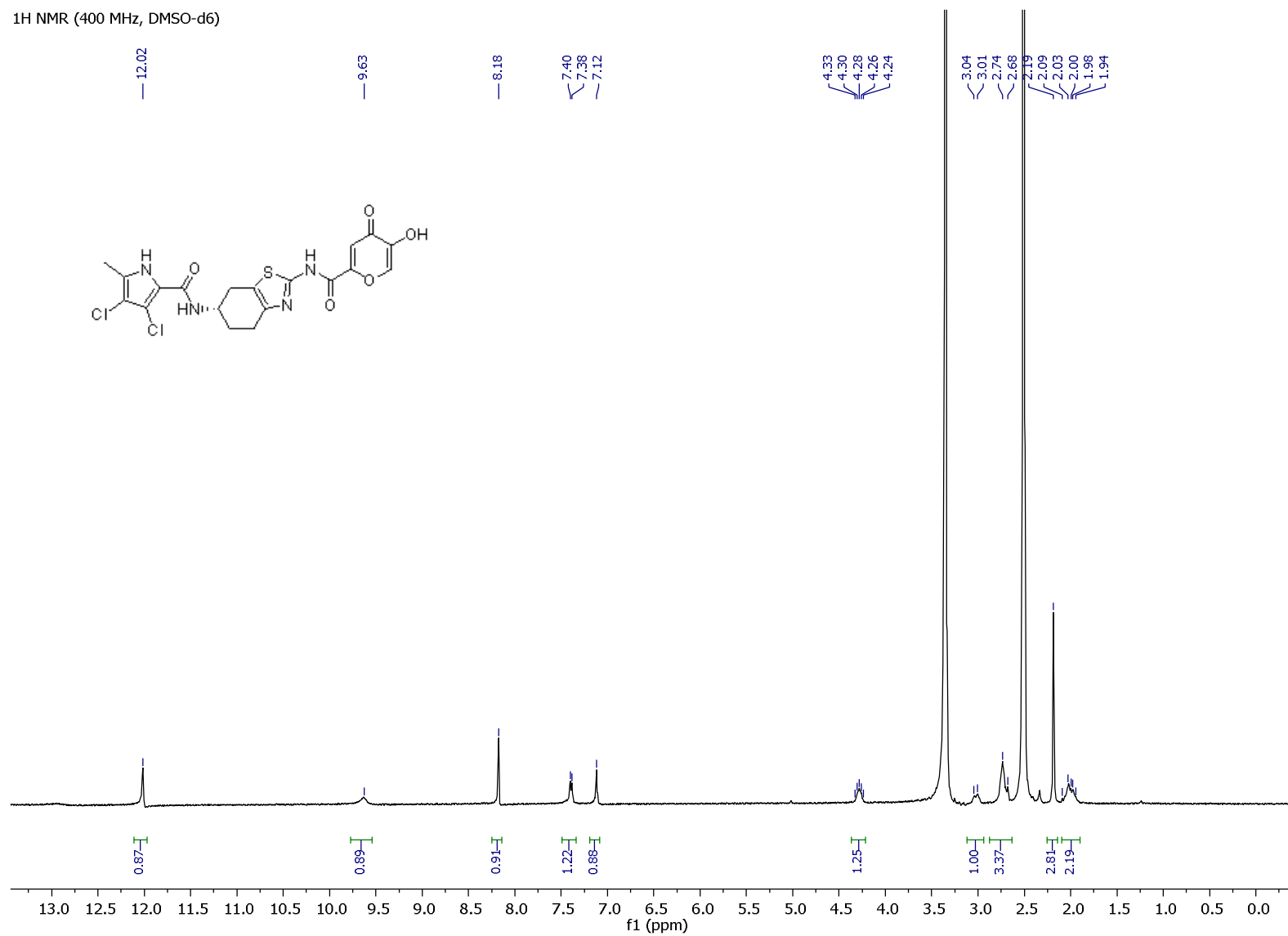


¹³C NMR (100 MHz, DMSO-d₆)

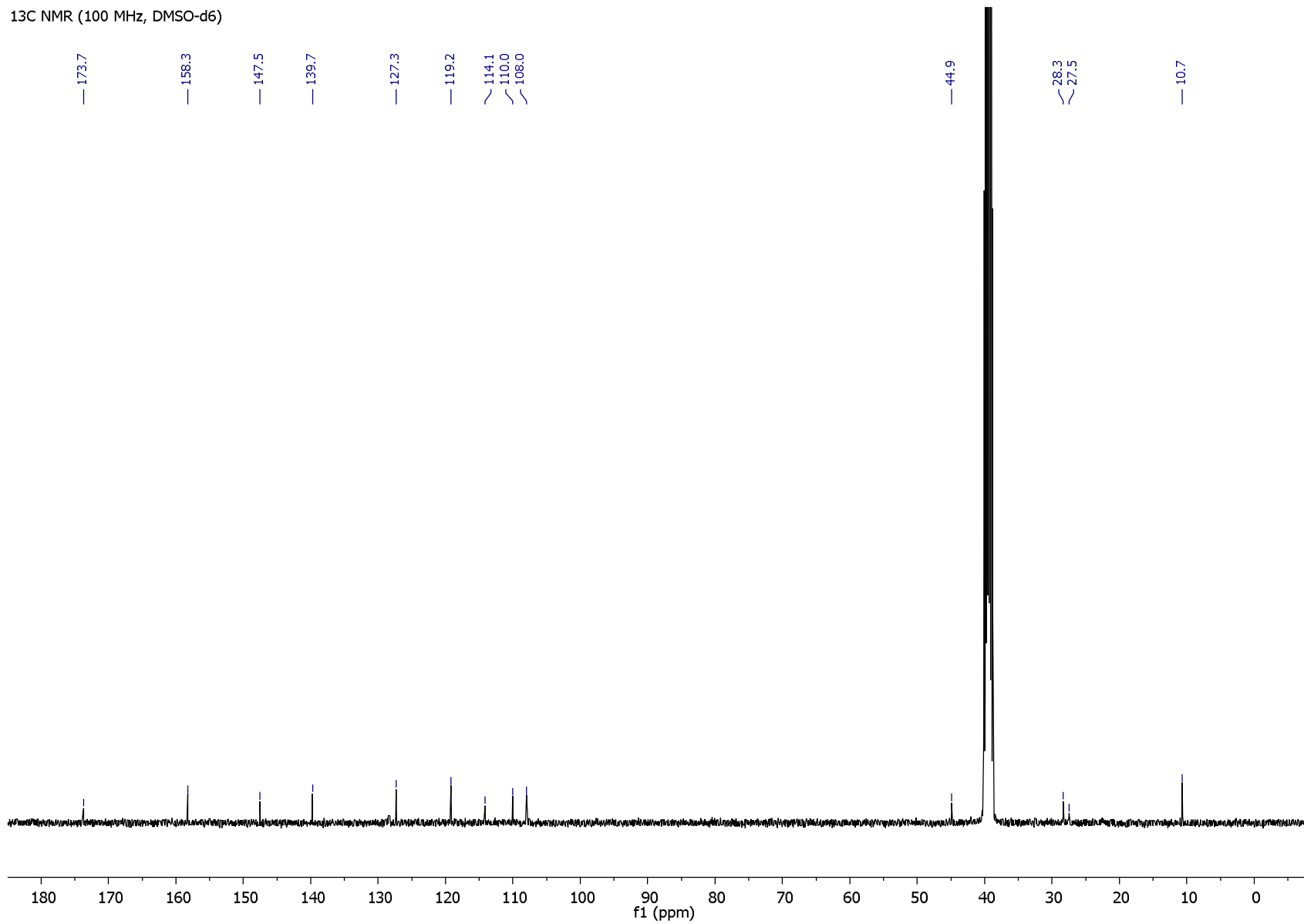


(S)-3,4-Dichloro-*N*-(2-(5-hydroxy-4-oxo-4*H*-pyran-2-carboxamido)-4,5,6,7-tetrahydrobenzo[*d*]thiazol-6-yl)-5-methyl-1*H*-pyrrole-2-carboxamide (**17**).

¹H NMR (400 MHz, DMSO-*d*₆)

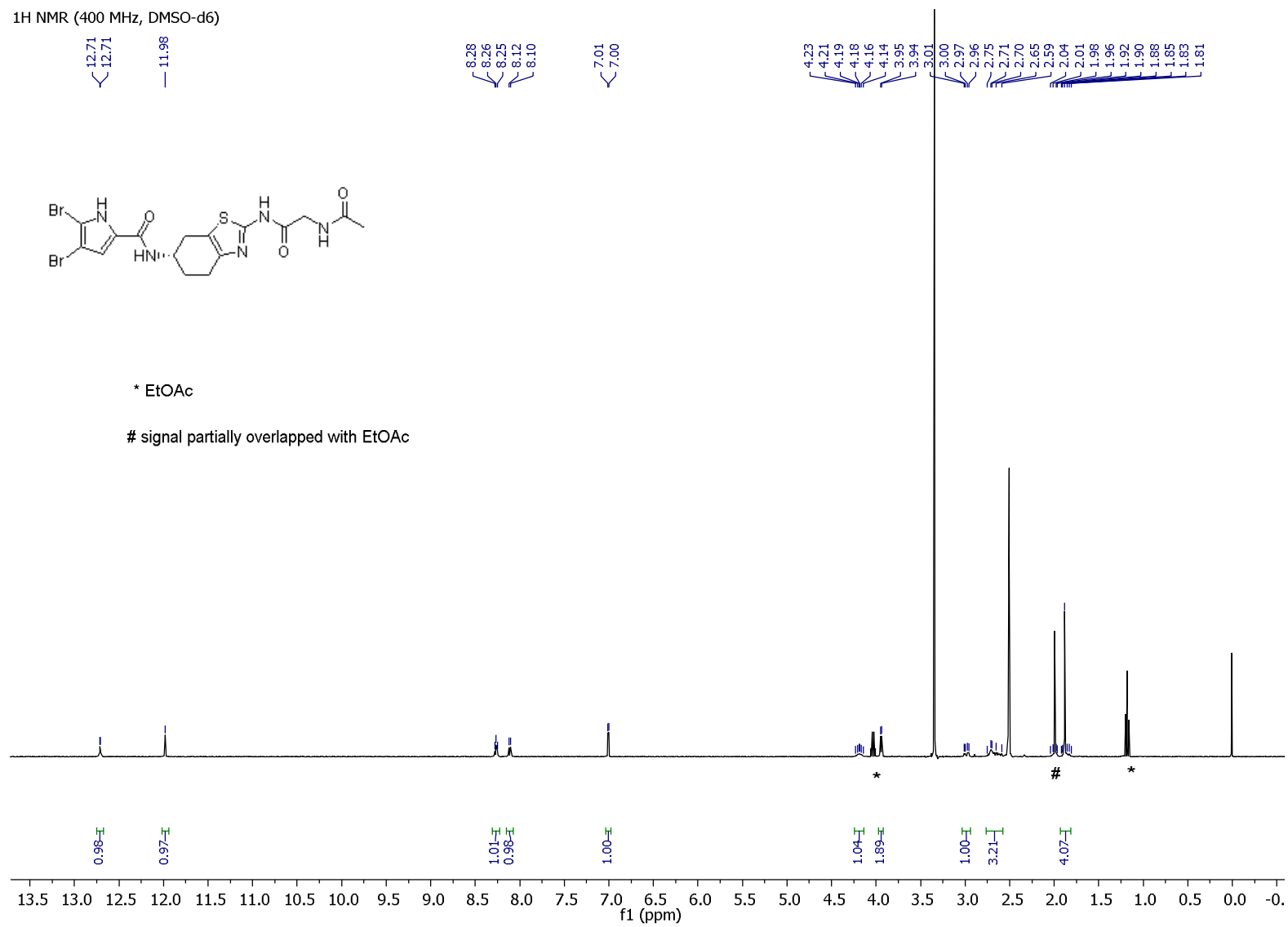


¹³C NMR (100 MHz, DMSO-d₆)

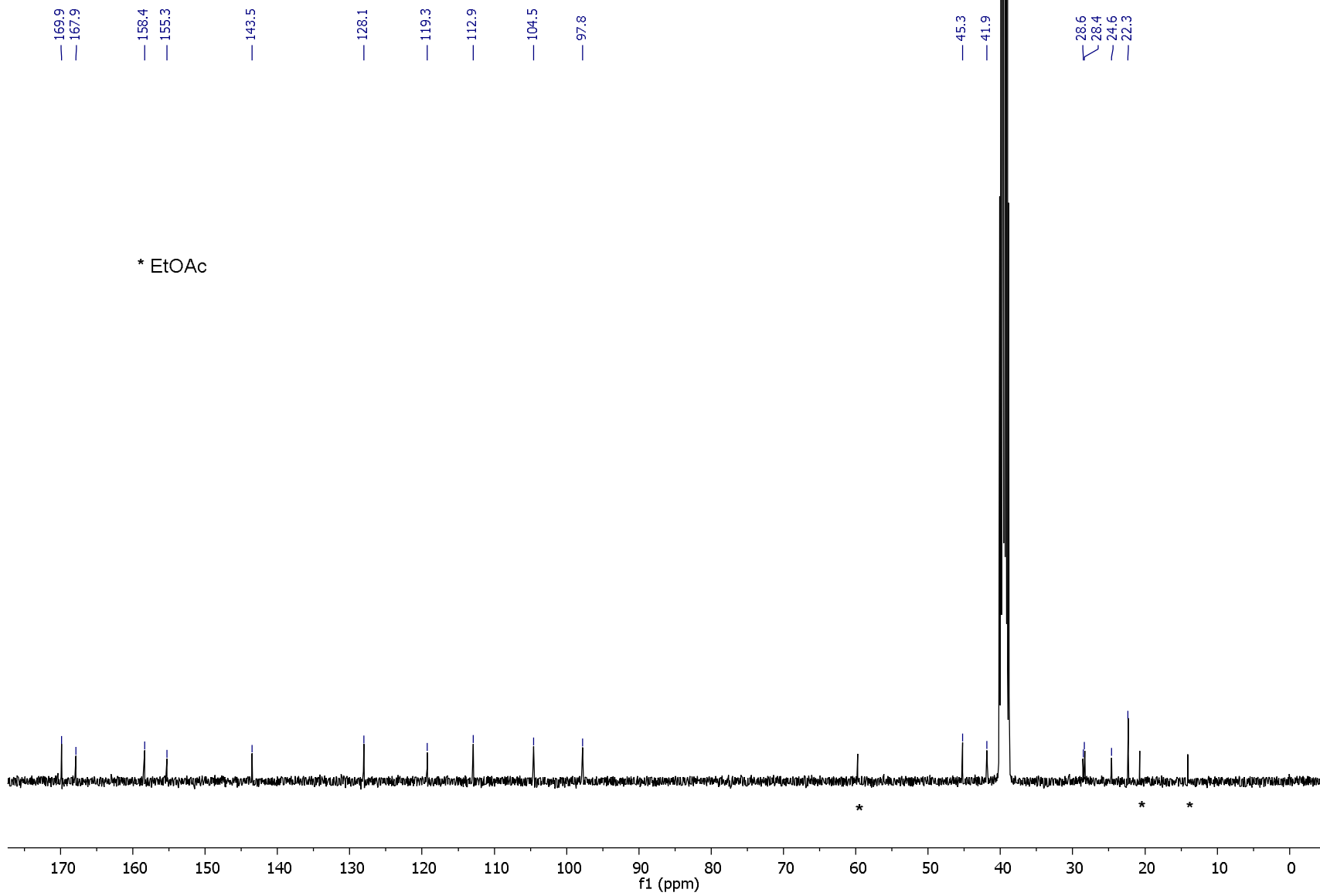


(S)-*N*-(2-(2-Acetamidoacetamido)-4,5,6,7-tetrahydrobenzo[*d*]thiazol-6-yl)-4,5-dibromo-1*H*-pyrrole-2-carboxamide (**18**).

¹H NMR (400 MHz, DMSO-*d*₆)

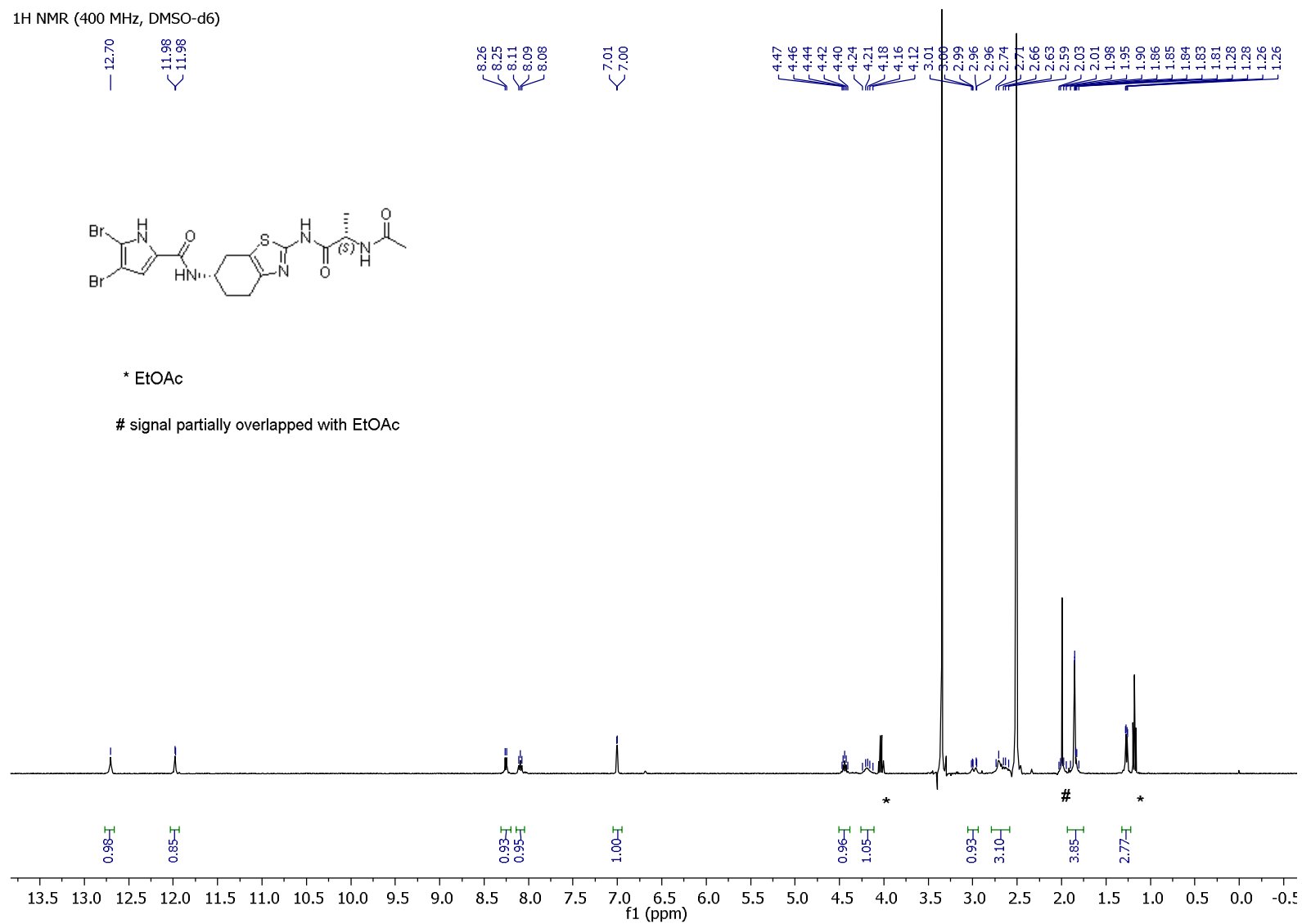


¹³C NMR (100 MHz, DMSO-d₆)

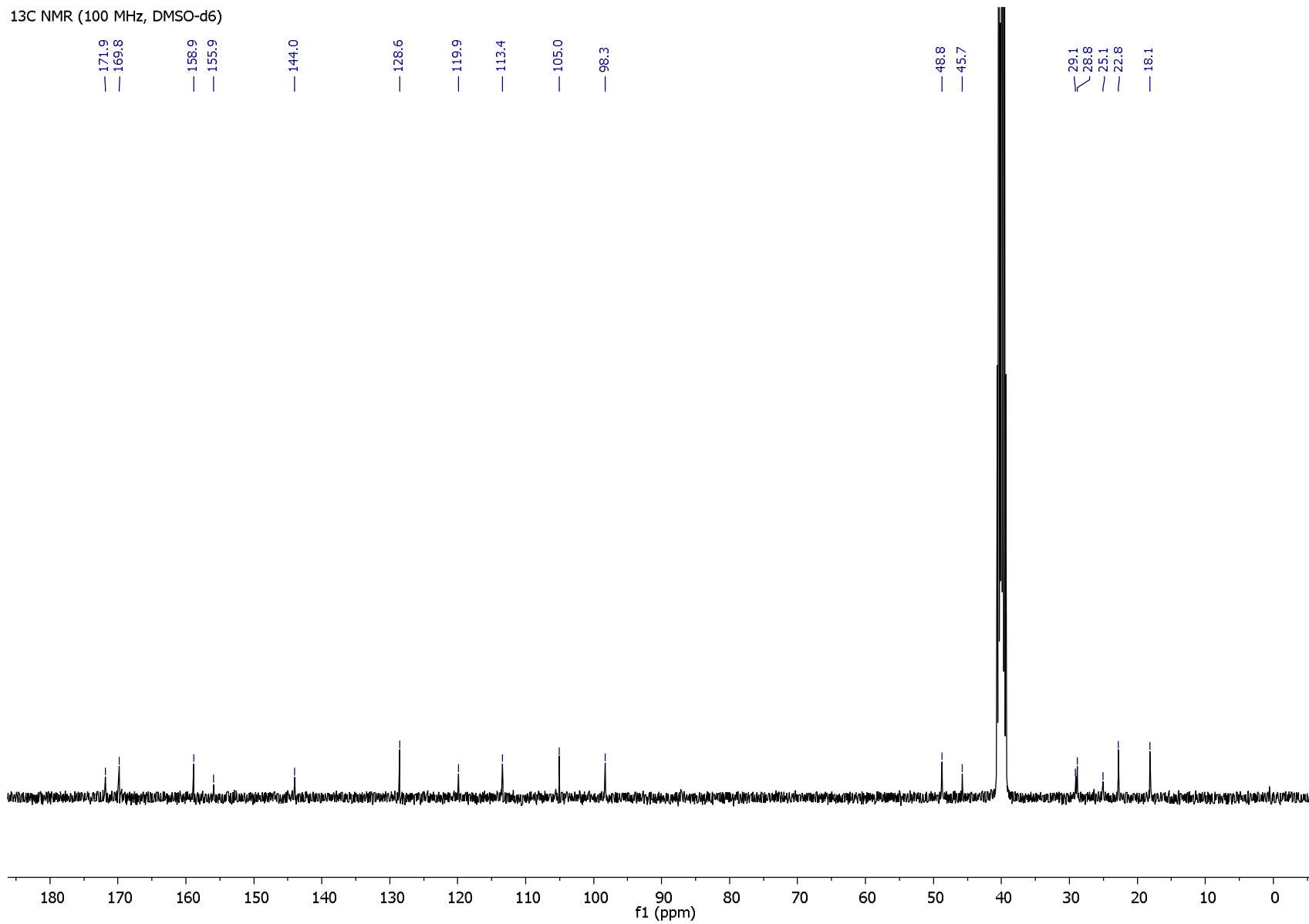


N-((*S*)-2-((*S*)-2-Acetamidopropanamido)-4,5,6,7-tetrahydrobenzo[*d*]thiazol-6-yl)-4,5-dibromo-1*H*-pyrrole-2-carboxamide (**20**).

¹H NMR (400 MHz, DMSO-*d*₆)



¹³C NMR (100 MHz, DMSO-d₆)



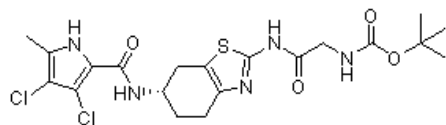
Tert-butyl (S)-2-((6-(3,4-dichloro-5-methyl-1H-pyrrole-2-carboxamido)-4,5,6,7-tetrahydrobenzo[d]thiazol-2-yl)amino)-2-oxoethyl)carbamate (25).

¹H NMR (400 MHz, DMSO-d₆)

12.02
11.95

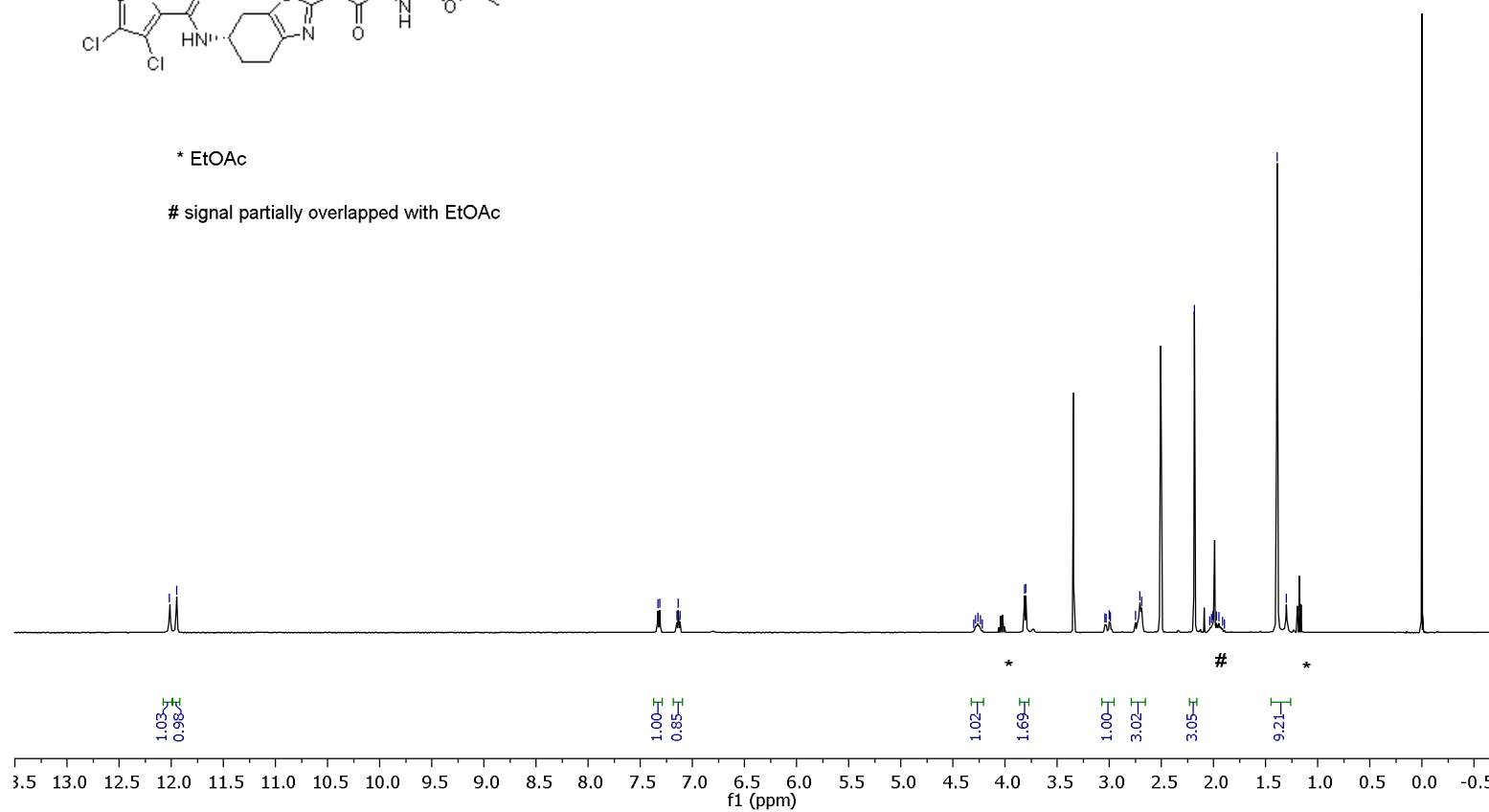
7.33
7.31
7.15
7.14
7.12

4.30
4.28
4.26
4.24
4.22
3.82
3.80
3.04
3.03
3.00
2.99
2.75
2.71
2.69
2.18
2.04
2.02
2.01
1.97
1.95
1.92
1.90
1.39
1.30

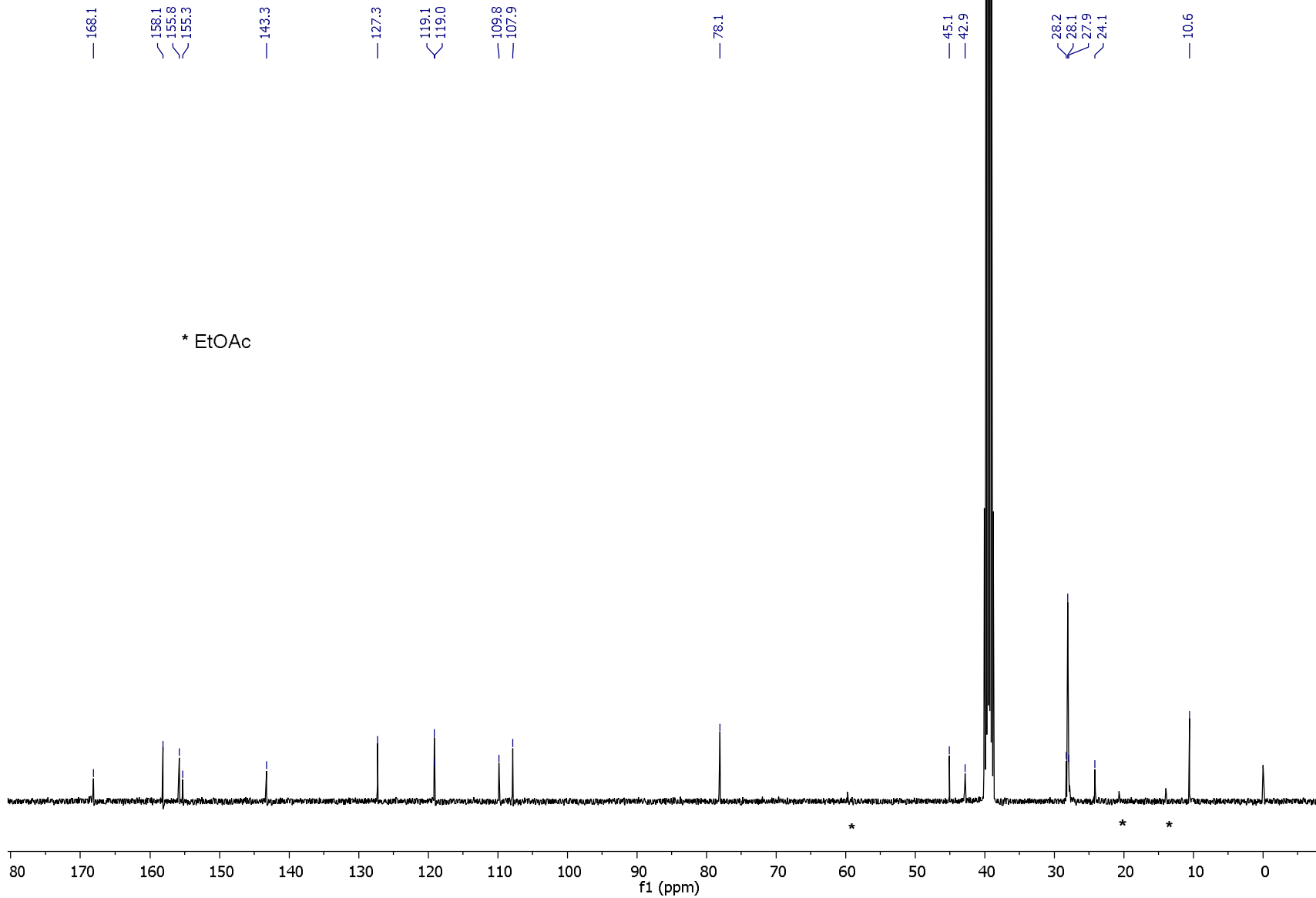


* EtOAc

signal partially overlapped with EtOAc

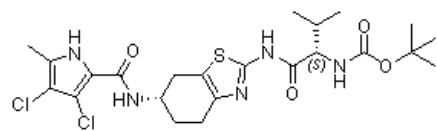


¹³C NMR (100 MHz, DMSO-d₆)



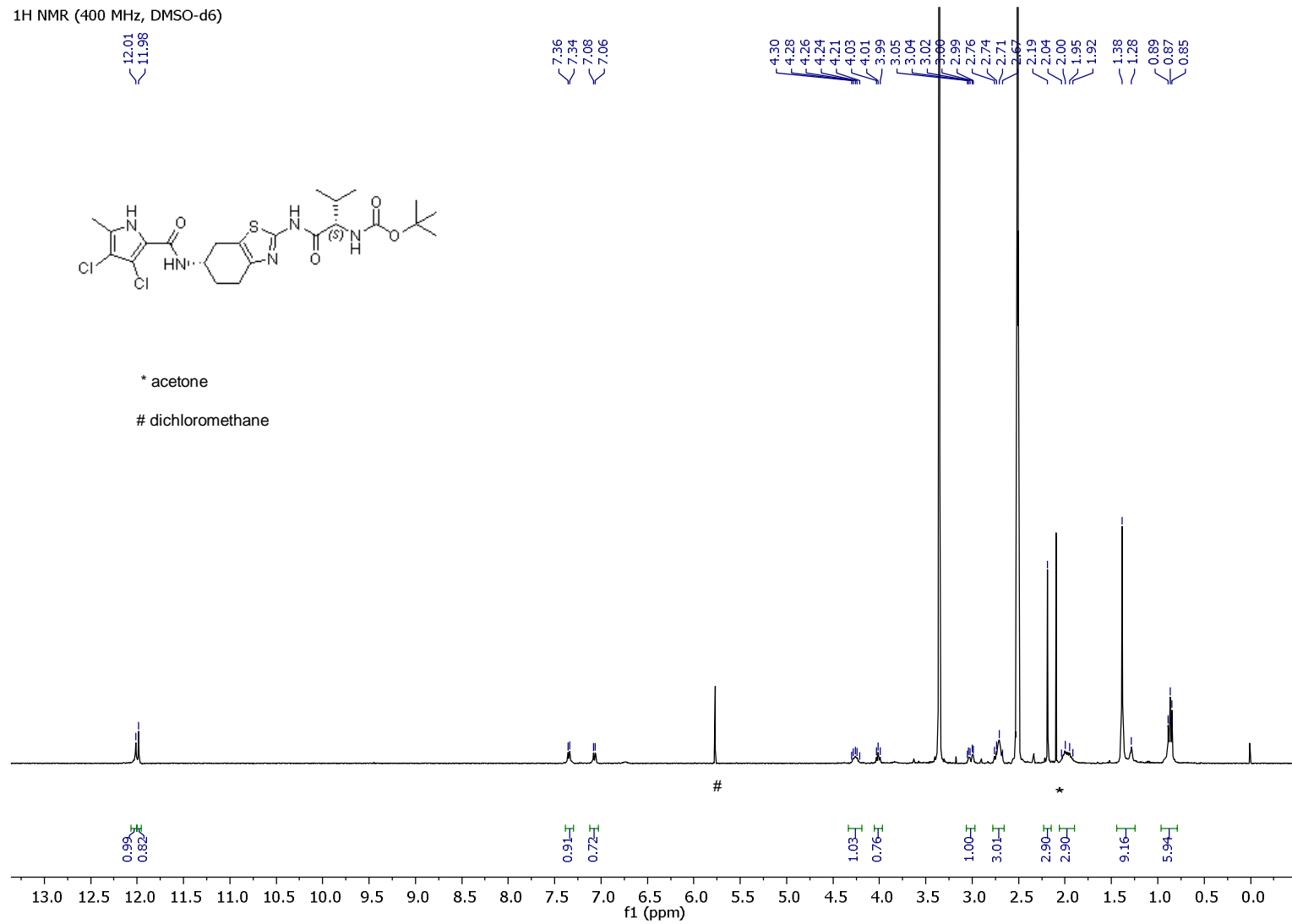
Tert-butyl ((S)-1-(((S)-6-(3,4-dichloro-5-methyl-1H-pyrrole-2-carboxamido)-4,5,6,7-tetrahydrobenzo[d]thiazol-2-yl)amino)-3-methyl-1-oxobutan-2-yl)carbamate (**27**).

¹H NMR (400 MHz, DMSO-d₆)

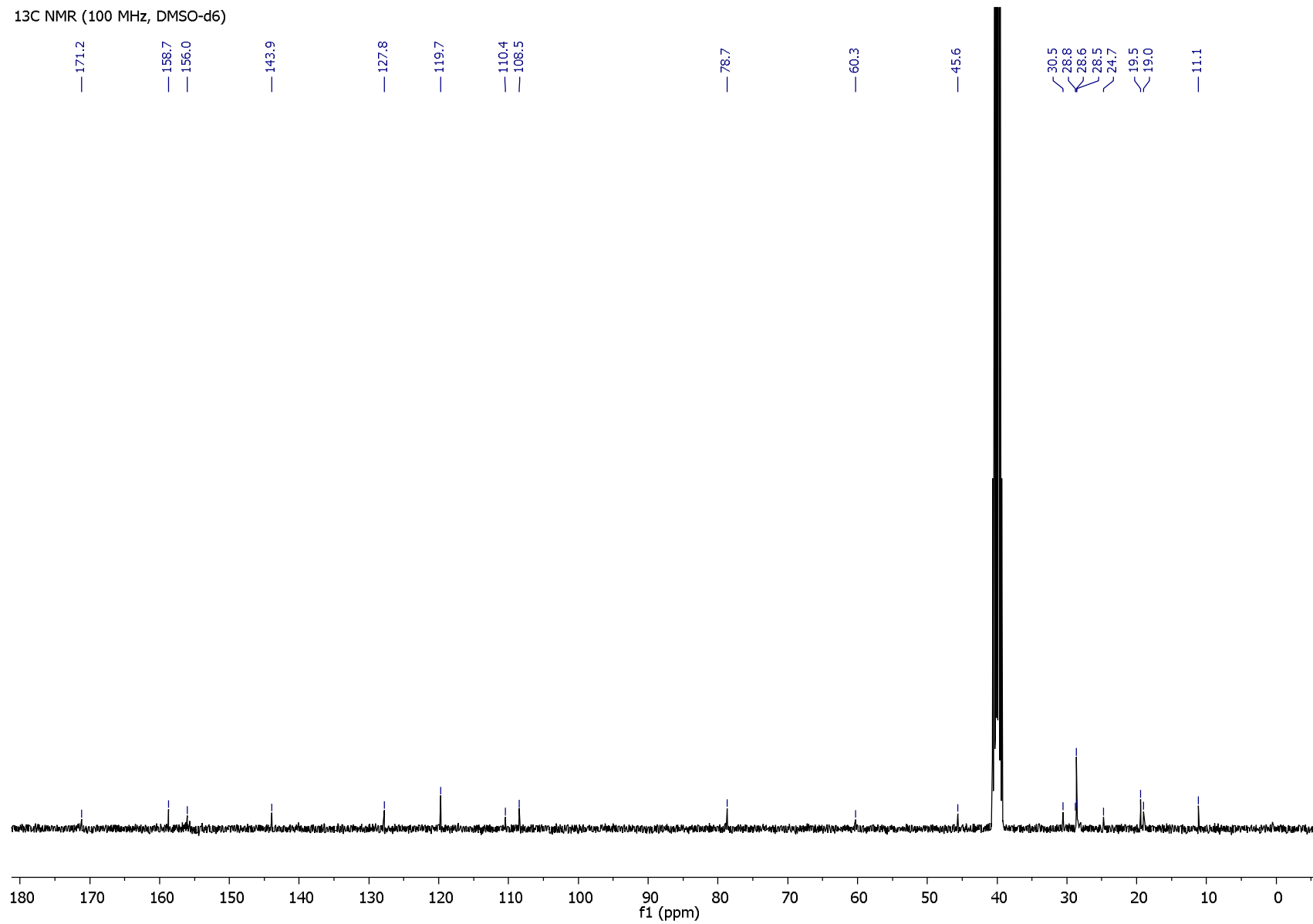


* acetone

dichloromethane

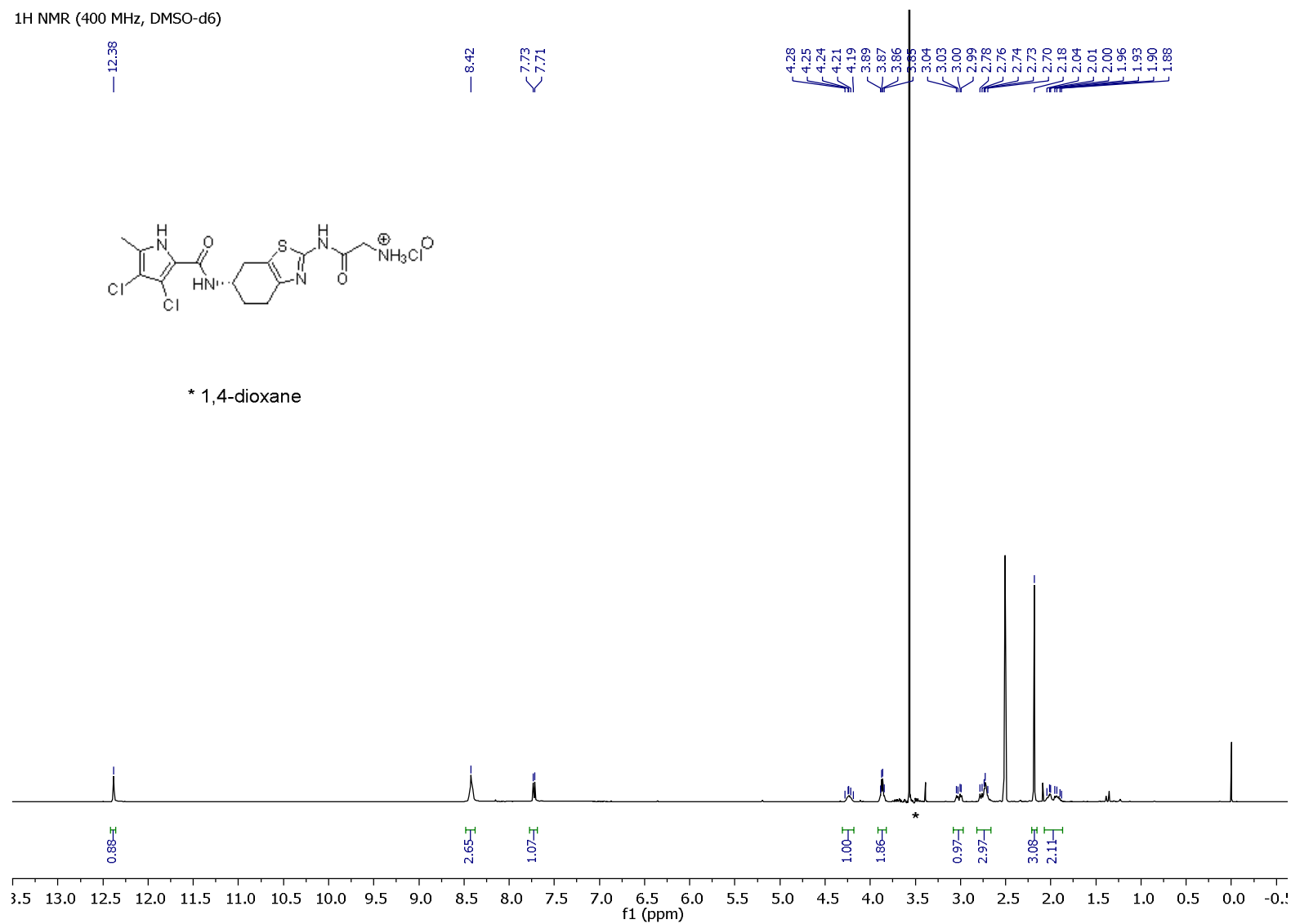


¹³C NMR (100 MHz, DMSO-d₆)



(S)-2-((6-(3,4-Dichloro-5-methyl-1H-pyrrole-2-carboxamido)-4,5,6,7-tetrahydrobenzo[d]thiazol-2-yl)amino)-2-oxoethan-1-aminium chloride (**30**).

¹H NMR (400 MHz, DMSO-d₆)



13C NMR (100 MHz, DMSO-d6)

— 164.9

— 158.1

— 127.1

119.8

119.0

— 110.4

— 107.9

— 45.0

— 40.5

28.2

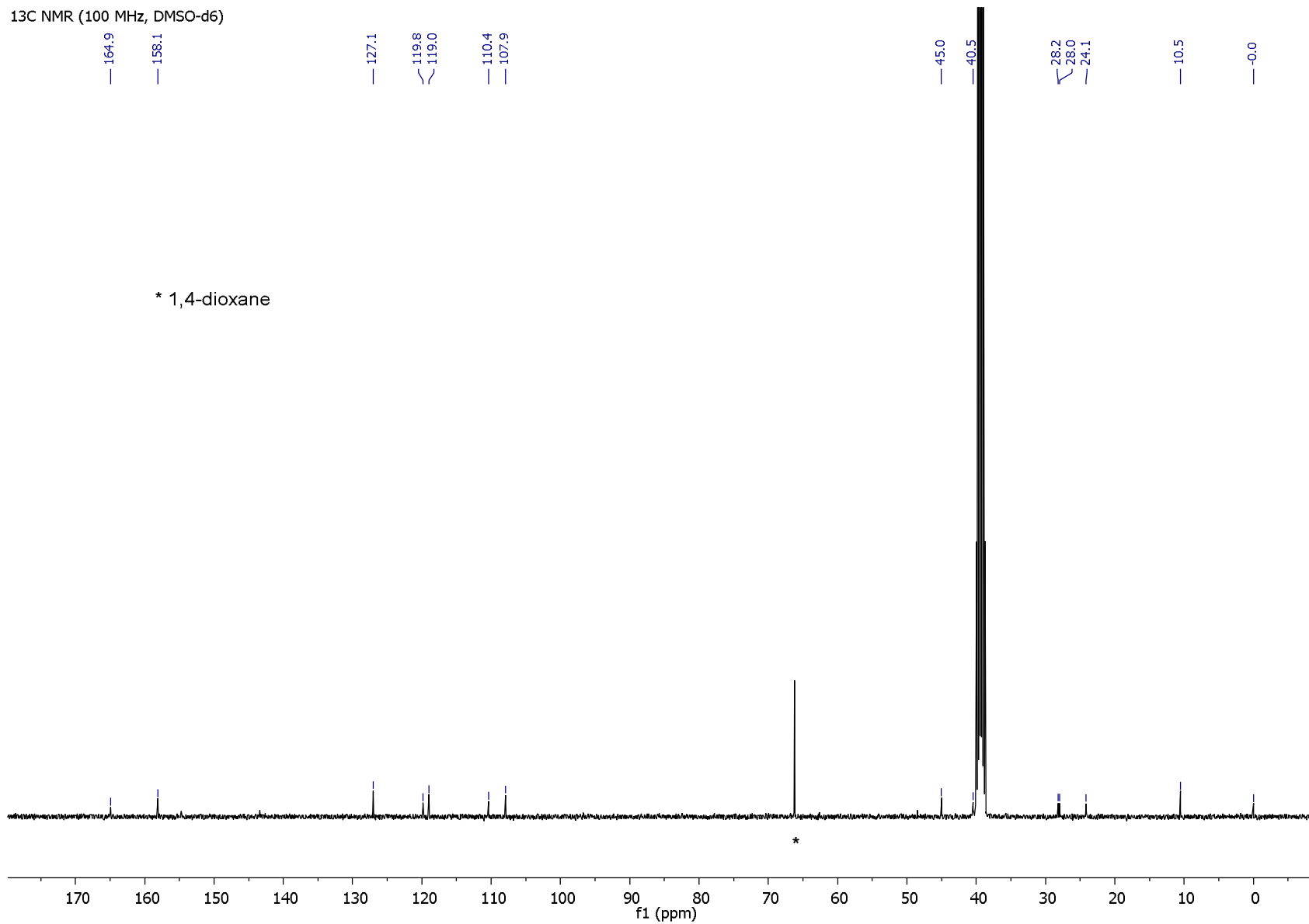
28.0

24.1

— 10.5

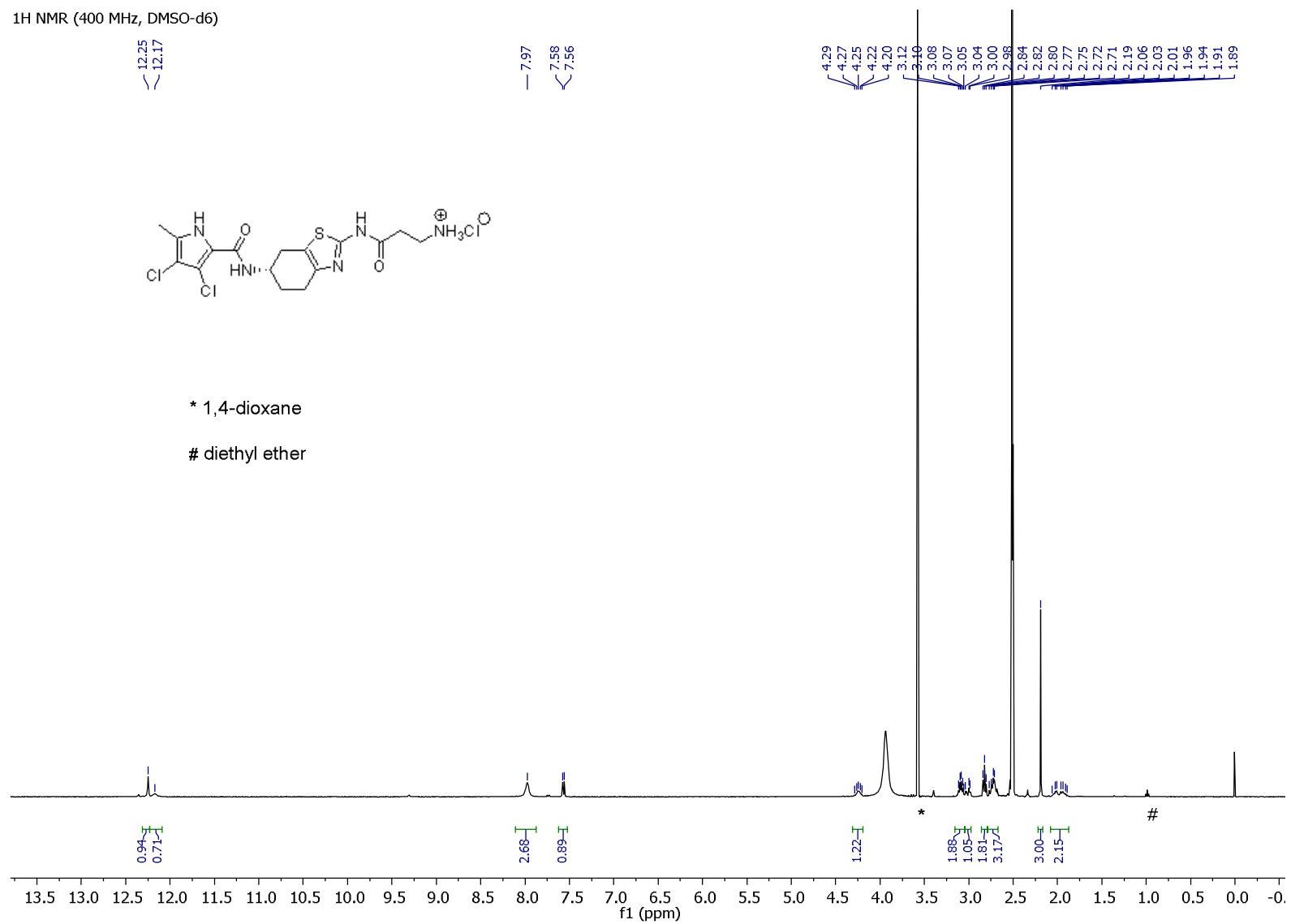
— 0.0

* 1,4-dioxane



(S)-3-((6-(3,4-Dichloro-5-methyl-1H-pyrrole-2-carboxamido)-4,5,6,7-tetrahydrobenzo[d]thiazol-2-yl)amino)-3-oxopropan-1-aminium chloride (**33**).

¹H NMR (400 MHz, DMSO-d₆)



¹³C NMR (100 MHz, DMSO-d₆)

— 168.7

— 158.6

— 155.7

— 143.7

— 127.5

119.8

119.5

— 111.1

— 108.5

— 45.7

34.8

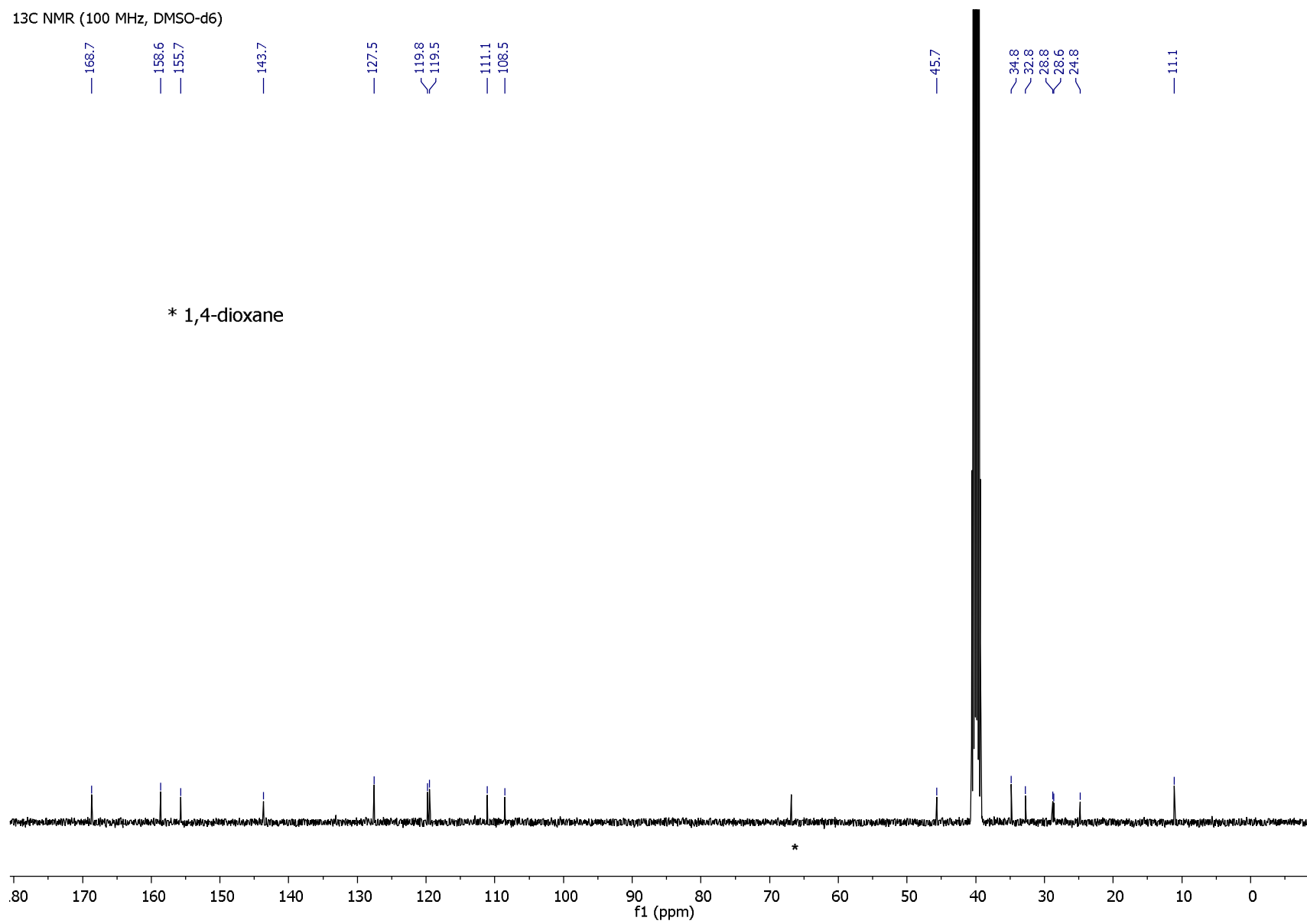
32.8

28.6

24.8

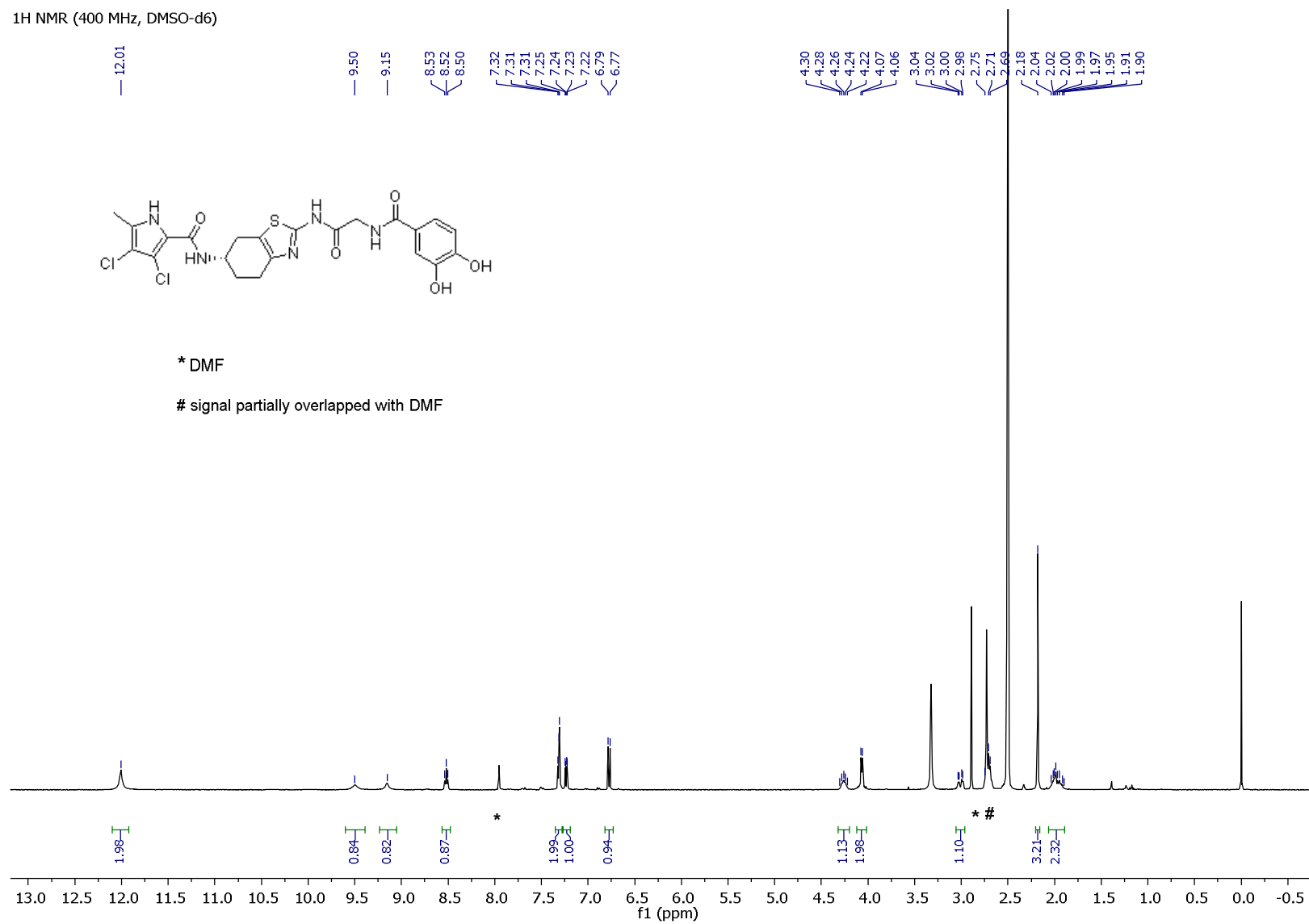
— 11.1

* 1,4-dioxane

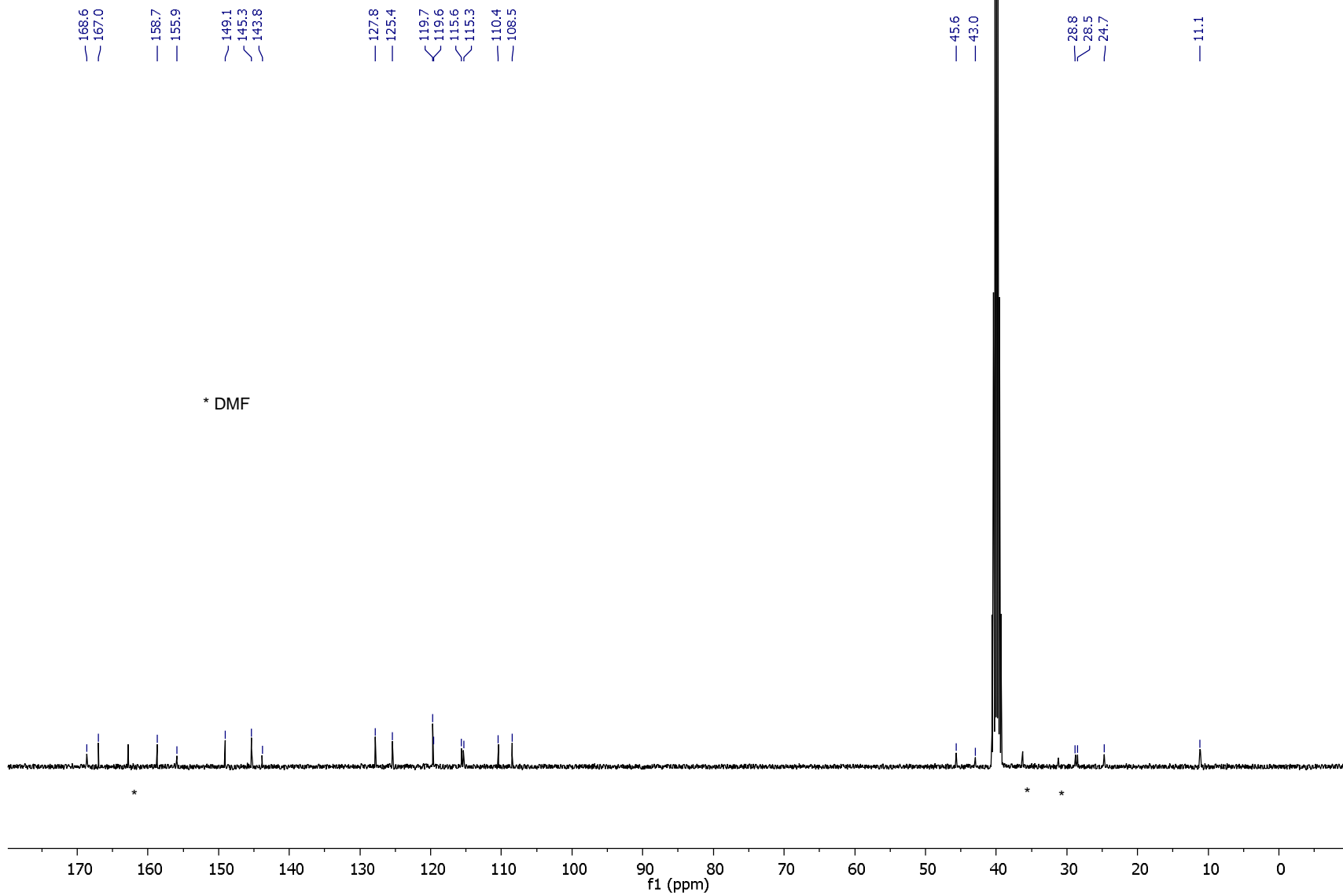


(S)-3,4-Dichloro-*N*-(2-(2-(3,4-dihydroxybenzamido)acetamido)-4,5,6,7-tetrahydrobenzo[*d*]thiazol-6-yl)-5-methyl-1*H*-pyrrole-2-carboxamide (**34**).

¹H NMR (400 MHz, DMSO-d₆)



13C NMR (100 MHz, DMSO-d6)



(S)-3,4-Dichloro-N-(2-(2-(2,3-dihydroxybenzamido)acetamido)-4,5,6,7-tetrahydrobenzo[d]thiazol-6-yl)-5-methyl-1H-pyrrole-2-carboxamide (35).

¹H NMR (400 MHz, DMSO-d₆)

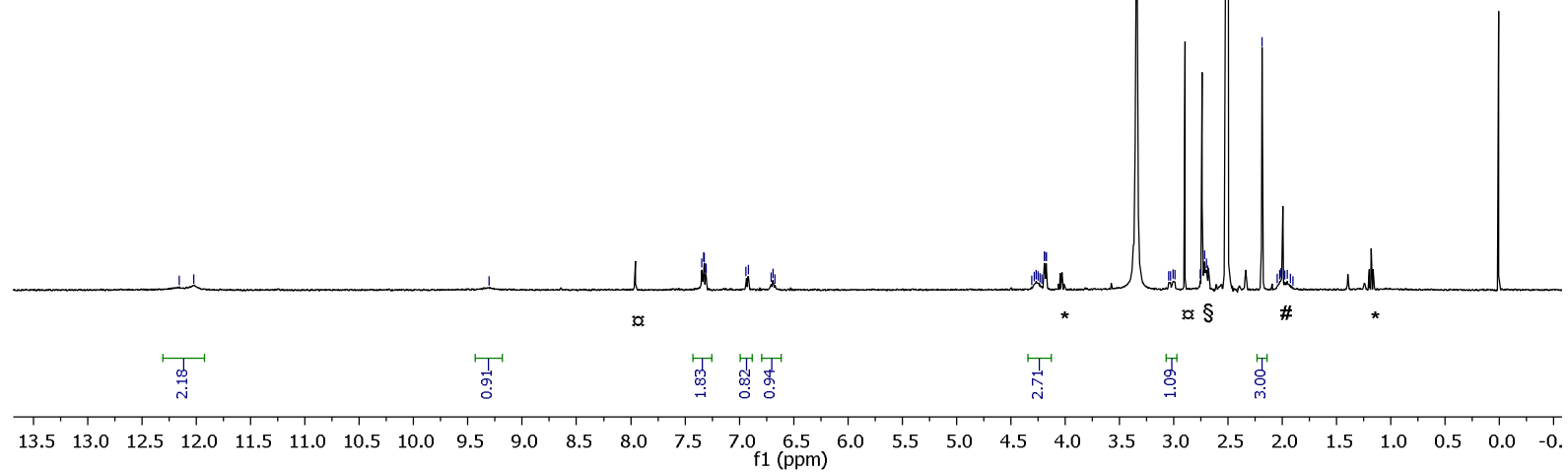


* EtOAc

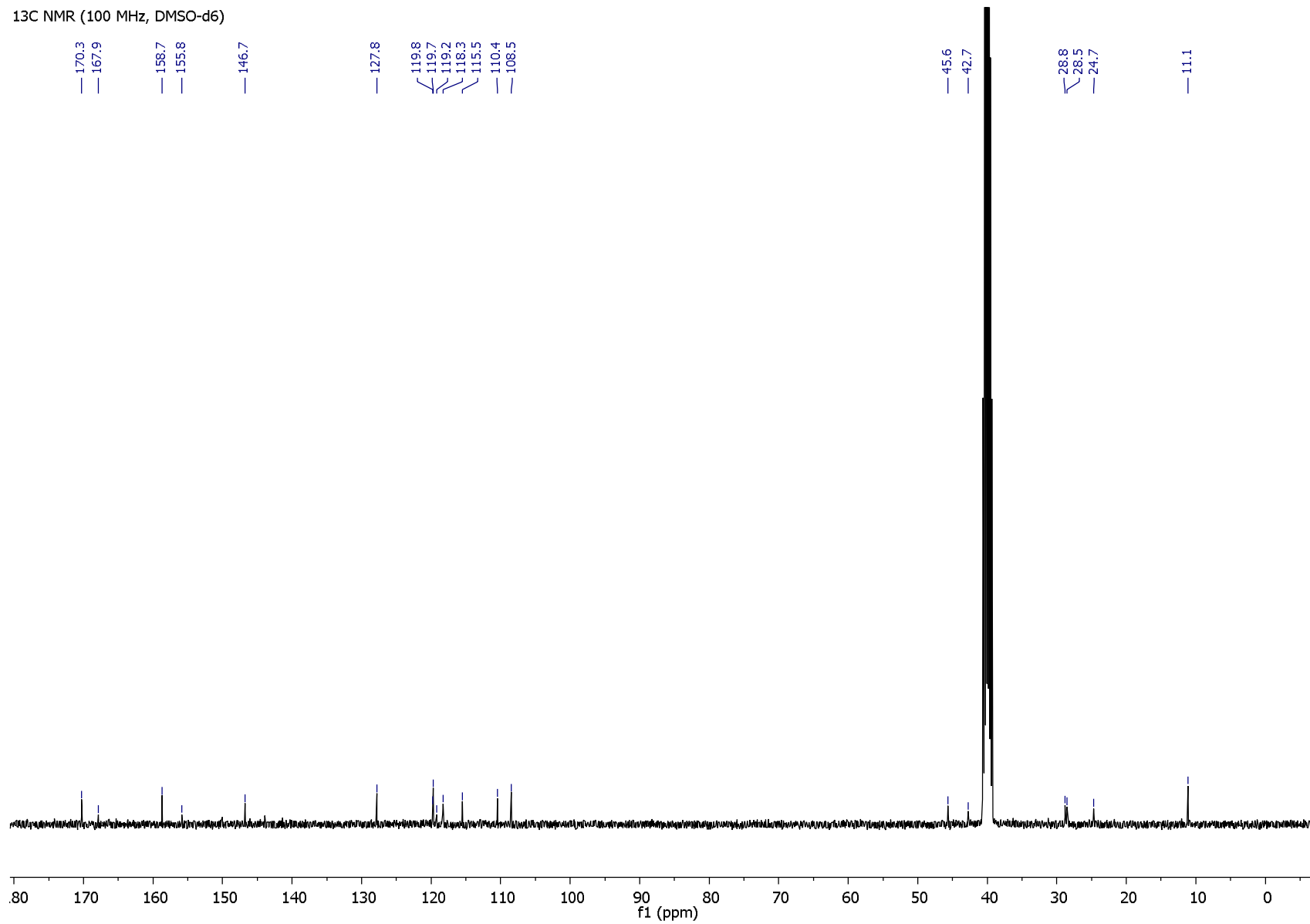
α DMF

signal partially overlapped with EtOAc

§ signal partially overlapped with DMF

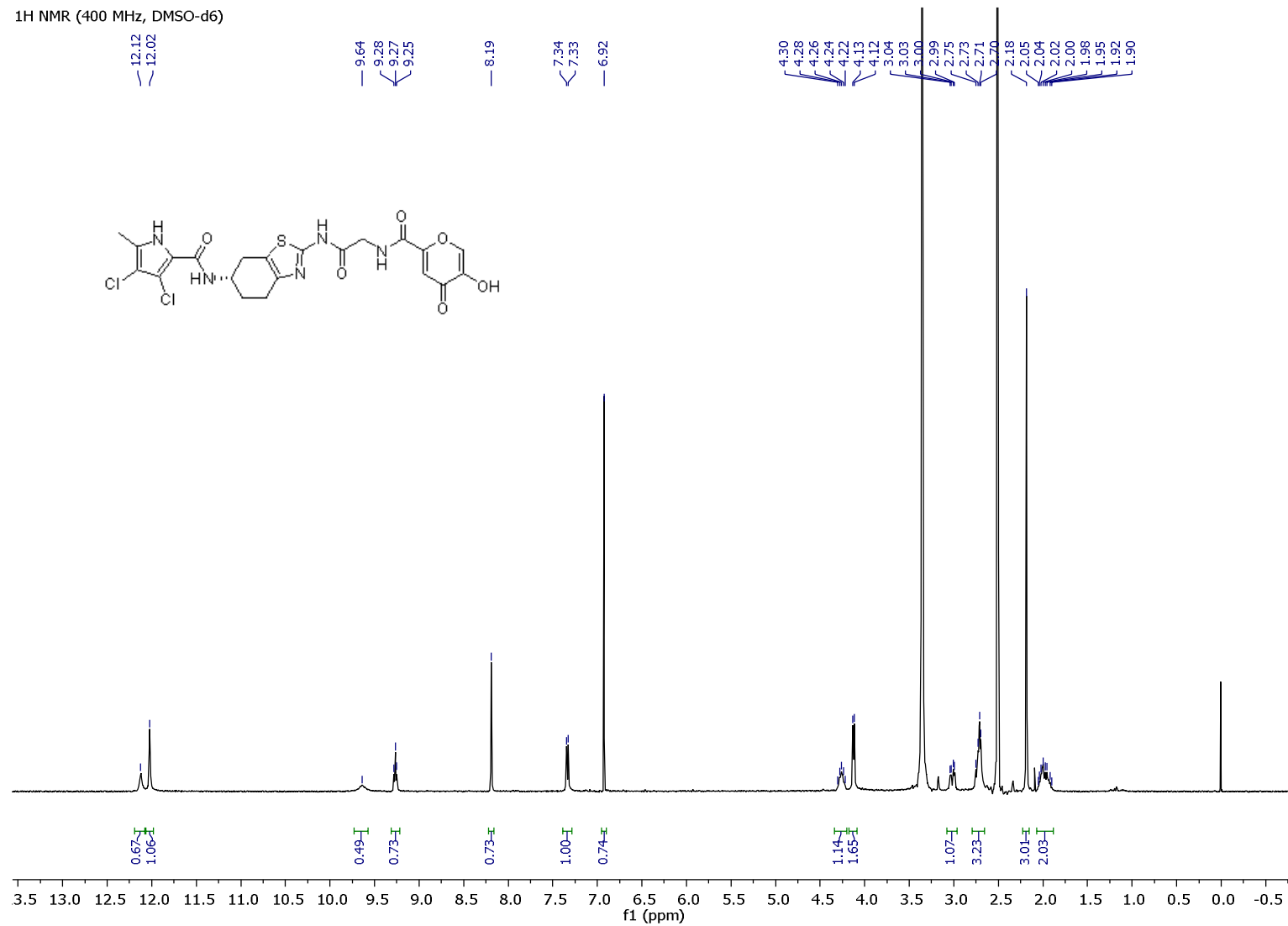


13C NMR (100 MHz, DMSO-d6)

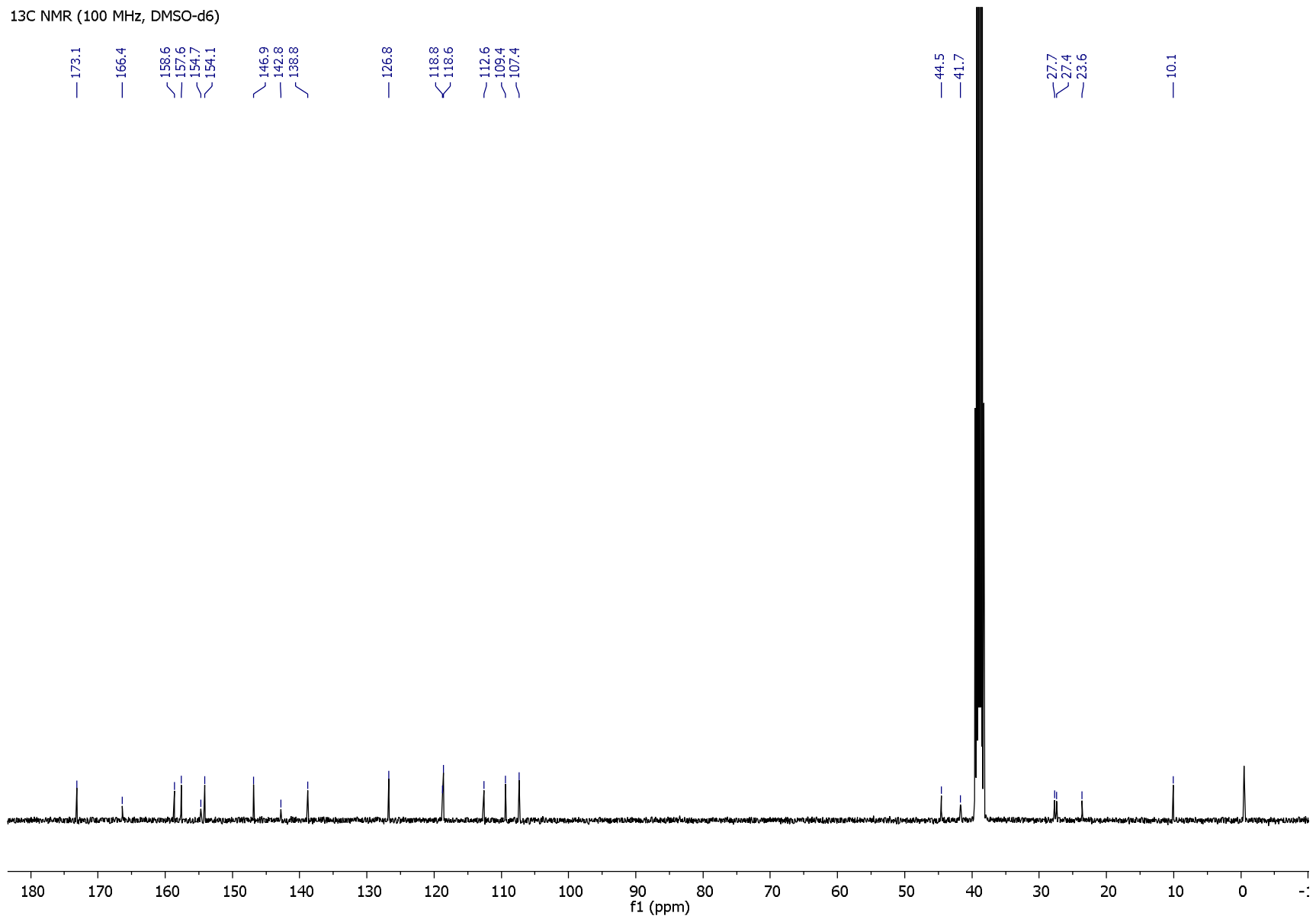


(S)-3,4-Dichloro-N-(2-(2-(5-hydroxy-4-oxo-4H-pyran-2-carboxamido)acetamido)-4,5,6,7-tetrahydrobenzo[d]thiazol-6-yl)-5-methyl-1H-pyrrole-2-carboxamide (**39**).

¹H NMR (400 MHz, DMSO-d₆)

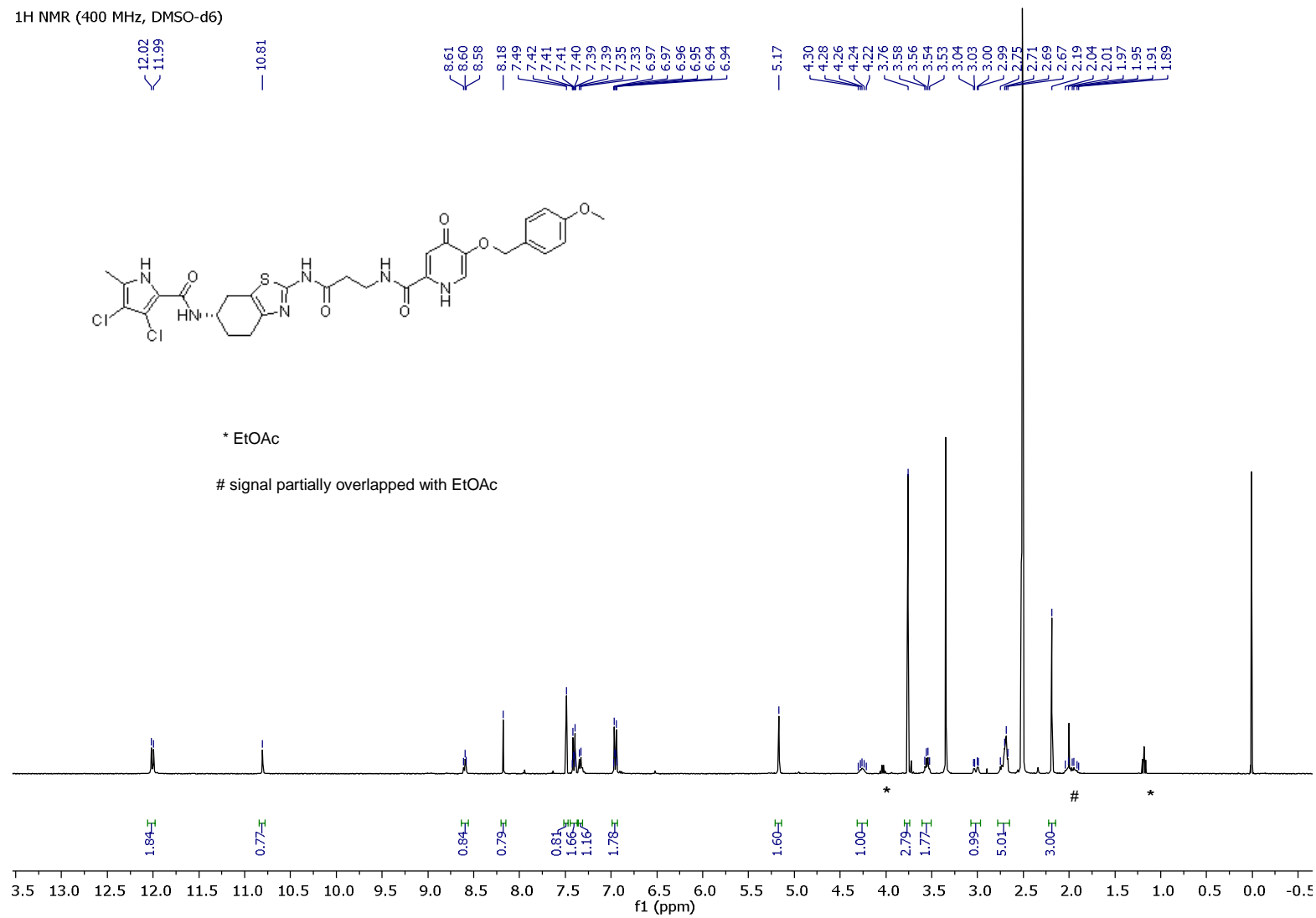


¹³C NMR (100 MHz, DMSO-d₆)

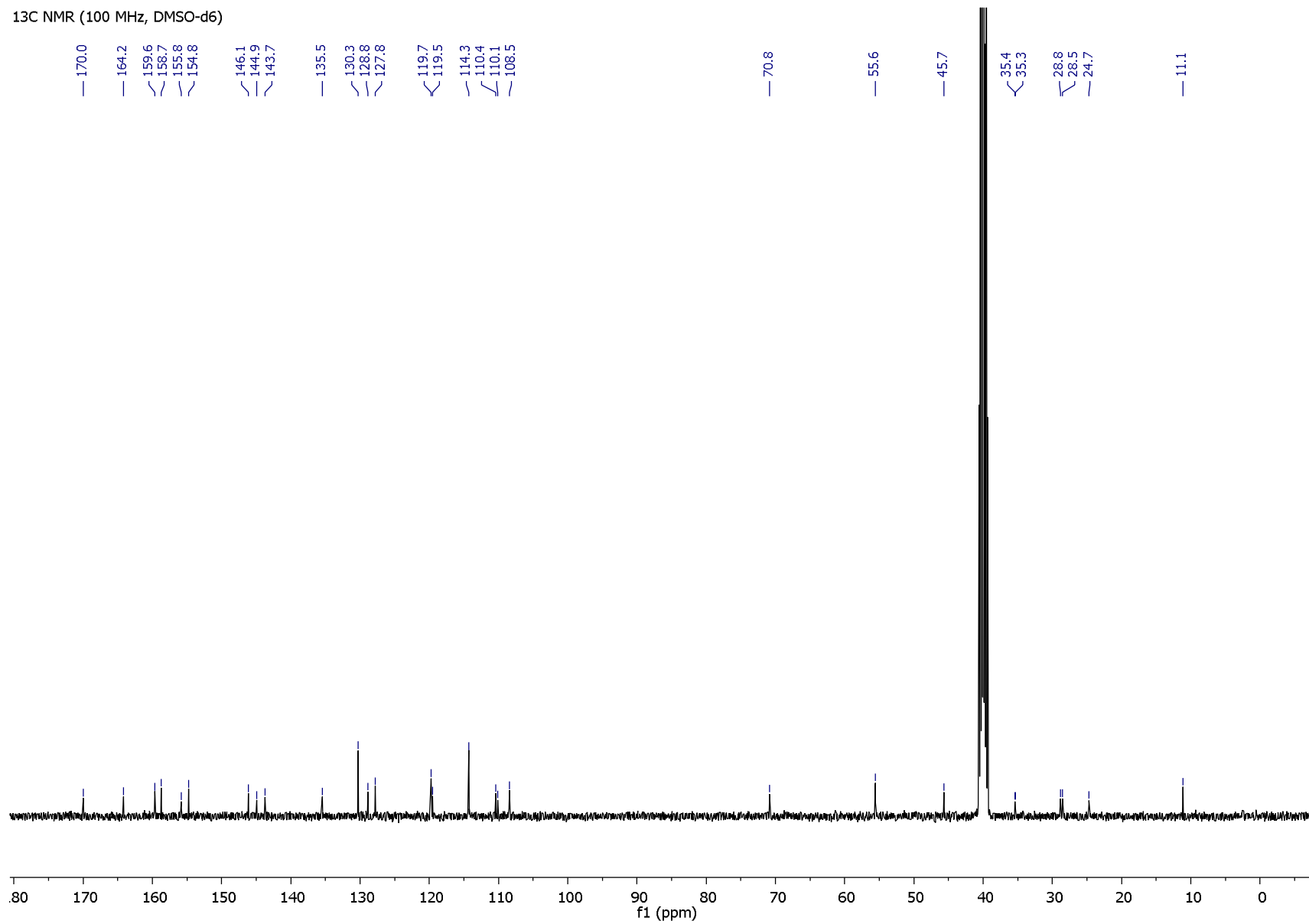


(S)-N-(3-((6-(3,4-Dichloro-5-methyl-1H-pyrrole-2-carboxamido)-4,5,6,7-tetrahydrobenzo[d]thiazol-2-yl)amino)-3-oxopropyl)-5-((4-methoxybenzyl)oxy)-4-oxo-1,4-dihydropyridine-2-carboxamide (**43**).

¹H NMR (400 MHz, DMSO-d₆)

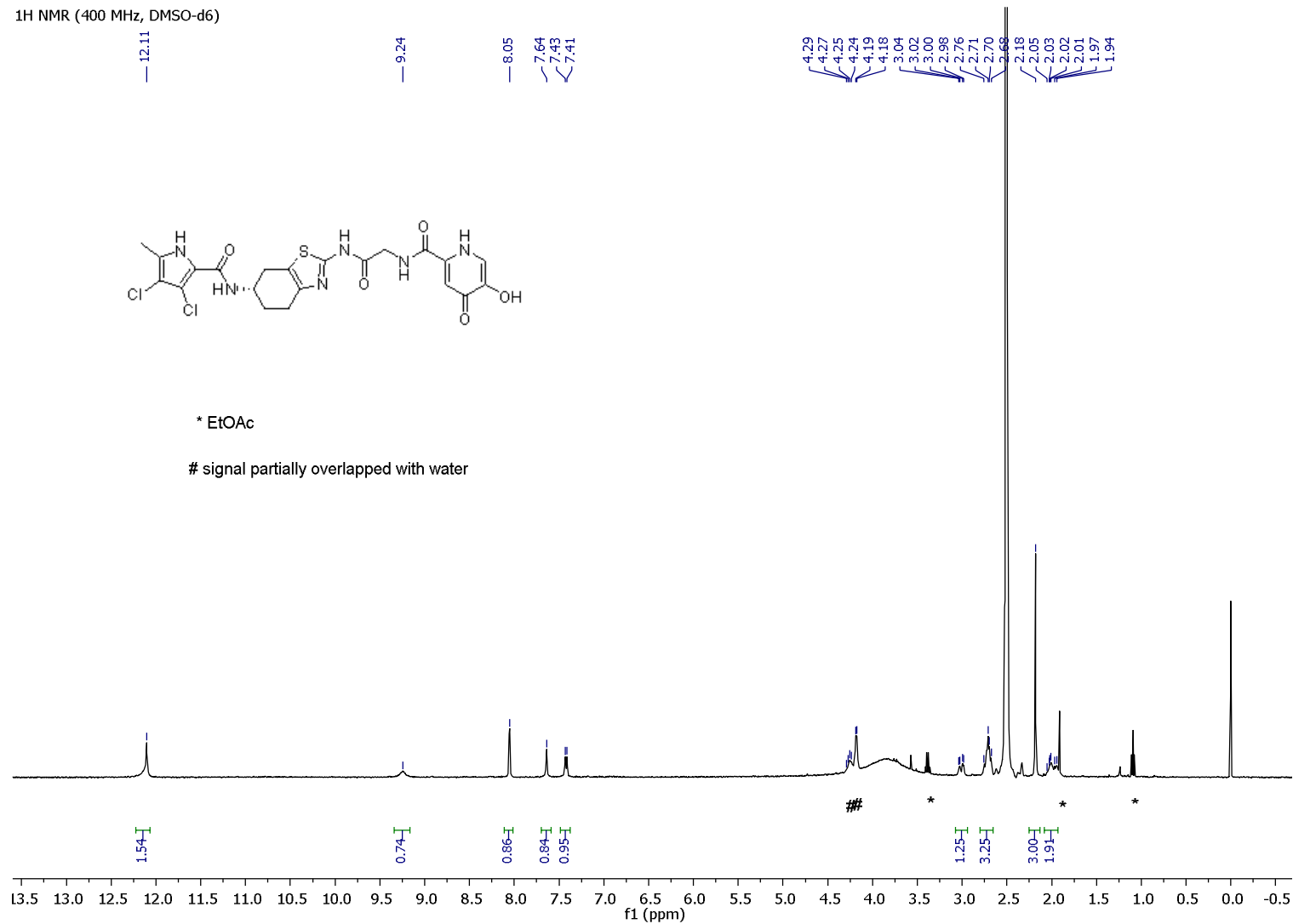


¹³C NMR (100 MHz, DMSO-d₆)

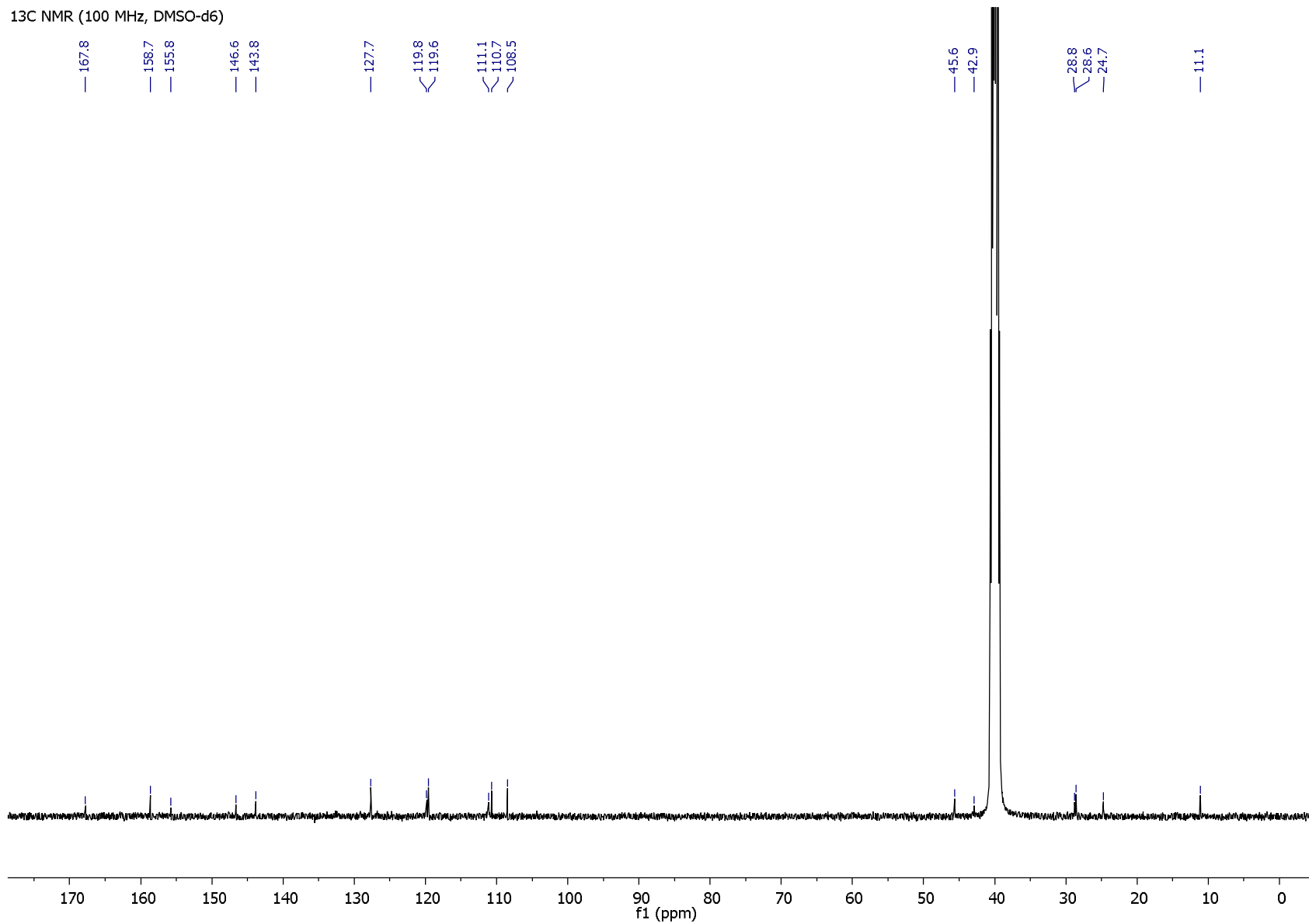


(*S*)-*N*-(2-((6-(3,4-Dichloro-5-methyl-1*H*-pyrrole-2-carboxamido)-4,5,6,7-tetrahydrobenzo[*d*]thiazol-2-yl)amino)-2-oxoethyl)-5-hydroxy-4-oxo-1,4-dihydropyridine-2-carboxamide (**44**).

¹H NMR (400 MHz, DMSO-*d*₆)

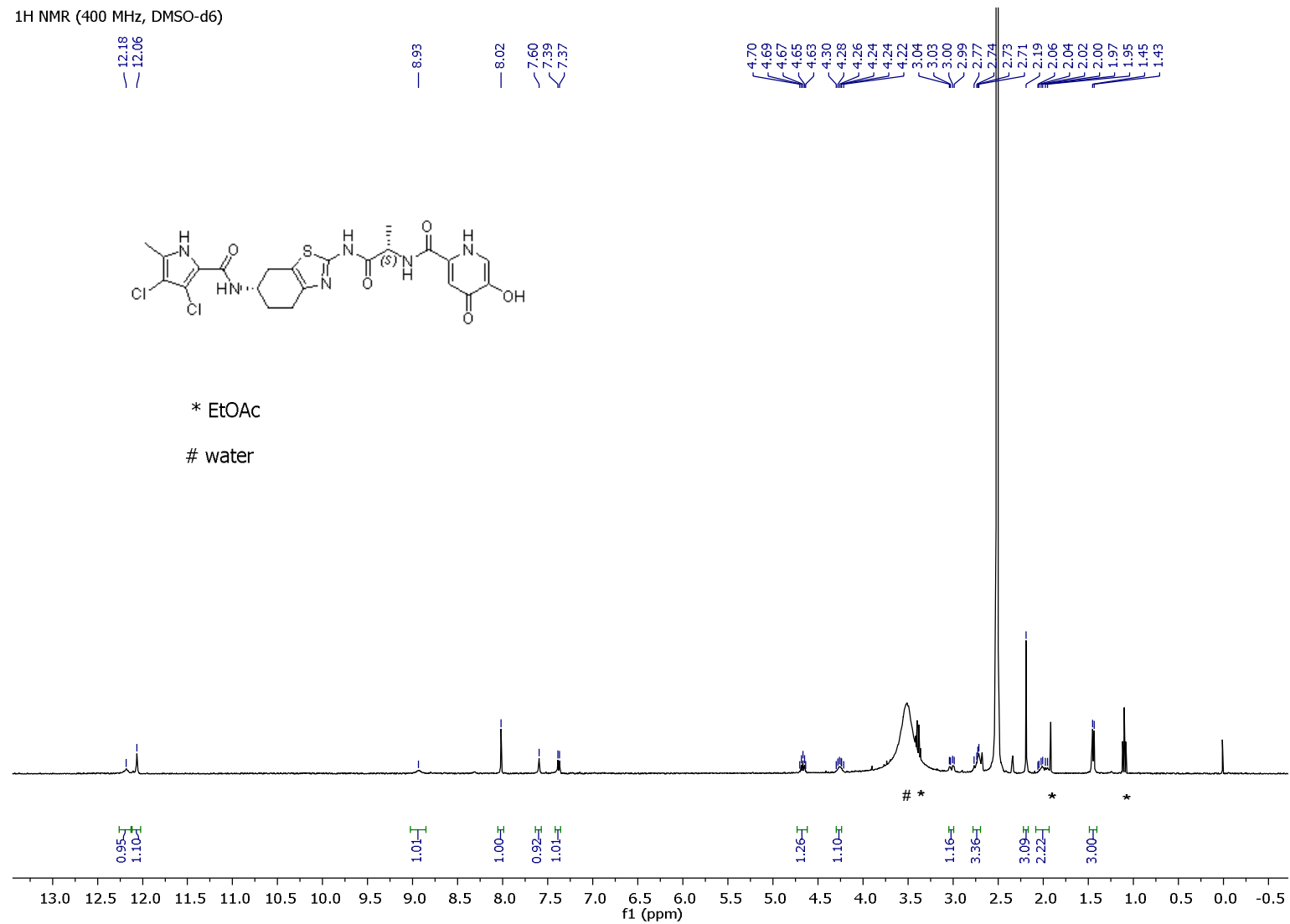


13C NMR (100 MHz, DMSO-d6)

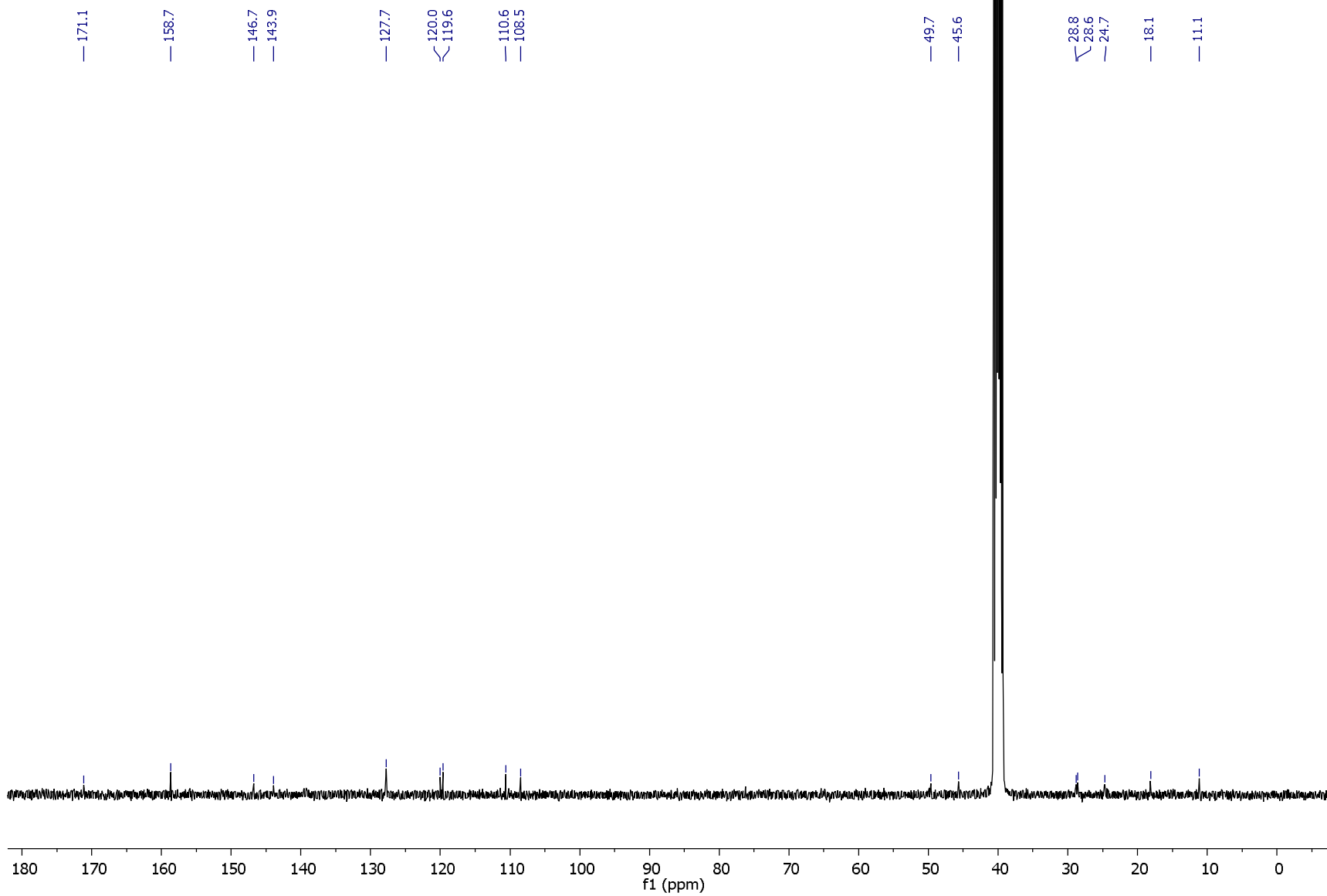


N-((*S*)-1-(((*S*)-6-(3,4-Dichloro-5-methyl-1*H*-pyrrole-2-carboxamido)-4,5,6,7-tetrahydrobenzo[*d*]thiazol-2-yl)amino)-1-oxopropan-2-yl)-5-hydroxy-4-oxo-1,4-dihydropyridine-2-carboxamide (**45**).

¹H NMR (400 MHz, DMSO-d₆)



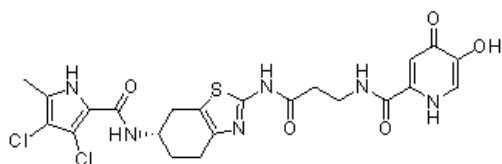
¹³C NMR (100 MHz, DMSO-d₆)



(S)-*N*-(3-((6-(3,4-Dichloro-5-methyl-1*H*-pyrrole-2-carboxamido)-4,5,6,7-tetrahydrobenzo[*d*]thiazol-2-yl)amino)-3-oxopropyl)-5-hydroxy-4-oxo-1,4-dihydropyridine-2-carboxamide (**47**).

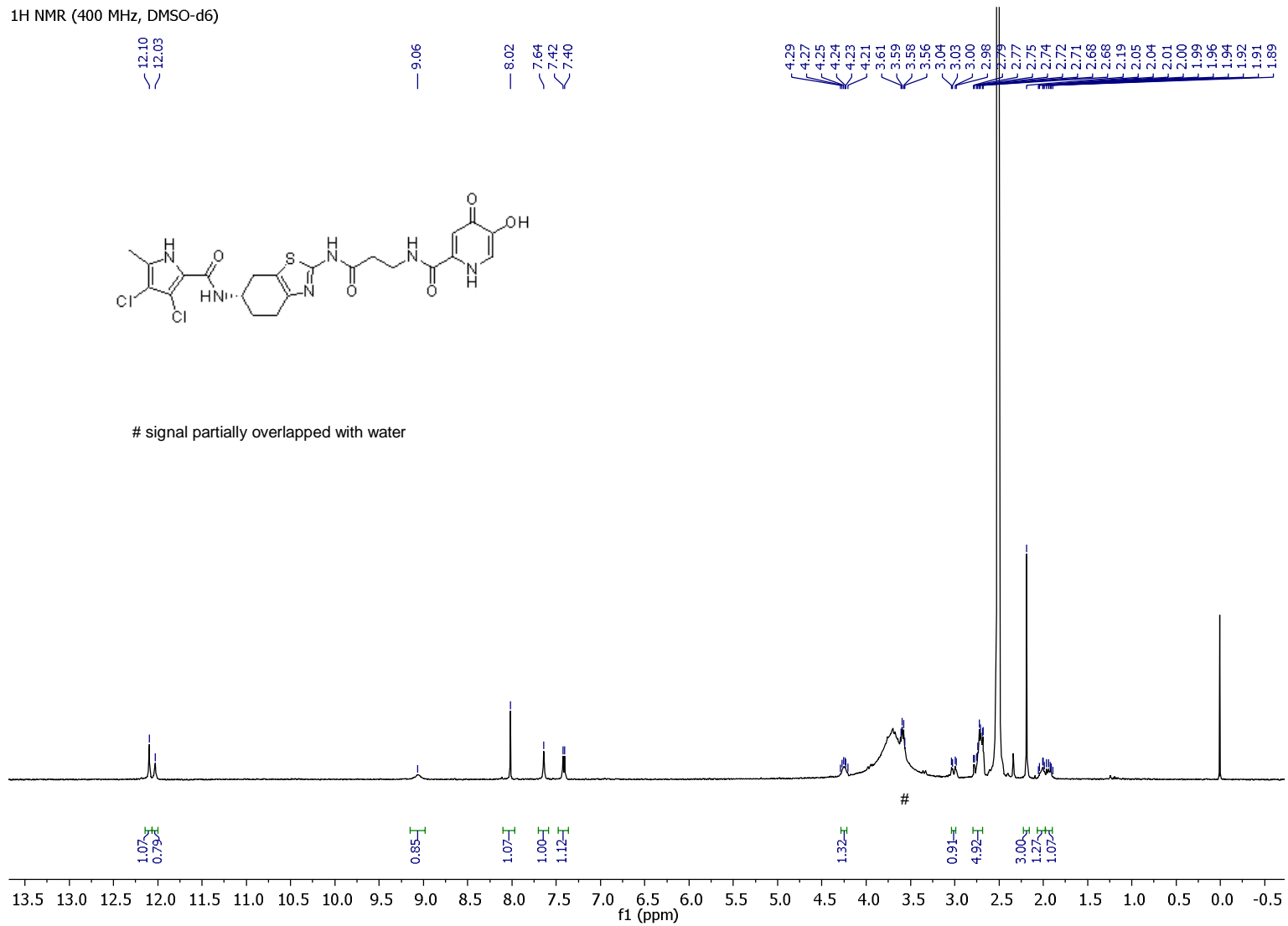
¹H NMR (400 MHz, DMSO-*d*₆)

12.10
12.03
9.06
8.02
7.64
7.42
7.40



signal partially overlapped with water

4.29
4.27
4.25
4.24
4.23
4.21
3.61
3.59
3.58
3.56
3.04
3.03
3.00
2.98
2.79
2.77
2.75
2.74
2.72
2.71
2.68
2.66
2.19
2.05
2.04
2.01
2.00
1.99
1.96
1.94
1.92
1.91
1.89



¹³C NMR (100 MHz, DMSO-d₆)

